

## An insight on the polyphase thermal history of the Internal Rif (Northern Morocco) through Raman micro-spectroscopy investigation

Journal:	<i>Italian Journal of Geosciences</i>
Manuscript ID	IJG-2021-0950.R1
Manuscript Type:	Original Article
Date Submitted by the Author:	n/a
Complete List of Authors:	Schito, Andrea; University of Aberdeen, Department of Geology and Geophysics; Roma Tre University, Dipartimento di Scienze Atouabat, Achraf; Roma Tre University, Dipartimento di Scienze Muirhead, David; University of Aberdeen, Department of Geology and Geophysics Calcagni, Rocco; Roma Tre University, Dipartimento di Scienze Galimberti, Roberto; Geolog Technologies S.r.l. , GEOTech Research and Laboratory Romano, Claudia; Roma Tre University, Dipartimento di Scienze Spina, Amalia; Università degli Studi di Perugia, Dipartimento di Fisica e Geologia Corrado, Sveva; Roma Tre University, Scienze
Keywords:	Internal Rif, Organic matter, Raman spectroscopy, Variscan orogenesis, Alpine thermal event

SCHOLARONE™  
Manuscripts

1  
2  
3 **An insight on the polyphase thermal history of the Internal Rif (Northern Morocco)**  
4  
5  
6 **through Raman micro-spectroscopy investigation**  
7  
8

9 A. SCHITO<sup>\*1,2</sup>, A. ATOUABAT<sup>2</sup>, D. K. MUIRHEAD<sup>1</sup>, R. CALCAGNI<sup>2</sup>, R. GALIMBERTI<sup>3</sup>, C. ROMANO<sup>2</sup>, A. SPINA<sup>4</sup> and  
10  
11 S. CORRADO<sup>2</sup>  
12  
13  
14  
15  
16

17 <sup>1</sup>*Department of Geology and Geophysics, School of Geosciences, University of Aberdeen, Aberdeen AB24*  
18  
19 *3UE, UK.*  
20

21 <sup>2</sup>*Università degli Studi di Roma Tre, Dipartimento di Scienze, Sezione di Scienze Geologiche, Largo San Leonardo*  
22  
23 *Murialdo 1, 00146 Rome, Italy*  
24

25 <sup>3</sup>*Geolog Technologies S.r.l. (GEOTech Research and Laboratory) – Viale Ortles 22/4, 20139, Milan, Italy*  
26  
27

28 <sup>4</sup>*Università degli Studi di Perugia, Dipartimento di Fisica e Geologia, Via Alessandro Pascoli, 06123 Perugia,*  
29  
30 *Italy*  
31  
32

33  
34  
35  
36  
37  
38 *\*Corresponding author (e-mail: andrea.schito@abdn.ac.uk)*  
39  
40

41 **Abstract**  
42  
43

44 Micro-Raman spectroscopy on carbonaceous material has been applied to estimate the maximum paleo-  
45 temperatures achieved by the Tectono-metamorphic units that constitute most of the backbone of the  
46 Internal domain of the Rif orogen in North Morocco. The Internal Rif is composed by the continental deep  
47 units of the Sebides, exhumed at the end of the Alpine cycle, overlain by the Variscan Ghomarides. Both  
48 units are thrust above the meta-carbonates of the Dorsale Calcaire. In the northern part of the Rif, the Sebide  
49 complex cropping out at the core of the Beni Mezala antiform suffered maximum paleo-temperatures  
50 derived from Raman parameters typical of greenschists facies, whereas in the flanks of the antiform the gap  
51 in temperatures between Lower Paleozoic (Silurian and Devonian) and Carboniferous Ghomarides probably  
52  
53  
54  
55  
56  
57  
58  
59  
60

1  
2  
3 reflect the temperatures peaks reached during Eo Variscan and Late Variscan phases. Moreover, our data  
4 suggest that one of the two analysed units in the Ghomarides always reached higher metamorphic conditions  
5 during both Variscan cycles. Further to the south, the increase in maximum temperatures towards the  
6 contact with the Beni-Bousera peridotite reflects an Alpine thermal overprinting, probably linked to slab  
7 retreat and delamination driven crustal anatexis, accompanied by magma emplacement during the last  
8 phases of the Alpine orogenesis.  
9  
10  
11  
12  
13  
14  
15  
16  
17  
18  
19

## 20 **1. Introduction**

21  
22 Maximum paleo-temperatures are strictly linked to rocks rheology and geochemical processes that occur at  
23 depth in different geodynamic settings, from passive margins to subduction systems. Thus, correct  
24 assessment of maximum paleo-temperatures experienced by rocks is an essential tool to unravel the  
25 evolution of the thermal structure of the crust during the main phases of an orogenesis. Classical  
26 metamorphic zones, based on metamorphic reactions and pseudosections, suffer from the superimposition  
27 of retrograde processes or by the presence/absence of diagnostic minerals that can undermine the accurate  
28 determination of the peak temperatures. On the other hand, maximum temperatures derived from the  
29 analyses of carbonaceous material (CM) dispersed in rocks have proven to provide robust and, sometimes,  
30 more precise data given the irreversible nature of organic matter transformation with temperature increase  
31 (TEICHMÜLLER, 1986; TAYLOR *et alii*, 1998, BEYSSAC *et alii*, 2002; LAHFID *et alii*, 2010). The most used  
32 thermal indicators for dispersed organic matter derive from optical analyses (e.g. vitrinite reflectance, color  
33 alteration indexes; HARTKOPF-FRÖDER *et alii*, 2015; SPINA *et alii*, 2018; SORCI *et alii*, 2020), although, in the  
34 last decades, an increasing interest raised towards the use of thermal parameters derived from Raman  
35 spectroscopy. This tool was initially developed for metamorphic temperature higher than about 300°C  
36 (PASTERIS AND WOPENKA, 1991; BEYSSAC *et alii*, 2002), but its use has recently been extended to lower  
37 metamorphic degrees (RAHL *et alii*, 2005; LAHFID *et alii*, 2010) and diagenesis (LI, 2007; GUEDES *et alii*, 2010;  
38 WILKINS *et alii*, 2014; LÜNSDORF *et alii*, 2017; SCHITO *et alii*, 2017, 2019; SCHMIDT *et alii*, 2017; HENRY *et*  
39 *alii*, 2018, 2019; SCHITO & CORRADO, 2018). Given the application in a wide range of temperature conditions,  
40  
41  
42  
43  
44  
45  
46  
47  
48  
49  
50  
51  
52  
53  
54  
55  
56  
57  
58  
59  
60

1  
2  
3 Raman spectroscopy on carbonaceous material (RSCM) has become one of the most used geothermometers  
4  
5 in geological studies to accurately unravel thermal metamorphic gradients (NEGRO *et alii*, 2006; DELCHINI *et*  
6  
7 *alii*, 2016; DUCOUX *et alii*, 2019; LAHFID *et alii*, 2019).

9  
10 The selected playground for new Raman studies on metamorphic rocks is the Internal Rif in Northern  
11  
12 Morocco. This area represents the innermost tectonic domain preserved on-shore of the wider Betic-Rif-Tell  
13  
14 orogenic chain that developed during the Mesozoic-Cenozoic complex convergence between Africa and  
15  
16 Eurasia plates forming the westernmost termination of the Mediterranean Alpine orogenic system (LEPRÊTRE  
17  
18 *et alii*, 2018; ROYDEN & FACCENNA, 2018).

19  
20 The Internal Rif offers a unique opportunity to observe at surface high-grade metamorphic rocks from an  
21  
22 alpine fossil subduction zone (Sebtide tectonic units) tectonically lying below low-grade metamorphic rocks  
23  
24 derived from a complex polyphase Variscan history (Ghomaride tectonic units). In detail, the Ghomarides  
25  
26 and Sebtides represent respectively the upper and lower plates preserved in a metamorphic core complex  
27  
28 (CHALOUAN *et alii*, 2008). They are composed by Paleozoic rocks with a partially preserved Mesozoic-  
29  
30 Cenozoic cover and by lower Paleozoic to Triassic deep-crustal mica-schists, migmatites and granulites  
31  
32 associated with peridotites (Beni Bousera complex), respectively (CHALOUAN *et alii*, 2008).

33  
34 Given its importance in the Alpine orogenic reconstruction in the western Mediterranean, the Sebtides have  
35  
36 been the subject of several studies aiming at the definition of their P-T deformation history, in particular of  
37  
38 their deepest units (MARRONE *et alii*, 2021; SOTO *et alii*, 1999; MICHARD *et alii*, 2006; BOOTH-REA *et alii*,  
39  
40 2007; ROSSETTI *et alii*, 2010, 2020; PLATT *et alii*, 2013; GUEYDAN *et alii*, 2015; MELCHIORRE *et alii*, 2017;  
41  
42 WILLIAMS & PLATT, 2018) . On the other hand, the Variscan metamorphic evolution of the Ghomarides  
43  
44 complex has been widely studied by CHALOUAN (1986) and CHALOUAN & MICHARD (1990) with the aim to  
45  
46 correlate it with the history of similar Variscan terranes in Spain (Betic Cordillera), northern Algeria (Kabylian  
47  
48 domain) and southern Italy (Calabro-Peloritain arc).

49  
50 An accurate study of the maximum paleo-temperatures achieved by Sebtides and Ghomarides in the Internal  
51  
52 Rif by means of Raman spectroscopic analyses on carbonaceous material has been already developed by  
53  
54 NEGRO *et alii* (2006). Nevertheless, using the RSCM method proposed by BEYSSAC *et alii* (2002), the authors  
55  
56 did not investigate in detail paleo-temperature distributions in tectonic units that suffered peak  
57  
58  
59  
60

1  
2  
3 metamorphisms lower than 330°C. This led the authors to provide interesting interpretation on the Alpine  
4 history of the units surrounding the Beni-Bousera and Ronda peridotites but failed to provide useful  
5 constraints for the low-metamorphic Variscan history of the Ghomarides.  
6  
7  
8

9  
10 The present work aims to fulfill this gap providing more accurate Raman paleo-temperature data, in  
11 particular for the Ghomaride succession and for the organic carbon-poor successions of the Upper Sebtides  
12 in northern part of the Rif belt.  
13  
14  
15

## 16 17 18 19 **2. Geological Setting**

20  
21 Located at the western edge of the West-Mediterranean Alpine systems, the Rif belt corresponds to the  
22 southern limb of Gibraltar Arc that developed in the framework of Africa-Eurasia collision (DOCHERTY &  
23 BANDA, 1995; PÉROUSE *et alii*, 2010; PLATT *et alii*, 2013; VAN HINSBERGEN *et alii*, 2014) and is a part of the  
24 Maghrebides orogenic system (Tell-Rif; DURAND-DELGA, 1980). The Maghrebides resulted from the closure  
25 of the Maghrebian Tethys and the docking of the Meso-Mediterranean blocks (i.e., Alboran and Kabily  
26 domains) onto the African margin during the Early Miocene (CHALOUAN & MICHARD, 2004; LEPRÊTRE *et alii*,  
27 2018).  
28  
29

30  
31 The Rif belt is classically divided into three main tectono-stratigraphic domains (FAVRE & STAMPFLI, 1992;  
32 FRIZON DE LAMOTTE *et alii*, 2011), namely from north to south and from internal to external portion of the  
33 chain: (i) Internal or Alboran Domain (MILLIARD, 1959; BOUILLIN, 1986; GARCÍA-DUEÑAS *et alii*, 1992), (ii)  
34 Maghrebian Flysch Basin Domain (GUERRERA *et alii*, 1993, 2005; LEPRÊTRE *et alii*, 2018; ATOUABAT *et alii*,  
35 2020), and (iii) External Domain (DIDON *et alii*, 1973; LEBLANC, 1979; MICHARD *et alii*, 2014; GIMENO-VIVES  
36 *et alii*, 2019; GIMENO-VIVES *et alii*, 2020). The internal domain, object of this work, is subdivided into three  
37 tectonic complexes, recognized from bottom to top as: Sebtides complex, Ghomarides complex and the  
38 'Dorsale Calcaire' (EL KADIRI *et alii*, 1992).  
39  
40  
41  
42  
43  
44  
45  
46  
47  
48  
49  
50  
51  
52  
53

54  
55 The Sebtide Complex represents the structurally deepest unit and it is composed by the Lower Sebtides (Filali  
56 and Beni Bousera Units) and Upper Sebtides (Federico Unit). The Beni Bousera consists of a peridotite body,  
57 with topmost discontinuous slivers of granulites (kinzigites, CHALOUAN *et alii*, 2008) that emplaced in the  
58  
59  
60

1  
2  
3 crust as a consequence of the Variscan orogen collapse (ROSSETTI *et alii*, 2020) and was finally exhumed  
4 during Alpine stages (AZDIMOUSA *et alii*, 2014). It is separated by the overlying gneisses of the Filali Unit  
5 through a ductile shear zone (MICHARD *et alii*, 2006; CHALOUAN *et alii*, 2008; ROSSETTI *et alii*, 2010). The  
6 Federico Unit in the northern part of the Rif is formed by four thrust imbrications, namely Tzigarine, Boquete  
7 de Anjera, Beni Mezala 1 and 2 (from here onward BM1 and BM2 respectively), each of them showing the  
8 same stratigraphy and a general downward increase in metamorphic grade. The uppermost Tizgarine Unit is  
9 composed by Permian-Triassic red pelites, and Middle-Upper Triassic dolomitic marbles. The Permian-  
10 Triassic successions of Boquete de Anjera, BM1 and BM2 Units are characterized by purple phyllites and dark  
11 quartz-phyllite respectively, overlain by Triassic marbles on top (BOUYBAOUENE *et alii*, 1998). Locally in both  
12 Beni Mezala Units, some Carboniferous-Permian schists occur.

13  
14 Lower and upper Sebtides are thought to have experienced metamorphic conditions that reached the  
15 eclogite facies in the Federico Unit under HP-LT conditions and granulite facies under a higher geothermal  
16 gradient in Filali and Beni-Bousera Units (CHALOUAN & MICHARD, 1990; ROSSETTI *et alii*, 2020), even if  
17 recent works (RODRÍGUEZ-RUIZ *et alii*, 2020) suggested lower metamorphic conditions for the inner BM1  
18 Unit in the northern sector of the study area. Federico Unit is characterized by pervasive planar and linear  
19 tectonic fabric with a top-to-the NNW sense of shearing (MICHARD *et alii*, 2006).

20  
21 The Ghomaride complex consists of an Ordovician to Carboniferous succession, unconformably overlain by  
22 Triassic red beds and, locally, Liassic limestones and Paleocene-Eocene calcarenites (CALVO *et alii*, 2001). This  
23 complex includes four Paleozoic tectonic units that, from the bottom to the top, are the Akaili Unit, the  
24 Koudiat Tizian Unit and the Beni Hozmar Unit. A fourth unit, Talembote Unit, is a klippe preserved above the  
25 Dorsale Calcaire in the Oued-Laou area (CHALOUAN & MICHARD, 1990; CHALOUAN *et alii*, 2008). In the  
26 different units the Ordovician to Silurian stratigraphy is rather homogeneous, characterized by Ordovician  
27 phyllites with quartzites and meta-conglomerates and by graptolitic shales and pillow basalts at the top of  
28 the Silurian section. Devonian sediments consist of distal calcareous flysch in the Akaili Unit and more  
29 proximal flysch and pelagic limestones in the Koudiat-Tizian and Beni-Hozmar (CHALOUAN, 1986). The  
30 Ordovician to Devonian succession was subjected to Eo-Variscan metamorphic event deformation  
31 characterized by NNE trending structures and white mica, chlorite and quartz recrystallization (CHALOUAN

1  
2  
3 & MICHARD, 1990). Visean-Bashkirian greywackes unconformably onlap, showing NW oriented structures  
4  
5 and limited recrystallization associated with a late Variscan low grade metamorphic event. Brittle Alpine  
6  
7 deformation was recorded in the unconformable Triassic red beds that mostly constitute the uppermost  
8  
9 deposits except for some Jurassic limestones and Upper Eocene conglomerates that locally crop out  
10  
11 (ZAGHLOUL *et alii*, 2010).  
12

13  
14 Finally, the 'Dorsale Calcaire', consists of Triassic-Middle Jurassic carbonate platform deposits, Jurassic-  
15  
16 Cretaceous sediments overlaid by Paleocene-Eocene clays and limestones and by Eocene to Aquitanian  
17  
18 clastic deposits and olistostromes (EL KADIRI *et alii*, 1992). It is detached along the Triassic levels, from most  
19  
20 likely the Ghomarides (DURAND-DELGA & OLIVIER, 1988) or partly from Ghomarides and Sebtides (WILDI,  
21  
22 1983). The Triassic successions are composed by dolostones, dolomitic breccias and stromatolitic dolostones,  
23  
24 while during the Jurassic, a transition to a more distal environment is represented by a condensed pelagic  
25  
26 sedimentation in the entire succession. Eocene deposits composed of arenites, bioclastic limestones and  
27  
28 chaotic breccias, are separated by an unconformity from the Mesozoic succession, indicative of an uplift in  
29  
30 early Eocene times (MICHARD & CHALOUAN, 1990; CHALOUAN *et alii*, 2008).  
31  
32  
33  
34  
35  
36  
37  
38  
39  
40  
41  
42  
43  
44  
45  
46  
47  
48  
49  
50  
51  
52  
53  
54  
55  
56  
57  
58  
59  
60

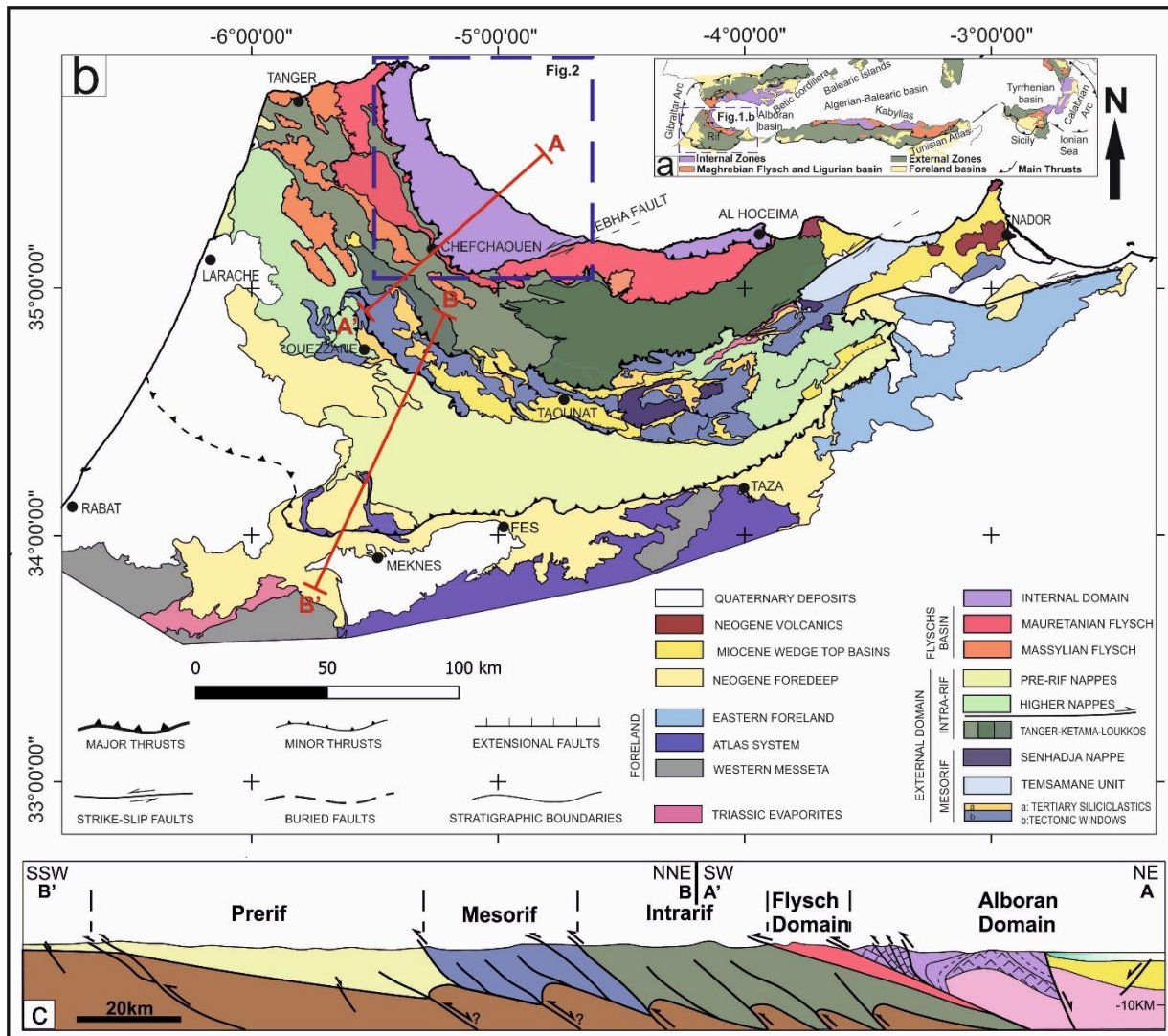


Figure 1 – Schematic geological map of the South Mediterranean (a) and of the Rif chain in North Morocco (b). Schematic cross section from the Alboran Sea to the external zones (c) (*modified after; SUTER, 1980; FRIZON DE LAMOTTE et alii, 2017; GIMENO-VIVES et alii, 2019; ATOUABAT et alii, 2020*).

### 3. Sampling areas and Materials

Sixteen samples from the Internal Rif have been collected and analysed from two areas (Fig. 2a): the Beni Mezala antiform to the North (Zone 1) and the region between Martil Village and Oued Laou, to the south of the town of Tetouan (Zone 2).

In Zone 1, sampling was performed along a NE-SW transect from the South of Ceuta town to the contact between the ‘Dorsale Calcaire’ and the Flysch domain (Fig. 2b) across the Beni Mezala antiform. Five samples



1  
2  
3 were collected in the Federico Units (Figs. 2b and 3a, b) in the core of the antiform and five from Ghomarides  
4 on both flanks of it (Figs. 2b and 3c, d). Samples from Ghomarides derived from Silurian and Carboniferous  
5 sections of the Akaili and Beni-Hozmar Units (Table 1). One sample (Mar 4.1) comes from a Silurian shaly  
6 horizon in the Beni-Hozmar Unit further to the South, close to the contact with the 'Dorsale Calcaire' (Fig.  
7 2a).  
8  
9  
10  
11  
12  
13

14 In Zone 2, samples were collected across a NW-SE oriented transect from Amsa village to Oued-Laou river  
15 (Fig. 2a and c) covering an area where mainly Ghomarides Akaili and Septides Filali Units crop out. In the  
16 Ghomarides, one sample comes from Carboniferous pelitic levels of the Akaili Unit cropping out in Ras Mazari  
17 cape area (close to the North of Amsa village), whereas all the others derive from Devonian to Ordovician  
18 Ghomarides (Akaili Unit). In this sector of the Septides, sample Mar 20.1 comes from Filali Unit (Tab. 1).  
19  
20  
21  
22  
23  
24  
25  
26  
27  
28  
29  
30  
31  
32  
33  
34  
35  
36  
37  
38  
39  
40  
41  
42  
43  
44  
45  
46  
47  
48  
49  
50  
51  
52  
53  
54  
55  
56  
57  
58  
59  
60

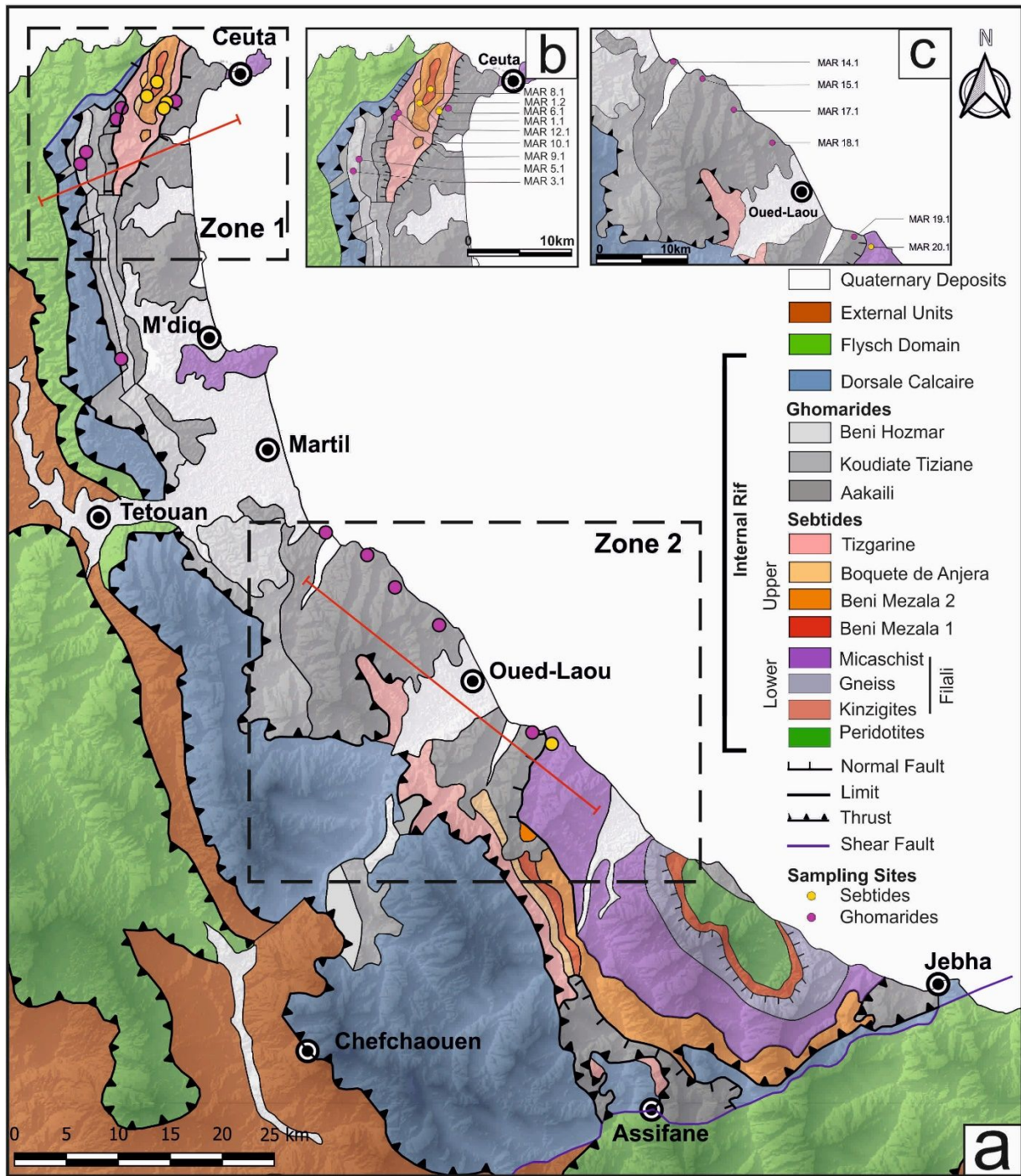


Figure 2 – A. Geological map of Internal Rif with indicated sampling zones (1 and 2) and sampling sites. Redrawn after CHALOUAN *et alii*, 2008.

**Table 1 – Sample distribution from the lowest tectonic units (bottom) to the shallowest (top) with indicated age, tectonic unit and coordinates (West Greenwich and North) of each sampling site.**

Complex	Sample name	Long.	Lat.	Tectonic Unit	Age
GHOMARIDES	MAR_5.1	05° 26' 51"	35° 49' 56"	Beni Hozmar	Silurian
	MAR_4.1	05° 26' 57"	34° 49' 40"	Beni Hozmar	Silurian
	MAR_3.1	05° 27' 10"	35° 49' 24"	Beni Hozmar	Carboniferous
	MAR_19.1	05° 02' 20"	35° 23' 59"	Akaili	Silurian
	MAR_18.1	05° 07' 27"	35° 28' 47"	Akaili	Silurian-Devonian?
	MAR_17.1	05° 09' 52"	35° 30' 29"	Akaili	Devonian
	MAR_15.1	05° 12' 24"	35° 32' 02"	Akaili	Devonian
	MAR_14.1	05° 13' 41"	35° 32' 56"	Akaili	Carboniferous
	MAR_10.1	05° 24' 57"	35° 51' 48"	Akaili	Silurian
	MAR_9.1	05° 24' 57"	35° 51' 48"	Akaili	Carboniferous
MAR_6.1	05° 21' 57"	35° 52' 12"	Akaili	Silurian	
SEBTIDES	MAR_1.2	05° 22' 27"	35° 52' 8"	Tizgarine	Permian
	MAR_1.1	05° 22' 26"	35° 52' 8"	Tizgarine	Permian
	MAR_12.1	05° 23' 31"	35° 52' 26"	Beni Mezala 2	Permian-Triassic
	MAR_8.1	05° 22' 50"	35° 52' 56"	Beni Mezala 1	Permian-Triassic
	MAR_20.1	05° 01' 16"	35° 23' 28"	Filali	Ordovician-Devonian

#### 4. Methods

TOC (total organic carbon) expresses the percentage of organic carbon weight related to the total weight of the analyzed rock. In this work data were acquired using a TOC Elementar model TOC VARIO Select analyzer, coupled with an oven (max temperature of 850°C).

1  
2  
3 Raman spectroscopic analyses allowed to determine the degree of order of the organic matter and thus  
4  
5 paleo-temperatures experienced by the rocks during prograde metamorphism (e.g. Raman spectroscopy on  
6  
7 carbonaceous material geothermometer – RSCM; BEYSSAC *et alii*, 2002; LAHFID *et alii*, 2010; LÜNSDORF *et*  
8  
9 *alii*, 2014).

10  
11  
12 The Raman spectrum of carbonaceous material consists of two main bands at  $\sim 1585\text{ cm}^{-1}$  (the graphite peak,  
13  
14 G ) and  $1350\text{ cm}^{-1}$  (the disorder peak, D; TUINSTRAN & KOENIG, 1970). These bands occur as the result of the  
15  
16 hybridised atomic orbital configuration of carbon atoms and the relative amount of  $sp^2$  carbon bonds  
17  
18 (graphite-like, trigonal planar symmetry) bounded by  $sp^3$  sites (diamond-like, tetrahedral symmetry;  
19  
20 ROBERTSON & OREILLY, 1987). The G band is assigned to the  $E_{2g}$  symmetry in-plane vibration of the carbon  
21  
22 atoms in the graphene sheets. On the other hand, the D band has been interpreted either by double resonant  
23  
24 Raman scattering ( $A_{1g}$ -mode of small graphite crystallites; THOMSEN & REICH, 2000) or to ring breathing  
25  
26 vibration in the graphite sub-unit or polycyclic aromatic compounds (CASTIGLIONI *et alii*, 2001; DI DONATO  
27  
28 *et alii*, 2004; NEGRI *et alii*, 2004; LÜNSDORF, 2016). Their mutual relationships change with maturity level of  
29  
30 organic matter (e.g. temperature; TUINSTRAN & KOENIG, 1970) up to the graphitic stage (BEYSSAC *et alii*,  
31  
32 2002). The number of bands that composes the carbonaceous material Raman spectrum, decreases with  
33  
34 increasing ordering (i.e. temperature increase) passing from more than five bands in diagenetic organic  
35  
36 matter to a single band in pure graphite (Fig. 4; HENRY *et alii*, 2019 for a complete review).  
37  
38  
39  
40  
41  
42  
43  
44  
45  
46  
47  
48  
49  
50  
51  
52  
53  
54  
55  
56  
57  
58  
59  
60

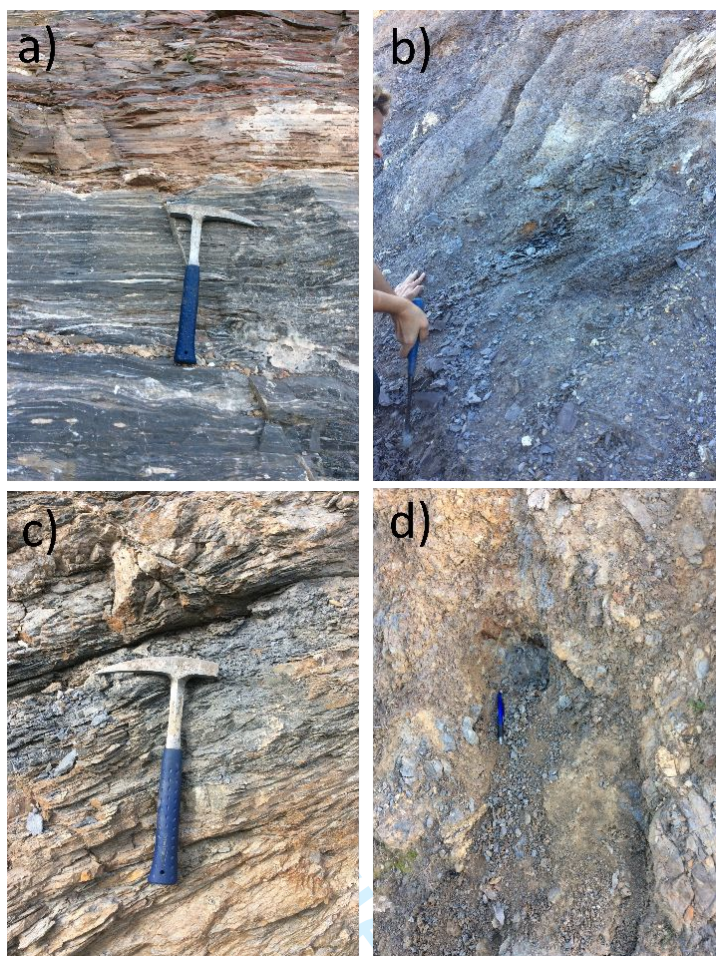


**Figure 3 Outcrop examples of a) schists from BM 2 Unit; b) black phyllites from Tizgarine Unit; c) Devonian pelites from the Ghomarides; d) Carboniferous pelites from the Ghomarides.**

Analyses in this work were performed on petrographic thin sections according to recommendation in BEYSSAC *et alii* (2002) and LÜNSDORF *et alii* (2017), using a Jobin Yvon micro-Raman LabRam system with a Neodymium-Yag laser of 532nm (green laser) as a light source and a CCD detector. Spectra were acquired in the first order Raman spectral range ( $700$  to  $2300$   $\text{cm}^{-1}$ ). The power of the laser was 40mW and was reduced to less than 0.4 mW by optical filters to avoid heating alteration of the organic matter. The integration time for each data was of 20 s repeated for three times under a 50x magnification lens (as defined by SCHITO *et alii*, 2017).

Temperatures were derived according to two different approaches in order to check the comparability between the relatively new method of LÜNSDORF *et alii*. (2017) with the classic fitting approach proposed by BEYSSAC *et alii*. (2002) for high metamorphism or by LAHFID *et alii*. (2010) for low metamorphism. The automatic method proposed by LÜNSDORF & LÜNSDORF (2016) and LÜNSDORF *et alii* (2017) is designed

1  
2  
3 to offer a comparability of Raman results at different stages of “organic metamorphism”. The method is  
4  
5 based on the IFORS software that curve-fits Raman spectra of carbonaceous material modelling  
6  
7 simultaneously the background with a fifth-order polynomial curve and the Raman signal with pseudo-Voight  
8  
9 bands. The optimization of the curve is an iterative process that adds pseudo-Voight functions (note that the  
10  
11 number of bands is not imposed *a priori*) until the best-representation of the baseline-subtracted spectrum  
12  
13 is reached (LÜNSDORF & LÜNSDORF, 2016; LÜNSDORF *et alii*, 2017). Among Raman parameters carried out  
14  
15 from this process, the normalized intensities of the D and G bands (STA-D, STA-G) are used to calculate paleo-  
16  
17 temperature by means of the third-degree polynomial equation proposed by LÜNSDORF *et alii* (2017). The  
18  
19 correlation against temperatures provided in LÜNSDORF *et alii* (2017) is based on a reference series of 26  
20  
21 samples collected across the central and western Alps in a range comprised between 100 and 700°C.  
22  
23

24  
25 RA2 or R2 parameters and related paleo-temperatures, were calculated, depending on the shape of the  
26  
27 spectra, by means of a four-to-three bands deconvolution as suggested by BEYSSAC *et alii* (2002) for graphitic  
28  
29 carbon (Figs. 4b and c) or by a five bands deconvolution proposed by LAHFID *et alii* (2010) for low-  
30  
31 metamorphic organic matter (Fig. 4a). Bands deconvolution was performed using LabSpec software by  
32  
33 Horiba. Paleo-temperatures were calculated according to the following equations:  
34  
35

$$36 \quad T (^{\circ}C) = -445 \times R2 + 641 \quad (1)$$

$$39 \quad T (^{\circ}C) = \frac{RA2 - 0.27}{0.0045} \quad (2)$$

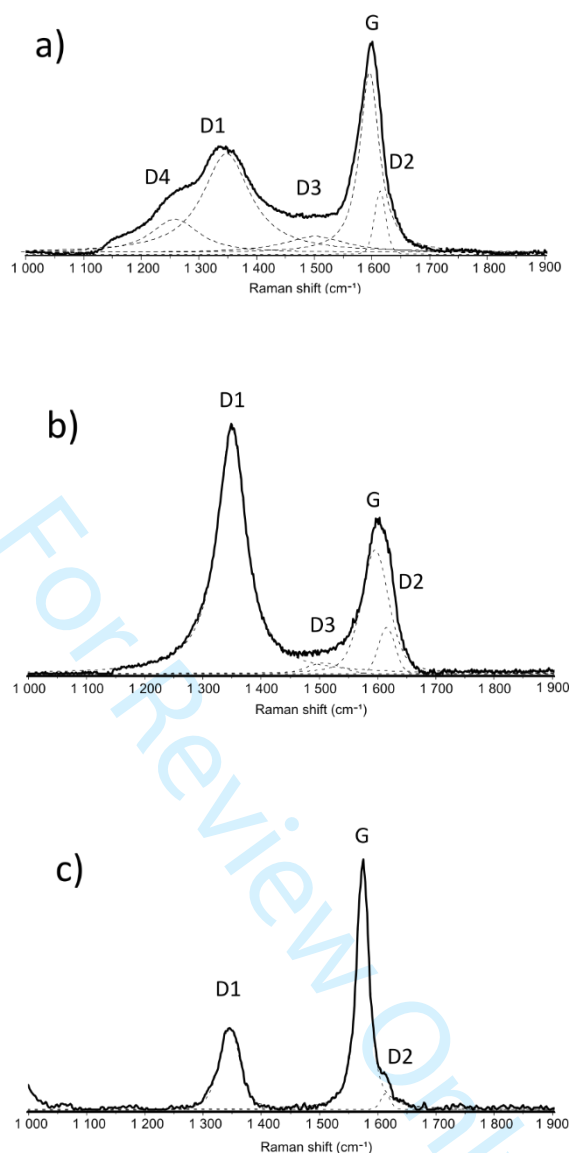


**Figure 4** Examples of Raman spectra and related bands assignment for different temperature intervals in the Internal Rif chain. a) Very disordered Raman spectrum from Carboniferous pelites of the Akaili Unit (Gomarides); b) spectrum from Silurian shales of the Akaili Unit (Ghomarides); c) spectrum of graphitic carbon from the Filali Unit (Sebtides).

## 5. Results

TOC data in Sebtide samples indicate values between 0.7 and 0.8% except for sample 12.1 from the Beni Mezala 2 Unit where TOC is higher than 2%. In the Ghomarides, samples show values ranging between about 0.6 and 3.9% in the Akaili Unit and between 0.6 and 1.6% in the Beni Hozmar Unit, generally indicating high organic carbon content (Tab. 2).

1  
2  
3 Between 14 to 35 Raman spectra on organic fragments were acquired for each sample, to obtain a reliable  
4 temperature estimation (Table 2). High fluorescing spectra with a low signal-to-noise ratio were discarded  
5 after acquisition during a first qualitative evaluation.  
6  
7

8  
9  
10 In zone 1, Raman spectra on organic matter from the BM 2 Unit show a well-developed D band and a strongly  
11 asymmetric G band due to the presence of a clearly defined D2 band. In the Tizgarine Unit, the G band shows  
12 lower intensities with respect to the D band and the D2 band shows lower intensities and wavenumber  
13 position. Such features correlate to paleo-temperatures of approximately 365°C in the BM 2 Unit and  
14 between 324 and 337°C (according to different approaches, see Tab. 2) in the Tizgarine Unit.  
15  
16

17  
18  
19 In zone 1, samples 10.1, 6.1 and 9.1 from the Ghomarides show very different spectral features. Spectra in  
20 sample 10.1 and 6.1 are characterized by two well-developed D and G bands with similar intensities (Fig. 5a),  
21 whereas in sample 9.1 the G band shows higher intensities with respect to the D band and a shoulder toward  
22 lower wavenumbers occurs on the D band (and 5c). Such differences, shown in Figs. 5a and c, correspond to  
23 a drop of more than 100°C between Lower Paleozoic (300-305°C in 10.1 and 296-299°C in 6.1) and  
24 Carboniferous samples (195-197°C in sample 9.1). A similar interval gap was also observed the Beni-Hozmar  
25 unit where paleo-temperatures range between 352 and 372°C in the Silurian sample 5.1 and between 285  
26 and 288 °C in the Carboniferous sample 3.1 (Tab. 2 and Figs. 5b and d).  
27  
28

29  
30  
31 In zone 2, the only sample from Filali unit shows spectra at an advanced stage of graphitization, characterized  
32 by a narrow G band with higher intensities with respect to the D band corresponding to temperature of 486-  
33 488°C (Fig 4c). Moving toward the NE in the Ghomarides, Raman spectra show a progressive increase of  
34 structural disorder with the increase of the D band intensity in samples 18.1 and 17.1 and with a broadening  
35 of both G and D bands in samples 15.1 and 14.1. Raman temperatures indicate a temperature decrease from  
36 the SW to the NE passing from 442-446°C in sample 19.1, to 340-370°C for samples 18.1 and 17.1 and 246-  
37 304°C at 15.1 and 14.1 sampling sites (Fig. 6, Tab. 2).  
38  
39  
40  
41  
42  
43  
44  
45  
46  
47  
48  
49  
50  
51  
52  
53  
54  
55  
56  
57  
58  
59  
60



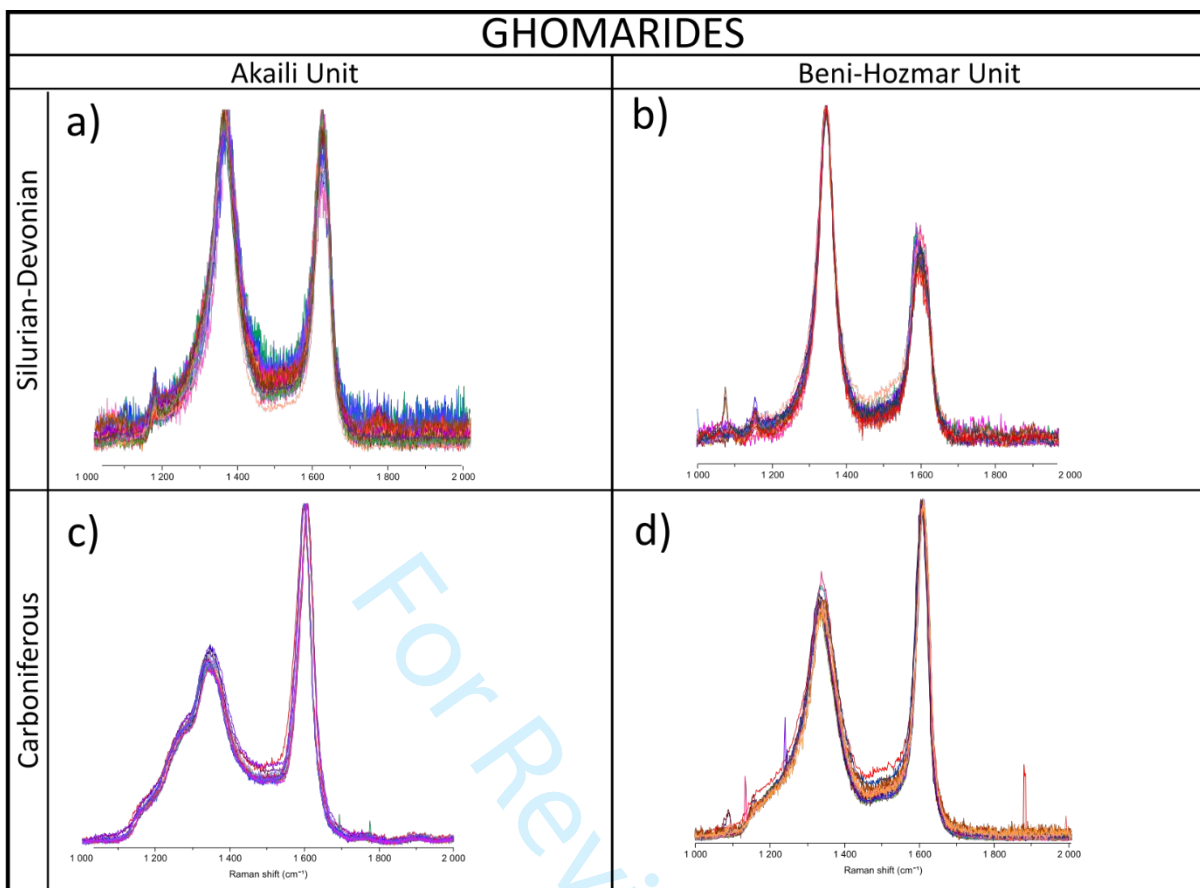


Figure 5 Differences between Carboniferous and pre- Carboniferous Raman spectra in the Akaili and Beni-Hozmar Units.

**Table 2.** TOC data and Raman derived temperatures for the analysed samples. \* Values in *Italic* represent R2 ratio according to *Beysac et alii, 2002* ; values in **bold** RA2 ratio according to *Lahfid et alii, 2010*.

Sample	Unit	TOC (%)	T°C mean (LÜNSDORF <i>et alii, 2014</i> )	std T°C	R2/RA2*	std R2/RA2*	T°C mean RA2/R2	std T°C	n° of spectra
Mar 8.1	Beni Mezala 1	0.4	n.d.	n.d.	n.d.	n.d.	n.d.	n.d.	n.d.
Mar 12.1	Beni Mezala 2	2	365.21	19.75	<i>0.62</i>	<i>0.03</i>	365.52	14.26	20
Mar 1.1	Tizgarine	0.7	324.62	17.39	<i>0.68</i>	<i>0.01</i>	337.87	6.80	20
Mar 1.2	Tizgarine	0.8	325.64	16.66	<i>0.66</i>	<i>0.04</i>	332.19	10.31	22
Mar 10.1	Akaili	0.7	298.11	15.39	<b>1.62</b>	<b>0.07</b>	300.91	15.97	32
Mar 9.1	Akaili	0.8	197.00	13.72	<b>0.89</b>	<b>0.13</b>	195.22	29.35	21
Mar 6.1	Akaili	0.4	299.35	21.91	<b>1.60</b>	<b>0.05</b>	296.57	11.13	32
Mar 5.1	Beni Hozmar	0.6	372.24	12.20	<i>0.65</i>	<i>0.03</i>	352.80	12.43	33
Mar 3.1	Beni Hozmar	1.6	285.76	10.95	<b>1.57</b>	<b>0.08</b>	288.57	18.49	27
Mar 4.1	Beni Hozmar	0.4	368.54	15.52	<i>0.64</i>	<i>0.02</i>	356.30	11.01	28
Mar 14.1	Akaili	1.5	246.55	8.93	<b>1.14</b>	<b>0.14</b>	246.86	30.96	21
Mar 15.1	Akaili	1.9	295.71	18.98	<b>1.64</b>	<b>0.08</b>	304.79	18.87	35
Mar 17.1	Akaili	0.7	368.27	9.38	<i>0.65</i>	<i>0.03</i>	380.84	8.02	22
Mar 18.1	Akaili	3.9	342.46	15.28	<i>0.66</i>	<i>0.03</i>	347.64	11.70	24
Mar 19.1	Akaili	1.2	442.23	13.16	<i>0.64</i>	<i>0.03</i>	446.34	7.67	22
Mar 20.1	Filalì	0.7	488.07	5.71	<i>0.36</i>	<i>0.06</i>	486.15	6.67	14

## 6. Discussion

### 6.1 RSCM temperatures

The RSCM geothermometer is one of the most used methods to assess the peak temperatures reached during prograde metamorphism (see HENRY *et alii*, 2019 for a complete review). It is based on the variation of the Raman spectrum of graphitic carbon at increasing temperatures, detected by curve-fit derived parameters (PASTERIS & WOPENKA, 1991). Different correlations between Raman parameters and temperatures have

1  
2  
3 been proposed depending on the fitting approach and the metamorphic types and degree (BEYSSAC *et alii*,  
4 2002; AOYA *et alii*, 2010; LAHFID *et alii*, 2010; LÜNSDORF *et alii*, 2017; MORI *et alii*, 2017; HENRY *et alii*, 2019;  
5 2002; AOYA *et alii*, 2010; LAHFID *et alii*, 2010; LÜNSDORF *et alii*, 2017; MORI *et alii*, 2017; HENRY *et alii*, 2019;  
6 2002; AOYA *et alii*, 2010; LAHFID *et alii*, 2010; LÜNSDORF *et alii*, 2017; MORI *et alii*, 2017; HENRY *et alii*, 2019;  
7 LI *et alii*, 2020). Among them the most used are those of BEYSSAC *et alii* (2002) and LAHFID *et alii* (2010),  
8 based on the R2 and RA2 parameters for high and low-grade metamorphism, respectively. At the highest-  
9 based on the R2 and RA2 parameters for high and low-grade metamorphism, respectively. At the highest-  
10 grades, CM spectrum is composed by one band in pure graphite and by four bands at about 330°C (BEYSSAC  
11 *et alii*, 2002), while in the interval between 200 and 320°C it can be adequately fitted with five Lorentzian  
12 bands (LAHFID *et alii*, 2010). While this fitting approach has been successfully applied in a number of studies  
13 (BEYSSAC *et alii*, 2004, 2019; NEGRO *et alii*, 2006; GALY *et alii*, 2008; DELCHINI *et alii*, 2016; COCHELIN *et alii*,  
14 2018; LAHFID *et alii*, 2019, among others) it has been demonstrated that the parameters calculation can be  
15 strongly influenced by the operator fitting approach (LÜNSDORF *et alii*, 2014). For this reason an automatic  
16 method has been proposed by LÜNSDORF & LÜNSDORF (2016) to provide higher comparability to the RSCM  
17 geothermometer.  
18 geothermometer.

19 In this work, the automatic approach of LÜNSDORF & LÜNSDORF (2016) is particularly suitable since many  
20 samples lie in the paleo-temperature range between 300 and 350°C (Tab. 2). This is the interval where the  
21 two geothermometers by BEYSSAC *et alii* (2002) and LAHFID *et alii* (2010) overlap and the choice of a bad  
22 fitting approach can lead to paleo-temperatures misinterpretation. Nevertheless, in order to constrain as  
23 much as possible our thermal data and avoid errors that can derived from the automatic processing of some  
24 spectra with low signal-to-noise ratio (Fig. 5), the RSCM temperatures derived with the IFORS software have  
25 been double checked by calculating the R2 or RA2 ratio and derived paleo-temperatures. Results shown in  
26 Table 2 indicate that maximum differences reached 20°C only in sample 3.1 and that they are lower than  
27 10°C in most of the dataset. This evidence indicate a general agreement in paleo-temperature results  
28 considering that the error of the RSCM methods is always comprised between 40-50°C (BEYSSAC *et alii*,  
29 2002); LAHFID *et alii*, 2010; LÜNSDORF & LÜNSDORF, 2016).

30 The approach based on a comparative between two fitting procedures strengthen the quality of the data  
31 presented in this work and further confirms the validity of the IFORS software.  
32 presented in this work and further confirms the validity of the IFORS software.  
33 presented in this work and further confirms the validity of the IFORS software.  
34 presented in this work and further confirms the validity of the IFORS software.  
35 presented in this work and further confirms the validity of the IFORS software.  
36 presented in this work and further confirms the validity of the IFORS software.  
37 presented in this work and further confirms the validity of the IFORS software.  
38 presented in this work and further confirms the validity of the IFORS software.  
39 presented in this work and further confirms the validity of the IFORS software.  
40 presented in this work and further confirms the validity of the IFORS software.  
41 presented in this work and further confirms the validity of the IFORS software.  
42 presented in this work and further confirms the validity of the IFORS software.  
43 presented in this work and further confirms the validity of the IFORS software.  
44 presented in this work and further confirms the validity of the IFORS software.  
45 presented in this work and further confirms the validity of the IFORS software.  
46 presented in this work and further confirms the validity of the IFORS software.  
47 presented in this work and further confirms the validity of the IFORS software.  
48 presented in this work and further confirms the validity of the IFORS software.  
49 presented in this work and further confirms the validity of the IFORS software.  
50 presented in this work and further confirms the validity of the IFORS software.  
51 presented in this work and further confirms the validity of the IFORS software.  
52 presented in this work and further confirms the validity of the IFORS software.  
53 presented in this work and further confirms the validity of the IFORS software.  
54 presented in this work and further confirms the validity of the IFORS software.  
55 presented in this work and further confirms the validity of the IFORS software.  
56 presented in this work and further confirms the validity of the IFORS software.  
57 presented in this work and further confirms the validity of the IFORS software.  
58 presented in this work and further confirms the validity of the IFORS software.  
59 presented in this work and further confirms the validity of the IFORS software.  
60 presented in this work and further confirms the validity of the IFORS software.

## 6.2 Thermal evolution of the Rif and comparison with previous works

The Rif-Betic orogen is a key area in the Mediterranean puzzle to decipher the western Mediterranean geodynamic evolution (ROYDEN & FACCENNA, 2018 for a review) and it offers the opportunity to study both exhumed root of the Alpine orogen (e.g. Sebides) and terranes derived from the fragmented Variscan chain (e.g. Ghomarides).

The metamorphic evolution of the internal units of the Rif-Betic orogen has been the subject of detailed studies focused on the outcrops of Beni Mzala antiform and around the Beni Bousera peridotite (KORNPROBST, 1974; DURAND-DELGA, 1980; CHALOUAN AND MICHARD, 1990; MICHARD *et alii*, 2006; NEGRO *et alii*, 2006; CHALOUAN *et alii*, 2008; PLATT *et alii*, 2013, MARRONE *et alii*, 2021).

In the Federico Unit, cropping out at the core of the Beni Mzala antiform, paleo-temperatures derived from the analyses of carbonaceous material were not present in literature given the moderate-to-low TOC content (NEGRO *et alii*, 2006 and Table 2). Despite this, we were able to carry out enough CM spectra whose RSCM geothermometer shows values of about 320°C in the Tizgarine Unit and of about 365°C in BM 2 one. Data from Tizgarine Unit suggest that it suffered slightly warmer conditions than those calculated by the cookeite-pyrophyllites-phengite association (about 300°C according to BOUYBAOUENE *et alii*, 1998). On the other hand, the average temperature calculated for BM2, even if slightly lower, seem to confirm the minimum temperatures of 380°C provided by the presence of relict Mg-Carpholite estimated by BOUYBAOUENE *et alii*, (1998) rather than those of 450°C calculated by VIDAL *et alii* (1999) by means of Chl-Cld thermometer. Results for the BM2 should be considered only as a first approximation, since we were able to derive Raman maximum temperature only on one sample and therefore need to be further validated in the future.

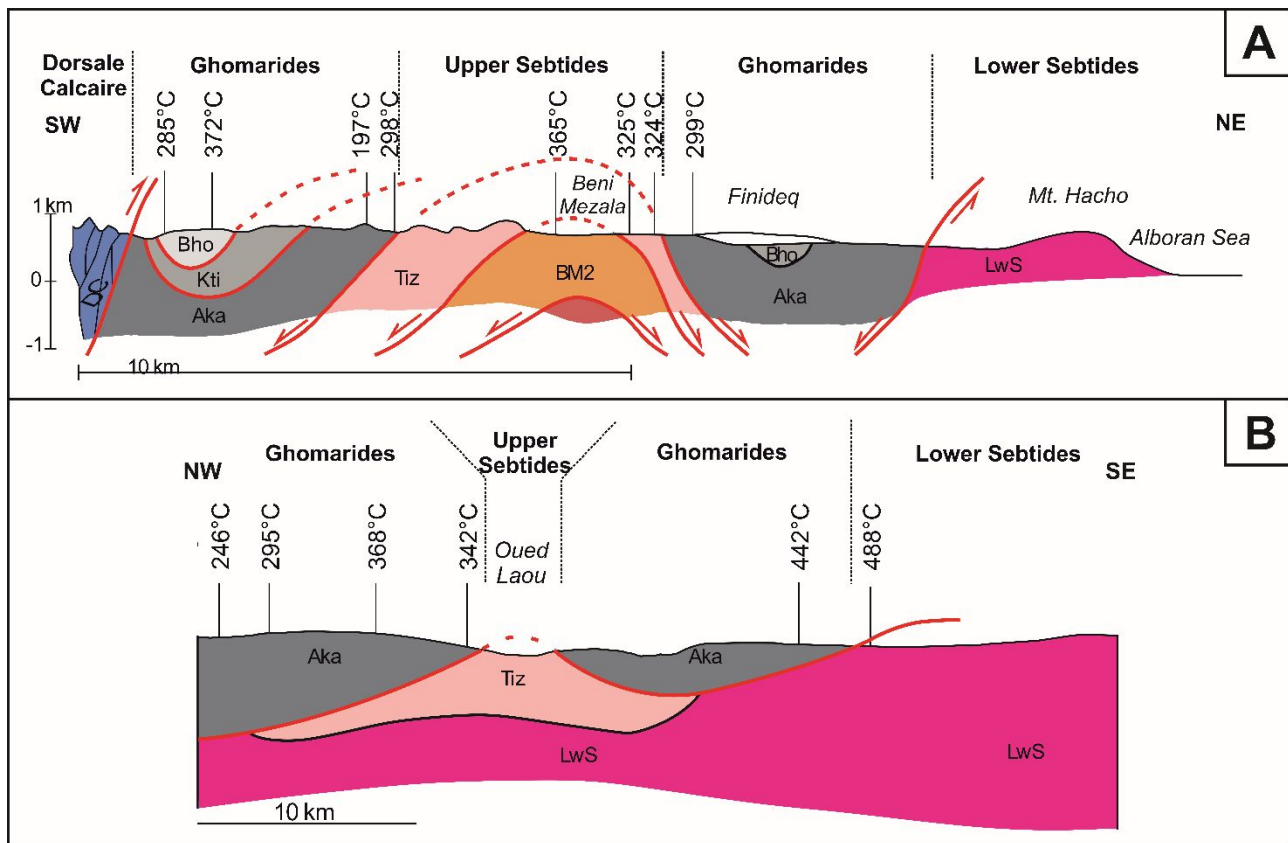


**Figure 6** Raman-derived temperatures plotted on cross-sections 1 and 2 located in Fig. 1. Redrawn and modified after NEGRO *et alii*, 2006 and CHALOUAN *et alii*, 2008. Temperature shown in the figure are derived from the IFORS software (LÜNSDORF & LÜNSDORF, 2016). For comparison with other RSCM approaches see Table 2 and section 6.1. Acronyms: DC – Dorsale Calcaire; BHo – Beni Hozmar; KTi – Koudiat Tiziane; Aka – Akaili; Tiz – Tizgarine; BM2 – Beni Mzala; Lws – Lower Sebides.

In the Ghomarides cropping out on the flanks of the Beni Mezala antiform, NEGRO *et alii* (2006) already provided Raman measurements on four samples from the Akaili Unit and on one sample from Koudiat Tiziane unit, suggesting temperature always below 330°C, as this is the lower calibration limit of the RSCM geothermometer based on R2 parameter proposed by BEYSSAC *et alii* (2002). This limit can now be overcome since new correlations at low metamorphism are now available in literature for low metamorphism (RAHL *et alii*, 2005; LAHFID *et alii*, 2010; LÜNSDORF *et alii*, 2017) and in diagenesis (SCHITO *et alii*, 2017; 2019; HENRY *et alii*, 2019) allowing to use the RSCM geothermometers in a variety of geological conditions (MUIRHEAD *et alii*, 2019; KEDAR *et alii*, 2020; NIRRENGARTEN *et alii*, 2020).

1  
2  
3 Our data on the Ghomarides in the northern sector of the Rif belt, outline a paleo-temperature jump between  
4 pre-Carboniferous and Carboniferous successions both in the Akaili and Beni Hozmar units. In detail, the  
5 maximum temperatures acquired during the Eo-Variscan phases by the pre-Carboniferous rocks are at the  
6 boundary between anchizone and epizone (about 300°C, FREY *et alii*, 1987) in the Akaili Unit and in the  
7 epizone (about 370°C) in the Beni-Hozmar (Table 2 and Fig. 7). On the contrary, Visean rocks in the Akaili  
8 Unit show values typical of deep diagenetic/low anchizone conditions (about 200°C) reached during the late  
9 Variscan phase, while temperatures in rocks with the same age are about 280°C in the Beni-Hozmar unit.  
10 Previous data from illite crystallinity (CHALOÛAN & MICHARD, 1985) also indicated lower metamorphism for  
11 Carboniferous rocks in the Ghomarides, but with no significant differences among their units (CHALOUAN &  
12 MICHARD, 1985; CHALOUAN & MICHARD, 1990). Thus our data show thus for the first time in detail the  
13 thermal structure across the Paleozoic Ghomarides, highlighting that the Beni-Hozmar Unit suffered  
14 metamorphism at higher temperatures with respect to the Akaili Unit both during Eo and Late Variscan  
15 events. It is particularly interestingly to note that almost the same gap in paleo-temperatures between 80  
16 and 100°C is recorded above and below the Variscan unconformity among the two units and this could  
17 suggest that they kept some similar structural relationship during both events.

18  
19 As matter of fact very little is known about the Variscan history of the Paleozoic units in the Ghomarides or in  
20 similar units in the Maghreb chain. In the Malaguides (southern Spain), the pre-Alpine deformation in  
21 Paleozoic rocks is very poorly constrained (MARTIN-ALGARRA *et alii*, 2009). HT/LP mineralogical assemblage,  
22 associated to paleo-temperatures of about 500°C were locally found in the lowermost Ordovician-Silurian  
23 rocks near the Ronda peridotite (RUIZ-CRUZ & GALÁN, 2002; RUIZ-CRUZ & NOVÁK, 2003; NEGRO *et alii*,  
24 2006), while clay mineralogical analyses (ABAD *et alii*, 2003) and CAI (Conodont Alteration Index)  
25 determination (MARTIN-ALGARRA *et alii*, 2009) failed to precisely detect variation at lower paleo-  
26 temperature and the whole Palaeozoic section is generally described to have suffered anchizone to epizone  
27 metamorphism. In both Greater and Lesser Kabylia (northern Algeria), similarly to the Ghomarides, MICHARD  
28 *et alii* (2006) describe a Late Devonian Eo-variscan phase that led to greenschists metamorphism and a Late-  
29 Variscan phase responsible for the folding of the unconformable Carboniferous deposits. These domains,  
30 together with the Calabria-Peloritan arc are thought to share a similar structural position in a western

1  
2  
3 (southwestern? RAUMER *et alii*, 2002) sector of the Paleotethys, rather than in the Rheic realm such as other  
4  
5 Variscan sectors in Iberia and Morocco ( i.e. Balearic, Iberian and Moroccan mesetas), and to suffered similar  
6  
7 metamorphisms (CHALOUAN & MICHARD, 1990; RAUMER *et alii*, 2002; MARTIN-ALGARRA *et alii*, 2009). This  
8  
9 hypothesis is mainly based on stratigraphic and structural affinities of the Paleozoic successions, even if at  
10  
11 low metamorphic degree the lack of a more comprehensive dataset hampers a full understanding. The RSCM  
12  
13 approach proposed in this work has shown to be promising. Thus it could be applied in similar areas and  
14  
15 provide evidence (or not) of a common metamorphic history of the Variscan terranes in the Mediterranean  
16  
17  
18  
19 area.  
20  
21  
22  
23  
24  
25  
26  
27  
28  
29  
30  
31  
32  
33  
34  
35  
36  
37  
38  
39  
40  
41  
42  
43  
44  
45  
46  
47  
48  
49  
50  
51  
52  
53  
54  
55  
56  
57  
58  
59  
60

For Review Only

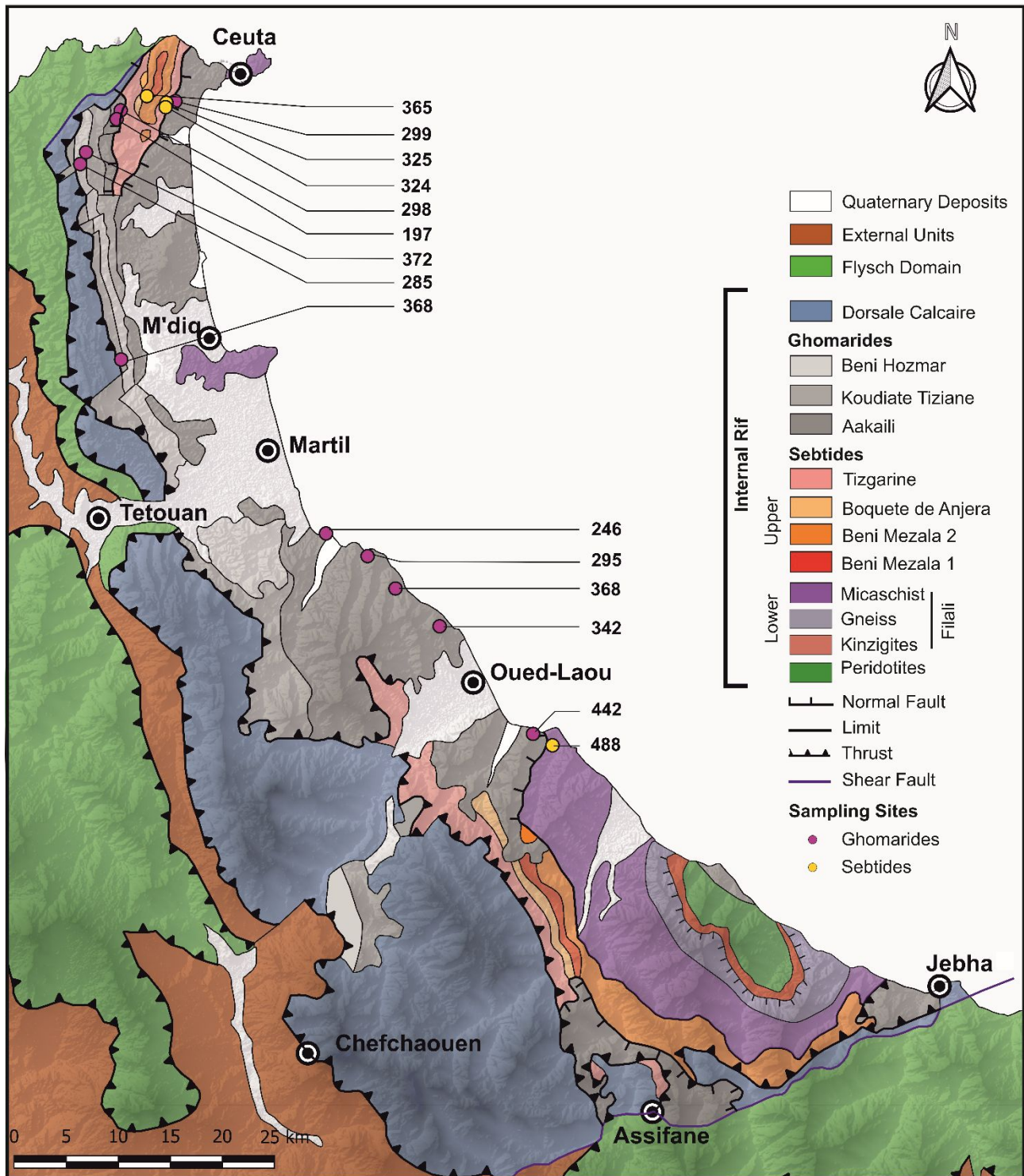


Figure 7. Geological map of internal Rif with indicated Raman-derived maximum paleo-temperatures. Temperature shown in the figure are derived from the IFORS software (LÜNSDORF & LÜNSDORF, 2016). For comparison with other RSCM approaches see Table 2 and section 6.1.



1  
2  
3 In the southern sector (Zone 2), samples were collected along the route from Ras Mazari to Cape Zaouia (Fig.  
4 7). The main contribution of this work was to unravel paleo-temperatures for the Devonian and  
5 Carboniferous rocks (samples 15.1 and 14.1) that were previously reported to be lower than 330°C by NEGRÒ  
6 *et alii* (2006). New data show a jump in paleo-temperature of about 50°C between Carboniferous and  
7 Devonian rocks moving from Ras Mazari to Tamrabete area south of Tetouan town (Fig. 7). This gap is lower  
8 than that observed in the northern sector for the Akaili unit. Moreover, the observation that paleo-  
9 temperatures of the pre-Carboniferous samples are similar, suggest that Carboniferous rocks here  
10 experienced higher thermal stress probably due to a Late Oligocene (Early Miocene?) thermal event that  
11 affected the area (see discussion below).

12  
13  
14  
15  
16  
17  
18  
19  
20  
21  
22  
23 As matter of fact, MICHARD *et alii*. (2006) showed in this area that K/Ar on white mica isotopic ages tend to  
24 increase moving from the Ghomaride–Sebtide tectonic contact (Zaouia Fault, 25My) to the Ras Mazari area  
25 where the apparent ages are of about 183 My. This age distribution, coupled with the increase of Raman  
26 temperature from Ras Mazari to the Zaouia Fault (Fig. 8 from NEGRÒ *et alii*, 2006) has been interpreted as a  
27 thermal event connected to the emplacement of the Beni-Boussera peridotites. Nevertheless, recent works  
28 recently questioned the hypothesis of “hot” exhumation of the Rif–Betic peridotites during the Alpine  
29 orogeny (ROSSETTI *et alii*, 2020; FARAH *et alii*, 2021). By means of geochronological data on the migmatitic  
30 rocks that form the envelopment of the Beni Bousera peridotite, ROSSETTI *et alii*, (2020) point out a main  
31 Hercynian thermal event, associated with intra-crustal emplacement of the peridotite, occurred and was  
32 followed by cooling and exhumation from deep to shallower crustal conditions. The final stage of exhumation  
33 is constrained by the authors to the Early Miocene and is coeval with the main stage of the Alboran basin  
34 back-arc extension. At this time, the westward retreat of the Tethyan subduction caused lithosphere  
35 delamination and asthenosphere upwelling that led to crustal partial melting and diffuse magmatism as  
36 outlined by the andalusite-bearing dykes that intruded the Beni Bousera units (ROSSETTI *et alii*, 2013). All  
37 these pieces of evidence suggest that the thermal gradient depicted by Raman data in the present work and  
38 in NEGRÒ *et alii* (2006), as well as the thermal reset of the K/Ar on white mica isotopic ages (MICHARD *et alii*,  
39 2006), related to an Alpine HT metamorphic event that is independent from the peridotite emplacement.  
40  
41  
42  
43  
44  
45  
46  
47  
48  
49  
50  
51  
52  
53  
54  
55  
56  
57  
58  
59  
60  
Given this, our data show some differences with respect to the paleo-temperature pattern provided by

1  
2  
3 NEGRÒ *et alii* (2006). This can be observed, particularly, in the area between Ras Mazari and R Mekkad, where  
4  
5 paleo-temperatures estimations differ for more than 100°C (Fig. 7). Considering that we followed the  
6  
7 analytical procedure for Raman spectra acquisition by BEYSSAC *et alii* (2002), a possible source of error could  
8  
9 be envisaged in different fitting methods. However, in our case, the paleo-temperatures from R2 shown in  
10  
11 Tab. 2 show a very good agreement with those calculated with the IFORS software, strengthening our  
12  
13 results. The fitting procedure or the user interpretation could in part justify differences observed among  
14  
15 similar spectra as shown in Fig. 7b (comparison spectra at 442-485°C and 488-508°C), but cannot be held  
16  
17 responsible for spectra related to samples near Tamkerte, which show very different features. In this case,  
18  
19 the differences are due to different heating conditions (Fig. 8b). Working with organic matter, differences in  
20  
21 thermal maturity (maximum paleo-temperature) can be usually ascribed to the presence of reworked  
22  
23 material (LACZO & JAMBOR, 1988; LUCCA *et alii*, 2018; QIN *et alii*, 2018; BALESTRA *et alii*, 2019), but this does  
24  
25 not seem to be the case, since spectra in our samples are very homogeneous. This piece of evidence suggests  
26  
27 that paleo-temperatures in this sector of the Ghomarides, has higher spread than previously assessed. One  
28  
29 possible explanation for this spread could be the effect of localized shear/strain (KITAMURA *et alii*, 2012;  
30  
31 KUO *et alii*, 2014, 2017; KEDAR *et alii*, 2020) that could have locally increased the thermal stress. Moreover,  
32  
33 as shown by MÜNCH *et alii*. (2021) in the area near Ceuta town, the internal zone of the Rif chain has been  
34  
35 dissected by E-W and NNW-SSE normal faults between about 18 and 11 My and this can explain why a regular  
36  
37 trend of increasing paleo-temperatures from Ras Mazari to Cape Zaouia has not been detected (Fig. 8).  
38  
39  
40  
41  
42  
43  
44  
45  
46  
47  
48  
49  
50  
51  
52  
53  
54  
55  
56  
57  
58  
59  
60

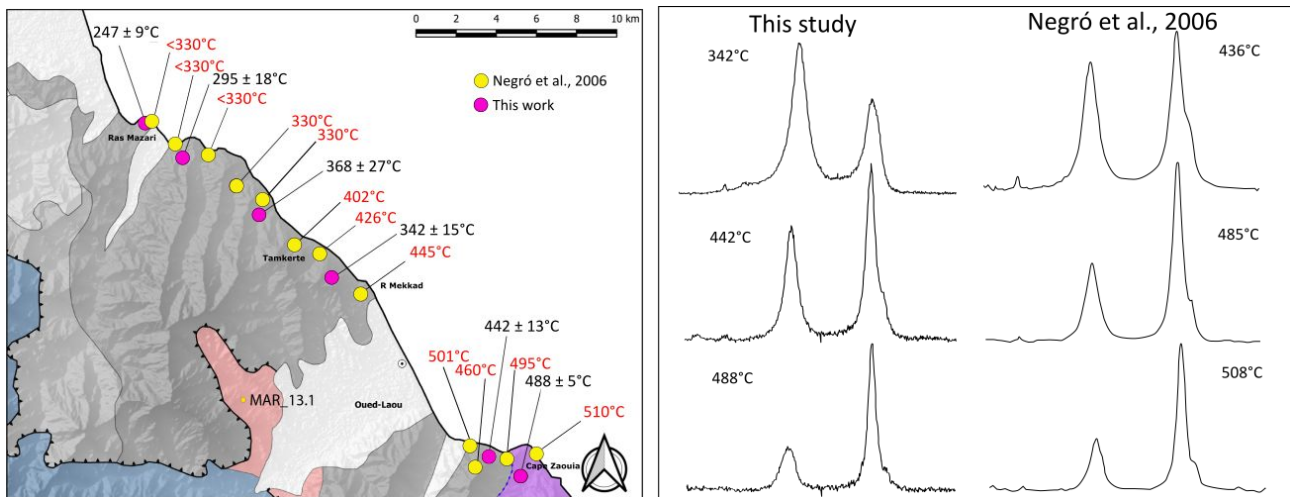


Figure 8 a) Raman paleo- temperatures from this work and from NEGRO *et alii.* (2006), plotted in zone 2 for comparison. b) Comparison between Raman spectra and related paleo-temperatures from this work and NEGRO *et alii.* (2006). Spectra on the same row correspond to samples from the same sampling area. Paleo-temperature shown in the figure are derived from the IFORS software (LÜNSDORF & LÜNSDORF, 2016). For comparison with other RSCM approaches see Table 2 and section 6.1.

## Conclusion

In this work we implemented the paleo-thermal database of the Internal Rif in Morocco providing a new set of data in the Sebtide and Ghomaride successions through Raman spectroscopy on dispersed organic matter. In the upper Sebtides cropping out in the Beni Mezala antiform we show that Tizgarine and BM 2 Units experienced maximum paleo-temperature of about 320 and 370°C, respectively. In the same area, data from Ghomarides show a temperature jump across the Eo-Variscan unconformity in both Akaili and Beni Hozmar Units. Interestingly, our data also indicate higher paleo-temperatures in Beni Hozmar suggesting higher metamorphic conditions suffered by this unit.

In the southern area between Ras Mazari and Cape Zaouia, samples collected from the Akaili Unit show increasing paleo-temperatures moving towards the tectonic contact with the Filali Unit connected with a Late Oligocene high temperature metamorphic event and not related to emplacement of the Beni-Bousera peridotite.

## Acknowledgments

We are greatly indebted with M.N. Zaghloul for fruitful discussions and for introduce us to Rif geology. We kindly acknowledge the Editor in chief Federico Rossetti, the associated editor Giulio Viola and two anonymous reviewers for their constructive criticisms that improved the original version of this paper.

## References

- ABAD I., NIETO F., PEACOR D.R. AND VELILLA N. (2003) - *Prograde and retrograde diagenetic and metamorphic evolution in metapelitic rocks of Sierra Espuna (Spain)*. Clay Minerals, **38**, 1–23.
- AOYA M. KOUKETSU Y., ENDO S., SHIMIZU H., MIZUKAMI T., NAKAMURA D., WALLIS S. (2010) - *Extending the applicability of the Raman carbonaceous-material geothermometer using data from contact metamorphic rocks*. Journal of Metamorphic Geology, **28**, 895–914,
- ATOUBAT A., CORRADO S., SCHITO A., HAISSAN F., GIMENO-VIVES O., MOHN G.,FRIZON DE LAMOTTE D. (2020) - *Validating Structural Styles in the Flysch Basin Northern Rif (Morocco) by Means of Thermal Modeling*. Geosciences, **10**, 325.
- AZDIMOUSA A., BOURGOIS J., POUPEAU G., VÁZQUEZ M., ASEBRIY L. ,LABRIN E. (2014) - *Fission track thermochronology of the Beni Bousera peridotite massif (Internal Rif, Morocco) and the exhumation of ultramafic rocks in the Gibraltar Arc*. Arabian Journal of Geosciences, **7**, 1993–2005.
- BALESTRA M., CORRADO S., ALDEGA L., MORTICELLI M.G., SULLI A., RUDKIEWICZ J.-L.,SASSI W. (2019) - *Thermal and structural modeling of the Scillato wedge-top basin source-to-sink system: Insights into the Sicilian fold-and-thrust belt evolution (Italy)*. GSA Bulletin, **131**, 1763–1782.
- BEYSSAC O., GOFFÉ B., CHOPIN C., ROUZAUD J. N. (2002). *Raman spectra of carbonaceous material in metasediments: a new geothermometer*. Journal of Metamorphic Geology, **20**(9), 859-871.
- BEYSSAC O., BOLLINGER L., AVOUAC J.P., GOFFÉ B. (2004) - *Thermal metamorphism in the lesser Himalaya of Nepal*

- 1  
2  
3 *determined from Raman spectroscopy of carbonaceous material. Earth and Planetary Science Letters,*  
4  
5 **225**, 233–241
- 6  
7 BEYSSAC O., PATTISON D.R.M., BOURDELLE F. (2019) - *Contrasting degrees of recrystallization of*  
8  
9 *carbonaceous material in the Nelson aureole, British Columbia and Ballachulish aureole, Scotland, with*  
10  
11 *implications for thermometry based on Raman spectroscopy of carbonaceous material. Journal of*  
12  
13 *Metamorphic Geology*, **37**, 71–95.
- 14  
15  
16 BOOTH-REA G., RANERO C.R., MARTÍNEZ-MARTÍNEZ J.M., GREVEMEYER I. (2007) - *Crustal types and Tertiary*  
17  
18 *tectonic evolution of the Alborán sea, western Mediterranean. Geochemistry, Geophysics, Geosystems,*  
19  
20 **8**(10).
- 21  
22  
23 BOUILLIN J. (1986) - *Le "bassin maghrebin"; une ancienne limite entre l'Europe et l'Afrique à l'ouest des Alpes.*  
24  
25 *Bulletin de la Société Géologique de France*, **2**, 547–558.
- 26  
27  
28 BOUYBAOUENE M., MICHARD A., GOFFE B. (1998) - *High-pressure granulites on top of the Beni Bousera*  
29  
30 *peridotites, Rif Belt, Morocco; a record of an ancient thickened crust in the Alboran Domain. Bulletin de*  
31  
32 *la Société Géologique de France*, **169**, 153–162.
- 33  
34  
35 CALVO M., CUEVAS J., TUBIA J.M. (2001) - *Preliminary palaeomagnetic results on Oligocene–early Miocene*  
36  
37 *mafic dykes from southern Spain. Tectonophysics*, **332**, 333–345.
- 38  
39  
40 CASTIGLIONI C., MAPELLI C., NEGRI F., ZERBI G. (2001) - *Origin of the D line in the Raman spectrum of graphite:*  
41  
42 *A study based on Raman frequencies and intensities of polycyclic aromatic hydrocarbon molecules.*  
43  
44 *Journal of Chemical Physics*, **114**, 963–974.
- 45  
46  
47 CHALOUAN A. (1986). *Les nappes Ghomarides (Rif septentrional, Maroc), un terrain varisque dans la chaîne*  
48  
49 *alpine. Thèse de doctorat Université Louis Pasteur (Strasbourg). Vol 1, 333 p.*
- 50  
51  
52 CHALOUAN A. & MICHARD A. (1990) - *The Ghomarides nappes, Rif coastal range, Morocco: a variscan chip in*  
53  
54 *the Alpine belt. Tectonics*, **9**, 1565–1583.
- 55  
56  
57 CHALOUAN A. & MICHARD A. (2004) - *The Alpine Rif Belt (Morocco): a case of mountain building in a*  
58  
59 *subduction-subduction-transform fault triple junction. Pure and Applied Geophysics*, **161**, 489–519.
- 60  
61  
62 CHALOUAN A., MICHARD A., EL KADIRI K., NEGRO F., FRIZON DE LAMOTTE D., SOTO J.-I., SADDIQUI O. (2008)-  
63  
64 *The Rif belt. In: Michard, A. (Ed.), The Geology of Morocco. Springer, Berlin*, **116**, 203–302,

1  
2  
3  
4  
5  
6  
7  
8  
9  
10  
11  
12  
13  
14  
15  
16  
17  
18  
19  
20  
21  
22  
23  
24  
25  
26  
27  
28  
29  
30  
31  
32  
33  
34  
35  
36  
37  
38  
39  
40  
41  
42  
43  
44  
45  
46  
47  
48  
49  
50  
51  
52  
53  
54  
55  
56  
57  
58  
59  
60

- CHALOUAN A. & MICHARD A. (1985) - *Age anté-Viséen de la phase varisque paroxysmale dans les nappes ghomarides du Rif interne (Maroc)/Pre-Visean age of the main Variscan folding in the Ghomarides nappes, Inner Rif, Morocco*. Sciences Géologiques, Bulletins et Mémoires, **38**, 165–174.
- COCHELIN B., LEMIRRE B., DENÈLE Y., DE SAINT BLANQUAT M., LAHFID A., DUCHÊNE S. (2018) - *Structural inheritance in the central pyrenees: The variscan to Alpine tectonometamorphic evolution of the Axial Zone*. Journal of the Geological Society, **175**, 336–351.
- DELCHINI S., LAHFID A., PLUNDER A., MICHARD A. (2016) - *Applicability of the RSCM geothermometry approach in a complex tectono-metamorphic context: The Jebilet massif case study (Variscan Belt, Morocco)*. Lithos, **256**, 1–12.
- DI DONATO E., TOMMASINI M., FUSTELLA G., BRAMBILLA L., CASTIGLIONI C., ZERBI G., SIMPSON C.D., MÜLLEN K., NEGRI F. (2004) - *Wavelength-dependent Raman activity of D2h symmetry polycyclic aromatic hydrocarbons in the D-band and acoustic phonon regions*. Chemical Physics, **301**, 81–93.
- DIDON J., DURAND-DELGA M., KORNPORST J. (1973) - *Homologies géologiques entre les deux rives du détroit de Gibraltar*. Bulletin de la Société Géologique de France, **7**, 77–105.
- DOCHERTYC. & BANDA E. (1995) - *Evidence for the eastward migration of the Alboran Sea based on regional subsidence analysis: a case for basin formation by delamination of the subcrustal lithosphere?* Tectonics, **14**, 804–818.
- DUCOUX M., JOLIVET L., CALLOT J. P., AUBOURG C., MASINI E., LAHFID A., HOMMONNAY E., CAGNARD F., GUMIAUX C., BAUDIN T. (2019) - *The Nappe des Marbres Unit of the Basque-Cantabrian Basin: The Tectono-thermal Evolution of a Fossil Hyperextended Rift Basin*. Tectonics, **38**, 3881–3915.
- DURAND-DELGA M. (1980) - *Le cadre structural de la Méditerranée occidentale*. Geologie des chaines alpines issues de la Tethys, BRGM ed., Orleans, pp. 67–85.
- DURAND-DELGA M. & OLIVIER P. (1988) - *Evolution of the Alboran block margin from Early Mesozoic to Early Miocene time*. In: The Atlas System of Morocco. Springer, Berlin, pp. 463–480.
- EL KADIRI K., LINARES A., OLORIZ F. (1992) - *La Dorsale calcaire rifaine (Maroc septentrional): Evolution stratigraphique et géodynamique durant le Jurassique-Crétacé*. Notes et mémoires du Service géologique, 217–265.

- 1  
2  
3 FARAH A., MICHARD A., SADDIQI O., CHALOUAN A., CHOPIN C. (2021) - *The Beni Bousera marbles, record of*  
4  
5 *a Triassic-Early Jurassic hyperextended margin in the Alpujarrides-Sebtides units (Rif belt)*, BSGF - Earth  
6  
7 Sciences Bulletin, **192**(1), 26.  
8  
9  
10 FAVRE P. & STAMPFLI G.M. (1992) - *From rifting to passive margin: the examples of the Red Sea, Central*  
11  
12 *Atlantic and Alpine Tethys*. Tectonophysics, **215**, 69–97.  
13  
14 FRIZON DE LAMOTTE D., RAULIN C., MOUCHOT N., WROBEL-DAVEAU J., BLANPIED C., RINGENBACH J. (2011)  
15  
16 - *The southernmost margin of the Tethys realm during the Mesozoic and Cenozoic: Initial geometry and*  
17  
18 *timing of the inversion processes*. Tectonics, **30**(3), TC3002.  
19  
20  
21 GALY V., BEYSSAC O., FRANCE-LANORD C., EGLINTON T. (2008) - *Recycling of graphite during Himalayan*  
22  
23 *erosion: A geological stabilization of carbon in the crust*. Science, **322**, 943–945.  
24  
25  
26 GARCÍA-DUEÑAS V., BALANYÁ J.C., MARTÍNEZ-MARTÍNEZ J.M. (1992) - *Miocene extensional detachments in*  
27  
28 *the outcropping basement of the northern Alboran basin (Betics) and their tectonic implications*. Geo-  
29  
30 Marine Letters, **12**, 88–95.  
31  
32  
33 GIMENO-VIVES O., FRIZON DE LAMOTTE D., LEPRÊTRE R., HAISSSEN F., ATOUABAT A., MOHN G. (2020) - *The*  
34  
35 *structure of the Central-Eastern External Rif (Morocco); Poly-phased deformation and role of the under-*  
36  
37 *thrusting of the North-West African paleo-margin*. Earth-Science Reviews, 103198.  
38  
39  
40 GIMENO-VIVES O., MOHN G., BOSSE V., HAISSSEN F., ZAGHLOUL M.N., ATOUABAT A., FRIZON DE LAMOTTE D.  
41  
42 (2019) - *The Mesozoic margin of the Maghrebian Tethys in the Rif belt (Morocco): Evidence for polyphase*  
43  
44 *rifting and related magmatic activity*. Tectonics, **38**, 2894–2918.  
45  
46  
47 GUEDES A., VALENTIM B., PRIETO A.C., RODRIGUES S., NORONHA F. (2010) - *Micro-Raman spectroscopy of*  
48  
49 *collotelinite, fusinite and macrinite*. International Journal of Coal Geology, **83**, 415–422.  
50  
51  
52 GUERRERA F., MARTÍN-ALGARRA A., PERRONE V. (1993) - *Late Oligocene-Miocene syn-/late-orogenic*  
53  
54 *successions in western and central Mediterranean chains from the Betic Cordillera to the southern*  
55  
56 *Apennines*. Terra Nova, **5**, 525–544.  
57  
58  
59 GUERRERA F., MARTÍN-MARTÍN M., PERRONE V., TRAMONTANA M. (2005) - *Tectono-sedimentary evolution*  
60  
*of the southern branch of the Western Tethys (Maghrebian Flysch Basin and Lucanian Ocean):*  
*consequences for Western Mediterranean geodynamics*. Terra Nova, **17**, 358–367.

- 1  
2  
3 GUEYDAN F., PITRA P., AFIRI A., POUJOL M., ESSAIFI A., PAQUETTE J. (2015). *Oligo-Miocene thinning of the*  
4 *Beni Bousera peridotites and their Variscan crustal host rocks, Internal Rif, Morocco*. *Tectonics*, **34**,  
5 1244–1268.  
6  
7  
8  
9  
10 HENRY D.G., JARVIS I., GILLMORE G., STEPHENSON M., EMMINGS J.F. (2018) - *Assessing low-maturity organic*  
11 *matter in shales using Raman spectroscopy: Effects of sample preparation and operating procedure*.  
12 *International Journal of Coal Geology*, **191**, 135–151.  
13  
14  
15  
16 HENRY D.G., JARVIS I., GILLMORE G., STEPHENSON M. (2019) - *Raman spectroscopy as a tool to determine*  
17 *the thermal maturity of organic matter: Application to sedimentary, metamorphic and structural*  
18 *geology*. *Earth-Science Reviews*, **198**, 102936.  
19  
20  
21  
22  
23 KEDAR L., BOND C.E., MUIRHEAD D. (2020). *Carbon ordering in an aseismic shear zone: Implications for*  
24 *Raman geothermometry and strain tracking*. *Earth and Planetary Science Letters*, **549**, 116536.  
25  
26  
27  
28 KITAMURA M., MUKOYOSHI H., FULTON P.M., HIROSE T. (2012) - *Coal maturation by frictional heat during*  
29 *rapid fault slip*. *Geophysical research letters*, **39**, L16302.  
30  
31  
32  
33 KORNPROBST J. (1974) - *Contribution h l' Ctude petrographique et structurale de la zone interne du Rif (Maroc*  
34 *Septentrional)*. *Notes et Memoirs de la Service Geologique de Maroc*, 251, 256 pp.  
35  
36  
37 KUO L.W., LI H., SMITH S.A.F., DI TORO G., SUPPE J., SONG S.R., NEILSEN S., SHEU H.S., SI J. (2014) - *Gouge*  
38 *graphitization and dynamic fault weakening during the 2008 Mw 7.9 Wenchuan earthquake*. *Geology*,  
39 **42**, 47–50.  
40  
41  
42  
43 KUO L.W., DI FELICE, F., SPAGNOLO E., DI TORO G., SONG S.R., ARETUSINI S., LI H., SUPPE J., SI J., WEN C.Y.  
44 (2017) - *Fault gouge graphitization as evidence of past seismic slip*. *Geology*, **45**, 979–982.  
45  
46  
47  
48 LACZO I. & JAMBOR A. (1988) - *Secondary Heating of Vitrinite: Some Geological Implications*. in *The*  
49 *Pannonian Basin: A Study in Basin Evolution*. AAPG Special Volumes. **M45**, 311-318.  
50  
51  
52 LAHFID A., BEYSSAC O., DEVILLE E., NEGRO F., CHOPIN C., GOFFÉ B. (2010) - *Evolution of the Raman spectrum*  
53 *of carbonaceous material in low-grade metasediments of the Glarus Alps (Switzerland)*. *Terra Nova*, **22**,  
54 354–360.  
55  
56  
57  
58 LAHFID A., BAIDDER L., OUANAIMI H., SOULAIMANI A., HOEPFFNER C., FARAH A., SADDIQUI O., MICHARD A.  
59 (2019) - *From extension to compression: high geothermal gradient during the earliest Variscan phase of*  
60



- 1  
2  
3 *the Moroccan Meseta; a first structural and RSCM thermometric study*. European Journal of Mineralogy,  
4  
5 **31**, 695–713.  
6  
7  
8 LEBLANC D. (1979) - *Étude Géologique Du Rif Externe Oriental Au Nord de Taza (Maroc)*. Éditions du Service  
9  
10 géologique du Maroc, **281**, 293 pp.  
11  
12 LEPRÊTRE R., FRIZON DE LAMOTTE D., COMBIER V., GIMENO-VIVES O., MOHN G., ESCHARD R. (2018) - *The*  
13  
14 *Tell-Rif orogenic system (Morocco, Algeria, Tunisia) and the structural heritage of the southern Tethys*  
15  
16 *margin*. BSGF-Earth Sciences Bulletin, **189**(2), 10.  
17  
18  
19 LI C.Z. (2007) - *Some recent advances in the understanding of the pyrolysis and gasification behaviour of*  
20  
21 *Victorian brown coal*. Fuel, **86**, 1664–1683.  
22  
23  
24 LI K., RIMMER S.M., PRESSWOOD S.M., LIU Q. (2020) - *Raman spectroscopy of intruded coals from the Illinois*  
25  
26 *Basin: Correlation with rank and estimated alteration temperature*. International Journal of Coal  
27  
28 Geology, **219**, 103369.  
29  
30  
31 LUCCA A., STORTI F., MOLLI G., MUCHEZ P., SCHITO A., ARTONI A., BALSAMO F., CORRADO S., SALVIOLI-  
32  
33 MARIANI E. (2018) - *Seismically enhanced hydrothermal plume advection through the process zone of*  
34  
35 *the Compione extensional Fault, Northern Apennines, Italy*. Bulletin of the Geological Society of America,  
36  
37 **131**, 547–571.  
38  
39  
40 LÜNSDORF N.K. (2016) - *Raman spectroscopy of dispersed vitrinite - Methodical aspects and correlation with*  
41  
42 *reflectance*. International Journal of Coal Geology, **153**, 75–86.  
43  
44  
45 LÜNSDORF N.K. & LÜNSDORF J.O. (2016) - *Evaluating Raman spectra of carbonaceous matter by automated,*  
46  
47 *iterative curve-fitting*. International Journal of Coal Geology, **160**, 51–62.  
48  
49  
50 LÜNSDORF N.K., DUNKL I., SCHMIDT B.C., RANTITSCH G., VON EYNATTEN H. (2014) - *Towards a higher*  
51  
52 *comparability of geothermometric data obtained by Raman spectroscopy of carbonaceous material.*  
53  
54 *Part I: evaluation of biasing factors*. Geostandards and Geoanalytical Research, **38**, 73–94.  
55  
56  
57 LÜNSDORF N.K., DUNKL I., SCHMIDT B.C., RANTITSCH G., VON EYNATTEN H. (2017) - *Towards a Higher*  
58  
59 *Comparability of Geothermometric Data Obtained by Raman Spectroscopy of Carbonaceous Material.*  
60  
*Part 2: A Revised Geothermometer*. Geostandards and Geoanalytical Research, **41**, 593–612.
- MARRONE S., MONIÉ P., ROSSETTI F., LUCCI F., THEYE T., BOUYBAOUENE M.L., NAJIB ZAGHLOUL M. (2020) -

1  
2  
3 *The Pressure-Temperature-time-deformation history of the Beni Mzala unit (Upper Sebtides, Rif belt,*  
4 *Morocco): Refining the Alpine tectono-metamorphic evolution of the Alboran Domain of the Western*  
5 *Mediterranean.* *Journal of Metamorphic Geology.* **39**(5), 591-615.

6  
7  
8  
9  
10 MARTIN-ALGARRA A., MAZZOLI S., PERRONE V., RODRIGUEZ-CANERO R., NAVAS-PAREJO P. (2009) - *Variscan*  
11 *tectonics in the Malaguide Complex (Betic Cordillera, southern Spain): stratigraphic and structural*  
12 *Alpine versus pre-Alpine constraints from the Ardales area (Province of Malaga). I. Stratigraphy.* *The*  
13 *Journal of geology,* **117**, 241–262.

14  
15  
16  
17  
18  
19 MELCHIORRE M., ÁLVAREZ-VALERO A.M., VERGÉS J., FERNANDEZ M., BELOUSOVA E.A., EL MAZ A.,  
20  
21 MOUKADIRI A. (2017). *In situ U-Pb zircon geochronology on metapelitic granulites of Beni Bousera*  
22 *(Betic-Rif system, N Morocco).* *Geological Society of America Special Papers,* **526**, 151–171.

23  
24  
25  
26  
27  
28  
29  
30  
31  
32  
33  
34  
35  
36  
37  
38  
39  
40  
41  
42  
43  
44  
45  
46  
47  
48  
49  
50  
51  
52  
53  
54  
55  
56  
57  
58  
59  
60  
MICHARD A., NEGRO F., SADDIQI O., BOUYBAOUENE M.L., CHALOUAN A., MONTIGNY R., GOFFÉ B. (2006) -  
*Pressure–temperature–time constraints on the Maghrebide mountain building: evidence from the Rif–*  
*Betic transect (Morocco, Spain), Algerian correlations, and geodynamic implications.* *Comptes Rendus*  
*Geoscience,* **338**, 92–114.

MICHARD A., MOKHTARI A., CHALOUAN A., SADDIQI O., ROSSI P., RJIMATI E.-C. (2014) - *New ophiolite slivers*  
*in the External Rif belt, and tentative restoration of a dual Tethyan suture in the western Maghrebides.*  
*Bulletin de la Société Géologique de France,* **185**, 313–328.

MILLIARD Y. (1959). *Les massifs métamorphiques et ultrabasiques de la zone paléozoïque interne du Rif.* *Notes*  
*Mem. Serv. Géol. Maroc,* **18**, 125–160.

MORI H., MORI N., WALLIS S., WESTAWAY R., ANNEN C. (2017). *The importance of heating duration for*  
*Raman CM thermometry: evidence from contact metamorphism around the Great Whin Sill intrusion,*  
*UK.* *Journal of Metamorphic Geology,* **35**, 165–180, <https://doi.org/10.1111/jmg.12225>.

MUIRHEAD D.K., BOND C.E., WATKINS H., BUTLER R.W.H., SCHITO A., CRAWFORD Z., MARPINO A. (2019) -  
*Raman Spectroscopy: an effective thermal marker in low temperature carbonaceous fold-thrust belts.*  
*Geological Society, London, Special Publications,* **490**, 135-151.

MÜNCH P., CAILLAUD J., MONIÉ P., GRAUBY O., CORSINI M., RICCI J., ROMAGNY A., PILIPPON M., LANSON B.,  
AZDIMOUSSA A., BEN MOUSSA A., ARNAUD N. (2021) - *Direct dating of brittle extensional deformation*

- 1  
2  
3 *contemporaneous of Neogene exhumation of the internal zones of the Rif Chain*. *Tectonophysics*, **807**,  
4  
5 228800.  
6  
7  
8 NEGRI F., DI DONATO E., TOMMASINI M., CASTIGLIONI C., ZERBI G., MÜLLEN K. (2004) - *Resonance Raman*  
9  
10 *contribution to the D band of carbon materials: Modeling defects with quantum chemistry*. *Journal of*  
11  
12 *Chemical Physics*, **120**, 11889–11900.  
13  
14 NEGRÒ F., BEYSSAC O., GOFFÉ B., SADDIQI O., BOUYBAOUENE M.L. (2006) - *Thermal structure of the Alboran*  
15  
16 *Domain in the Rif (northern Morocco) and the Western Betics (southern Spain). Constraints from Raman*  
17  
18 *spectroscopy of carbonaceous material*. *Journal of Metamorphic Geology*, **24**, 309–327.  
19  
20  
21 NIRRENGARTEN M., MOHN G., SCHITO A., CORRADO S., GUTIÉRREZ-GARCÍA L., BOWDEN S.A. AND DESPINOIS  
22  
23 F. (2020) - *The thermal imprint of continental breakup during the formation of the South China Sea*.  
24  
25 *Earth and Planetary Science Letters*, **531**, 115972.  
26  
27  
28 PASTERIS J.D. & WOPENKA B. (1991) - *Raman spectra of graphite as indicators of degree of metamorphism*.  
29  
30 *The Canadian Mineralogist*, **29**, 1–9.  
31  
32 PÉROUSE E., VERNANT P., CHÉRY J., REILINGER R., MCCLUSKYS. (2010) - *Active surface deformation and sub-*  
33  
34 *lithospheric processes in the western Mediterranean constrained by numerical models*. *Geology*, **38**,  
35  
36 823–826.  
37  
38  
39 PLATT J.P., BEHR W.M., JOHANESSEN K., WILLIAMS J.R. (2013) - *The Betic-Rif arc and its orogenic hinterland:*  
40  
41 *a review*. *Annual Review of Earth and Planetary Sciences*, **41**, 313–357.  
42  
43  
44 QIN J., WANG S., SANEI H., JIANG C., CHEN Z., REN S., XU X., YANG J., ZHONG N. (2018) - *Revelation of organic*  
45  
46 *matter sources and sedimentary environment characteristics for shale gas formation by petrographic*  
47  
48 *analysis of middle Jurassic Dameigou formation, northern Qaidam Basin, China*. *International Journal of*  
49  
50 *Coal Geology*, **195**, 373–385.  
51  
52  
53 RAHL J.M., ANDERSON K.M., BRANDON M.T., FASSOULAS C. (2005) - *Raman spectroscopic carbonaceous*  
54  
55 *material thermometry of low-grade metamorphic rocks: Calibration and application to tectonic*  
56  
57 *exhumation in Crete, Greece*. *Earth and Planetary Science Letters*, **240**, 339–354.  
58  
59  
60 ROBERTSON J. & OREILLY E.P. (1987). *Electronic and atomic structure of amorphous carbon*. *Physical Review*  
  
B, **35**, 2946–2957.

- 1  
2  
3 RODRÍGUEZ-RUIZ M.D., ABAD I., BENTABOL M., CRUZ M.D.R. (2020) - *Evidences of talc-white mica*  
4 *assemblage in low-grade metamorphic rocks from the internal zone of the Rif Cordillera (N Morocco).*  
5 *Applied Clay Science*, **195**, 105723.  
6  
7  
8  
9  
10 ROSSETTI F., THEYE, T., LUCCI F., BOUYBAOUENNE M.L., DINI A., GERDES A., PHILLIPS D., COZZUPOLI D. (2010)  
11 - *Timing and modes of granite magmatism in the core of the Alboran Domain, Rif chain, northern*  
12 *Morocco: implications for the Alpine evolution of the western Mediterranean.* *Tectonics*, **29**(2), TC2017.  
13  
14  
15  
16  
17 ROSSETTI F., DINI A., LUCCI F., BOUYBAOUENNE M., FACCENNA C. (2013) - *Early Miocene strike-slip tectonics*  
18 *and granite emplacement in the Alboran Domain (Rif Chain, Morocco): significance for the geodynamic*  
19 *evolution of Western Mediterranean.* *Tectonophysics*, **608**, 774–791.  
20  
21  
22  
23  
24 ROSSETTI F., LUCCI F., THEYE T., BOUYBAOUENNE M.L., GERDES A., OPITZ J., DINI A., LIPP C. (2020). *Hercynian*  
25 *anatexis in the envelope of the Beni Bousera peridotites (Alboran Domain, Morocco): Implications for*  
26 *the tectono-metamorphic evolution of the deep crustal roots of the Mediterranean region.* *Gondwana*  
27 *Research*. **83**, 157-182.  
28  
29  
30  
31  
32  
33 ROYDENL. & FACCENNA C. (2018). *Subduction orogeny and the Late Cenozoic evolution of the Mediterranean*  
34 *Arcs.* *Annual Review of Earth and Planetary Sciences*, **46**, 261–289.  
35  
36  
37  
38 RUIZ-CRUZ M.D. & GALÁN E. (2002). *Mineralogy and origin of spots in spotted slate from the Maláguide*  
39 *complex, betic cordilleras, spain: an XRD, EMPA and TEM–AEM study.* *The Canadian Mineralogist*, **40**,  
40 1483–1503.  
41  
42  
43  
44 RUIZ-CRUZ M.D. & NOVÁK J.K. (2003) - *Metamorphic chlorite and “vermiculitic” phases in mafic dikes from*  
45 *the Maláguide Complex (Betic Cordillera, Spain).* *European Journal of Mineralogy*, **15**, 67–80.  
46  
47  
48  
49 SCHITO A. & CORRADO S. (2018) - *An automatic approach for characterization of the thermal maturity of*  
50 *dispersed organic matter Raman spectra at low diagenetic stages.* *Geological Society, London, Special*  
51 *Publications*, **484**, 107-119.  
52  
53  
54  
55 SCHITO A., ROMANO C., CORRADO S., GRIGO D., POE B. (2017) - *Diagenetic thermal evolution of organic*  
56 *matter by Raman spectroscopy.* *Organic Geochemistry*, **106**, 57–67.  
57  
58  
59  
60 SCHITO A., SPINA A., CORRADO S., CIRILLI S., ROMANO C. (2019) - *Comparing optical and Raman*  
*spectroscopic investigations of phytoclasts and sporomorphs for thermal maturity assessment: the case*

- 1  
2  
3 *study of Hettangian continental facies in the Holy cross Mts. (central Poland). Marine and Petroleum*  
4  
5 *Geology, 104, 331–345.*  
6
- 7 SCHMIDT J.S., HINRICHS R., ARAUJO C. V. (2017) - *Maturity estimation of phytoclasts in strew mounts by*  
8  
9 *micro-Raman spectroscopy. International Journal of Coal Geology, 173, 1–8.*  
10
- 11 SORCI A., CIRILLI S., CLAYTON G., CORRADO S., HINTS O., GOODHUE R., SCHITO A., SPINA A. (2020).  
12  
13 *Palynomorph optical analyses for thermal maturity assessment of Upper Ordovician (Katian-Hirnantian)*  
14  
15 *rocks from Southern Estonia. Marine and Petroleum Geology, 120, 104574.*  
16  
17
- 18 SOTO J.I., PLATT J.P., SÁNCHEZ-GÓMEZ M., AZAÑÓN J.M. (1999) - *Pressure–temperature evolution of the*  
19  
20 *metamorphic basement of the Alboran Sea: thermobarometric and structural observations. In:*  
21  
22 *Proceedings of the Ocean Drilling Program, Scientific Results. pp. 263–279.*  
23  
24
- 25 TAYLOR G.H., TEICHMÜLLER M., DAVIS A., DIESEL C.F.K., LITKE R., ROBERT P. (1998) - *Organic petrology.*  
26  
27 *Gebrüder Borntraeger, Berlin, Stuttgart. pp. 704.*  
28  
29
- 30 TEICHMÜLLER M. (1986) - *Organic petrology of source rocks, history and state of the art. Organic*  
31  
32 *Geochemistry, 10, 581–599.*  
33  
34
- 35 THOMSEN C. & REICH S. (2000) - *Double resonant raman scattering in graphite. Physical Review Letters, 85,*  
36  
37 *5214–5217.*  
38  
39
- 40 TUINSTRA F. & KOENIG J.L. (1970) - *Raman Spectrum of Graphite. The Journal of Chemical Physics, 53, 1126–*  
41  
42 *1130.*  
43  
44
- 45 VAN HINSBERGEN D.J.J., VISSERS R.L.M., SPAKMAN W. (2014) - *Origin and consequences of western*  
46  
47 *Mediterranean subduction, rollback, and slab segmentation. Tectonics, 33, 393–419.*  
48
- 49 VON RAUMER J., STAMPFLI G., BOREL G., BUSSY F. (2002) - *Organization of pre-Variscan basement areas at*  
50  
51 *the north-Gondwanan margin. International Journal of Earth Sciences, 91, 35–52.*  
52
- 53 WILKINS R.W.T., BOUDOU R., SHERWOOD N., XIAO X. (2014) - *Thermal maturity evaluation from inertinites*  
54  
55 *by Raman spectroscopy : The ‘ RaMM ’ technique. International Journal of Coal Geology, 128–129, 143–*  
56  
57 *152.*  
58  
59
- 60 WILLIAMS J.R. & PLATT J.P. (2018) - *A new structural and kinematic framework for the Alborán Domain*

1  
2  
3 (*Betic–Rif arc, western Mediterranean orogenic system*). *Journal of the Geological Society*, **175**, 465–  
4  
5 496.

6  
7 ZAGHLOUL M.N., CRITELLI S., PERRI F., MONGELLI G., PERRONE V., SONNINO M., TUCKER M., AIELLO M.,  
8  
9 VENTIMIGLIA C. (2010). *Depositional systems, composition and geochemistry of Triassic*  
10  
11 *rifted-continental margin redbeds of the Internal Rif Chain, Morocco*. *Sedimentology*, **57**, 312–350.  
12  
13  
14  
15  
16  
17  
18  
19  
20  
21  
22  
23  
24  
25  
26  
27  
28  
29  
30  
31  
32  
33  
34  
35  
36  
37  
38  
39  
40  
41  
42  
43  
44  
45  
46  
47  
48  
49  
50  
51  
52  
53  
54  
55  
56  
57  
58  
59  
60

For Review Only

1  
2  
3 **An insight on the polyphase thermal history of the Internal Rif (Northern Morocco)**  
4  
5  
6 **through Raman micro-spectroscopy investigation**  
7  
8

9 A. SCHITO<sup>\*1,2</sup>, A. ATOUABAT<sup>2</sup>, D. K. MUIRHEAD<sup>1</sup>, R. CALCAGNI<sup>2</sup>, R. GALIMBERTI<sup>3</sup>, C. ROMANO<sup>2</sup>, A. SPINA<sup>4</sup> and  
10  
11 S. CORRADO<sup>2</sup>  
12  
13  
14  
15  
16

17 <sup>1</sup>*Department of Geology and Geophysics, School of Geosciences, University of Aberdeen, Aberdeen AB24*  
18  
19 *3UE, UK.*  
20

21  
22 <sup>2</sup>*Università degli Studi di Roma Tre, Dipartimento di Scienze, Sezione di Scienze Geologiche, Largo San Leonardo*  
23  
24 *Murialdo 1, 00146 Rome, Italy*  
25

26 <sup>3</sup> *Geolog Technologies S.r.l. (GEOTech Research and Laboratory) – Viale Ortles 22/4, 20139, Milan, Italy*  
27

28  
29 <sup>4</sup> *Università degli Studi di Perugia, Dipartimento di Fisica e Geologia, Via Alessandro Pascoli, 06123 Perugia,*  
30  
31 *Italy*  
32  
33  
34  
35  
36  
37

38 *\*Corresponding author (e-mail: andrea.schito@abdn.ac.uk)*  
39  
40

41 **Abstract**  
42  
43

44 Micro-Raman spectroscopy on carbonaceous material has been applied to estimate the maximum paleo-  
45 temperatures achieved by the **Tectono-metamorphic** units that constitute most of the backbone of the  
46 Internal domain of the Rif orogen in North Morocco. **The** Internal Rif is composed by the continental deep  
47 units of the Sebides, exhumed at the end of the Alpine cycle, overlain by the Variscan Ghomarides. Both  
48 units **are** trust above the meta-carbonates of the Dorsale Calcaire. **In the norther part of the Rif, the** Sebide  
49 complex cropping out **at the core of** the Beni Mezala antiform suffered maximum paleo-temperatures  
50 derived from Raman parameters **typical of greenschists facies, whereas** in the flanks of the antiform **the gap**  
51 **in temperatures between Lower Paleozoic (Silurian and Devonian) and Carboniferous Ghomarides**  
52  
53  
54  
55  
56  
57  
58  
59  
60

1  
2  
3 **probably reflect the temperatures peaks reached during Eo Variscan and Late Variscan phases. Moreover,**  
4  
5 **our data suggest that one of the two analysed units in the Ghomarides always reached higher metamorphic**  
6  
7 **conditions during both Variscan cycles. Further to the south, the increase in maximum** temperatures  
8  
9 towards the contact with the **Beni-Bousera peridotite** reflects an Alpine thermal overprinting, **probably**  
10  
11 linked to slab retreat and delamination driven crustal anatexis, accompanied **by** magma emplacement during  
12  
13 the last phases of the Alpine orogenesis.  
14  
15  
16  
17  
18  
19

## 20 **1. Introduction**

21  
22 **Maximum** paleo-temperatures are strictly linked to rocks rheology and geochemical processes that occur at  
23  
24 depth in different geodynamic settings, from passive margins to subduction systems. Thus, correct  
25  
26 assessment of maximum paleo-temperatures experienced by rocks is an essential tool to unravel the  
27  
28 evolution of the thermal structure of the crust during the main phases of an orogenesis. Classical  
29  
30 metamorphic zones, based on metamorphic reactions and pseudosections, suffer from the superimposition  
31  
32 of retrograde processes **or by the presence/absence of diagnostic minerals** that can undermine the accurate  
33  
34 determination of the peak temperatures. On the other hand, maximum temperatures derived from the  
35  
36 analyses of carbonaceous material (**CM**) dispersed in rocks have proven to provide robust and, sometimes,  
37  
38 more precise data given the irreversible nature of organic matter transformation with temperature increase  
39  
40 (TEICHMÜLLER, 1986; TAYLOR *et alii*, 1998, BEYSSAC *et alii*, 2002; LAHFID *et alii*, 2010). The most used  
41  
42 thermal indicators for **dispersed** organic matter derive from optical analyses (e.g. vitrinite reflectance, color  
43  
44 alteration indexes; HARTKOPF-FRÖDER *et alii*, 2015; SPINA *et alii*, 2018; **SORCI *et alii*, 2020**), although, in the  
45  
46 last **decades**, an increasing interest raised towards the use of thermal parameters derived from Raman  
47  
48 spectroscopy. This tool was **initially** developed for metamorphic temperature higher than about 300°C  
49  
50 (PASTERIS AND WOPENKA, 1991; BEYSSAC *et alii*, 2002), but its use has recently been extended **to** lower  
51  
52 metamorphic degrees (RAHL *et alii*, 2005; LAHFID *et alii*, 2010) and diagenesis (LI, 2007; GUEDES *et alii*, 2010;  
53  
54 WILKINS *et alii*, 2014; LÜNSDORF *et alii*, 2017; SCHITO *et alii*, 2017, 2019; SCHMIDT *et alii*, 2017; HENRY *et*  
55  
56 *alii*, 2018, 2019; SCHITO & CORRADO, 2018). Given the application in a wide range of temperature conditions,  
57  
58  
59  
60



1  
2  
3 Raman spectroscopy **on carbonaceous material (RSCM)** has become one of the **most used** geothermometers  
4  
5 in geological studies to accurately **unravel** thermal metamorphic gradients (NEGRO *et alii*, 2006; DELCHINI *et*  
6  
7 *alii*, 2016; DUCOUX *et alii*, 2019; LAHFID *et alii*, 2019).

9  
10 The selected playground for new Raman studies on metamorphic rocks is the Internal Rif in Northern  
11  
12 Morocco. This area represents the innermost tectonic domain preserved on-shore of the wider Betic-Rif-Tell  
13  
14 orogenic chain that developed during the Mesozoic-Cenozoic complex convergence between Africa and  
15  
16 Eurasia plates forming the westernmost termination of the Mediterranean Alpine orogenic system (LEPRÊTRE  
17  
18 *et alii*, 2018; ROYDEN & FACCENNA, 2018).

19  
20 The Internal Rif offers a unique opportunity to observe at surface **high-grade** metamorphic rocks from an  
21  
22 alpine fossil subduction zone (Sebtide tectonic units) **tectonically** lying below low-grade metamorphic rocks  
23  
24 derived from a complex polyphase Variscan history (Ghomaride tectonic units). In detail, the Ghomarides  
25  
26 and Sebtides represent respectively the upper and lower plates preserved in a metamorphic core complex  
27  
28 (CHALOUAN *et alii*, 2008). They are composed by Paleozoic rocks with a partially preserved Mesozoic-  
29  
30 Cenozoic cover and by lower Paleozoic to Triassic deep-crustal mica-schists, migmatites and granulites  
31  
32 associated with peridotites (Beni Bousera complex), respectively (**CHALOUAN *et alii*, 2008**).

33  
34 Given its importance in the Alpine orogenic reconstruction in the western Mediterranean, the Sebtides have  
35  
36 been the subject of several studies aiming at the definition of **their** P-T deformation history, in particular of  
37  
38 their deepest units (MARRONE *et alii*, 2021; SOTO *et alii*, 1999; MICHARD *et alii*, 2006; BOOTH-REA *et alii*,  
39  
40 2007; ROSSETTI *et alii*, 2010, 2020; PLATT *et alii*, 2013; GUEYDAN *et alii*, 2015; MELCHIORRE *et alii*, 2017;  
41  
42 WILLIAMS & PLATT, 2018) . On the other hand, the Variscan metamorphic evolution of the Ghomarides  
43  
44 complex has been widely studied by CHALOUAN (1986) and CHALOUAN & MICHARD (1990) with the aim to  
45  
46 correlate it with the history of similar Variscan terranes in Spain (Betic Cordillera), northern Algeria (Kabylian  
47  
48 **domain**) and southern Italy (Calabro-Peloritain **arc**).

49  
50 An accurate study of the maximum **paleo**-temperatures achieved by Sebtides and Ghomarides in the Internal  
51  
52 Rif by means of Raman spectroscopic analyses on carbonaceous material has been already developed by  
53  
54 NEGRO *et alii* (2006). Nevertheless, **using the RSCM method proposed by BEYSSAC *et alii* (2002)**, the authors  
55  
56 did not investigate in detail **paleo**-temperature distributions in tectonic units that suffered peak  
57  
58  
59  
60

1  
2  
3 metamorphisms lower than 330°C. **This led the authors to provide interesting interpretation on the Alpine**  
4 **history of the units surrounding the Beni-Bousera and Ronda peridotites but failed to provide useful**  
5 **constraints for the low-metamorphic Variscan history of the Ghomarides.**  
6  
7

8  
9 **The present work aims to fulfill this gap providing more accurate Raman paleo-temperature data**, in  
10 particular for the Ghomaride succession and for the organic carbon-poor successions of the Upper Sebtides  
11 in northern part of the Rif **belt**.  
12  
13  
14  
15

## 20 **2. Geological Setting**

21 Located at the western edge of the West-Mediterranean Alpine systems, the Rif belt corresponds to the  
22 southern limb of Gibraltar Arc that developed in the framework of Africa-Eurasia collision (DOCHERTY &  
23 BANDA, 1995; PÉROUSE *et alii*, 2010; PLATT *et alii*, 2013; VAN HINSBERGEN *et alii*, 2014) and is a part of the  
24 Maghrebides orogenic system (Tell-Rif; DURAND-DELGA, 1980). The Maghrebides resulted from the closure  
25 of the Maghrebian Tethys and the docking of the Meso-Mediterranean blocks (i.e., Alboran and Kabily  
26 domains) onto the African margin during the Early Miocene (CHALOUAN & MICHARD, 2004; LEPRÊTRE *et alii*,  
27 2018).  
28  
29

30 The Rif belt is classically divided into three main tectono-stratigraphic domains (FAVRE & STAMPFLI, 1992;  
31 FRIZON DE LAMOTTE *et alii*, 2011), namely from north to south and from internal to external **portion** of the  
32 chain: (i) Internal or Alboran Domain (MILLIARD, 1959; BOUILLIN, 1986; GARCÍA-DUEÑAS *et alii*, 1992), (ii)  
33 Maghrebian Flysch Basin Domain (GUERRERA *et alii*, 1993, 2005; LEPRÊTRE *et alii*, 2018; ATOUABAT *et alii*,  
34 2020), and (iii) External Domain (DIDON *et alii*, 1973; LEBLANC, 1979; MICHARD *et alii*, 2014; GIMENO-VIVES  
35 *et alii*, 2019; GIMENO-VIVES *et alii*, 2020). The internal domain, object of this work, is subdivided into three  
36 tectonic complexes, recognized from bottom to top as: Sebtides complex, Ghomarides complex and the  
37 'Dorsale Calcaire' (EL KADIRI *et alii*, 1992).  
38  
39

40 The Sebtide Complex represents the **structurally** deepest unit and it is composed by the Lower Sebtides (Filali  
41 and Beni Bousera Units) and Upper Sebtides (Federico Unit). The Beni Bousera consists of a peridotite body,  
42 with topmost discontinuous slivers of granulites (kinzigites, CHALOUAN *et alii*, 2008) that emplaced in the  
43  
44  
45  
46  
47  
48  
49  
50  
51  
52  
53  
54  
55  
56  
57  
58  
59  
60

1  
2  
3 crust as a consequence of the Variscan orogen collapse (ROSSETTI *et alii*, 2020) and was finally exhumed  
4 during Alpine stages (AZDIMOUSA *et alii*, 2014). It is separated by the overlying gneisses of the Filali Unit  
5  
6  
7 **through** a ductile shear zone (MICHARD *et alii*, 2006; CHALOUAN *et alii*, 2008; ROSSETTI *et alii*, 2010). The  
8  
9 Federico Unit in the northern part of the Rif is formed by four thrust imbrications, namely Tzigarine, Boquete  
10  
11 de Anjera, Beni Mezala 1 and 2 (from here onward BM1 and BM2 **respectively**), each of them showing the  
12  
13 same stratigraphy and a general downward increase in metamorphic grade. The uppermost Tizgarine Unit is  
14  
15 composed by Permian-Triassic red pelites, and Middle-Upper Triassic dolomitic marbles. The Permian-  
16  
17 Triassic successions of Boquete de Anjera, BM1 and BM2 Units are characterized by purple phyllites and dark  
18  
19 quartz-phyllite respectively, overlain by Triassic marbles on top (BOUYBAOUENE *et alii*, 1998). Locally in both  
20  
21 Beni Mezala Units, some Carboniferous-Permian schists occur.

22  
23  
24  
25 Lower and upper Sebtides are thought to have experienced metamorphic conditions that reached the  
26  
27 eclogite facies in the Federico Unit under HP-LT conditions and granulite facies under a higher geothermal  
28  
29 gradient in Filali and Beni-Bousera Units (CHALOUAN & MICHARD, 1990; ROSSETTI *et alii*, 2020), even if  
30  
31 recent works (RODRÍGUEZ-RUIZ *et alii*, 2020) suggested lower metamorphic conditions for the inner BM1  
32  
33 Unit in the northern sector of the study area. Federico Unit is characterized by pervasive planar and linear  
34  
35 tectonic fabric with a top-to-the NNW sense of shearing (MICHARD *et alii*, 2006).

36  
37  
38 The Ghomaride complex consists of an Ordovician to Carboniferous succession, unconformably overlain by  
39  
40 Triassic red beds and, locally, Liassic limestones and Paleocene-Eocene calcarenites (CALVO *et alii*, 2001). This  
41  
42 complex includes four Paleozoic tectonic units that, from the bottom to the top, are the Akaili Unit, the  
43  
44 Koudiat Tizian Unit and the Beni Hozmar Unit. A fourth unit, Talembote Unit, is a klippe preserved above the  
45  
46 Dorsale Calcaire in the Oued-Laou area (CHALOUAN & MICHARD, 1990; CHALOUAN *et alii*, 2008). In the  
47  
48 different units the Ordovician to Silurian stratigraphy is rather homogeneous, characterized by Ordovician  
49  
50 phyllites with quartzites and meta-conglomerates and by graptolitic shales and pillow basalts at the top of  
51  
52 the Silurian section. Devonian sediments consist of distal calcareous flysch in the Akaili Unit and more  
53  
54 proximal flysch and pelagic limestones in the Koudiat-Tizian and Beni-Hozmar (CHALOUAN, 1986). The  
55  
56 Ordovician to Devonian succession was subjected to Eo-Variscan metamorphic event deformation  
57  
58 characterized by NNE trending structures and white mica, chlorite and quartz recrystallization (CHALOUAN  
59  
60

1  
2  
3 & MICHARD, 1990). Visean-Bashkirian greywackes unconformably onlap, showing NW oriented structures  
4  
5 and limited recrystallization associated with a late Variscan low grade metamorphic event. Brittle Alpine  
6  
7 deformation was recorded in the unconformable Triassic red beds that mostly constitute the uppermost  
8  
9 deposits except for some Jurassic limestones and Upper Eocene conglomerates that locally crop out  
10  
11 (ZAGHLOUL *et alii*, 2010).  
12

13  
14 Finally, the 'Dorsale Calcaire', consists of Triassic-Middle Jurassic carbonate platform deposits, Jurassic-  
15  
16 Cretaceous sediments overlaid by Paleocene-Eocene clays and limestones and by Eocene to Aquitanian  
17  
18 clastic deposits and olistostromes (EL KADIRI *et alii*, 1992). It is detached along the Triassic levels, from most  
19  
20 likely the Ghomarides (DURAND-DELGA & OLIVIER, 1988) or partly from Ghomarides and Sebtides (WILDI,  
21  
22 1983). The Triassic successions are composed by dolostones, dolomitic breccias and stromatolitic dolostones,  
23  
24 while during the Jurassic, a transition to a more distal environment is represented by a condensed pelagic  
25  
26 sedimentation in the entire succession. Eocene deposits composed of arenites, bioclastic limestones and  
27  
28 chaotic breccias, are separated by an unconformity from the Mesozoic succession, indicative of an uplift in  
29  
30 early Eocene times (MICHARD & CHALOUAN, 1990; CHALOUAN *et alii*, 2008).  
31  
32  
33  
34  
35  
36  
37  
38  
39  
40  
41  
42  
43  
44  
45  
46  
47  
48  
49  
50  
51  
52  
53  
54  
55  
56  
57  
58  
59  
60

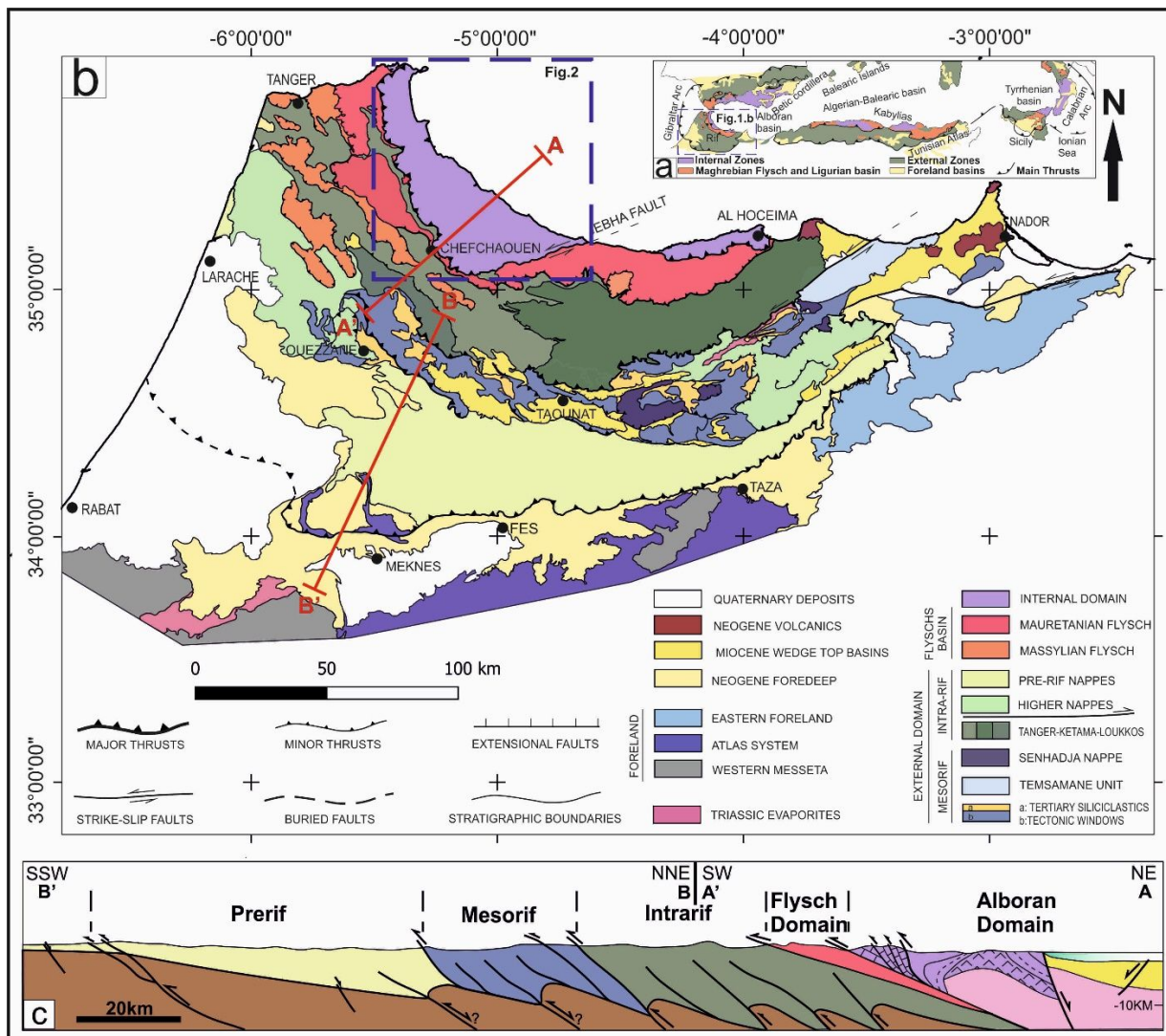


Figure 1 – Schematic geological map of the South Mediterranean (a) and of the Rif chain in North Morocco (b). Schematic cross section from the Alboran Sea to the external zones (c) (*modified after; SUTER, 1980; FRIZON DE LAMOTTE et alii, 2017; GIMENO-VIVES et alii, 2019; ATOUABAT et alii, 2020*).

### 3. Sampling areas and Materials

Sixteen samples from the Internal Rif have been collected and analysed from two areas (Fig. 2a): the Beni Mezala antiform to the North (Zone 1) and the region between Martil Village and Oued Laou, **to the south of** the town of Tetouan (Zone 2).

In Zone 1, sampling **was performed** along a NE-SW transect from the South of Ceuta town to the contact between the 'Dorsale Calcaire' and the Flysch domain (Fig. 2b) across the Beni Mezala antiform. Five samples

1  
2  
3 were collected in the Federico Units (Figs. 2b and 3a, b) in the core of the antiform and five from Ghomarides  
4 on both flanks of it (Figs. 2b and 3c, d). Samples from Ghomarides derived from Silurian and Carboniferous  
5 sections of the Akaili and Beni-Hozmar Units (Table 1). One sample (Mar 4.1) comes from a Silurian shaly  
6 horizon in the Beni-Hozmar Unit further to the South, close to the contact with the 'Dorsale Calcaire' (Fig.  
7 2a).  
8  
9  
10  
11  
12  
13

14 In Zone 2, samples were collected across a NW-SE oriented transect from Amsa village to Oued-Laou river  
15 (Fig. 2a and c) covering an area where mainly Ghomarides Akaili and Septides Filali Units crop out. In the  
16 Ghomarides, one sample comes from Carboniferous pelitic levels of the Akaili Unit cropping out in Ras Mazari  
17 cape area (close to the North of Amsa village), whereas all the others derive from Devonian to Ordovician  
18 Ghomarides (Akaili Unit). In this sector of the Septides, sample Mar 20.1 comes from Filali Unit (Tab. 1).  
19  
20  
21  
22  
23  
24  
25  
26  
27  
28  
29  
30  
31  
32  
33  
34  
35  
36  
37  
38  
39  
40  
41  
42  
43  
44  
45  
46  
47  
48  
49  
50  
51  
52  
53  
54  
55  
56  
57  
58  
59  
60

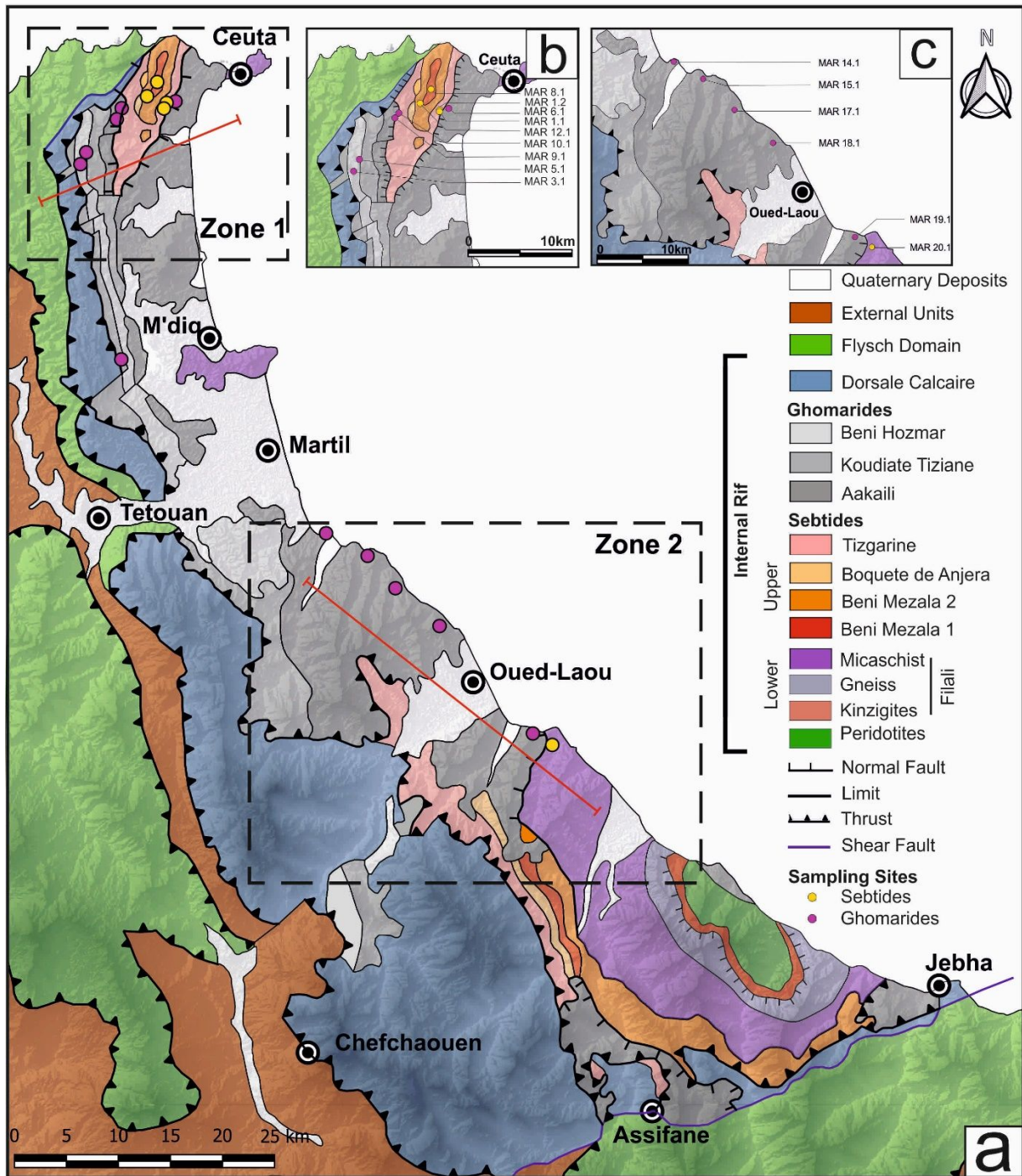


Figure 2 – A. Geological map of Internal Rif with indicated sampling zones (1 and 2) and sampling sites. Redrawn after CHALOUAN *et alii*, 2008.

**Table 1 – Sample distribution from the lowest tectonic units (bottom) to the shallowest (top) with indicated age, tectonic unit and coordinates (West Greenwich and North) of each sampling site.**

Complex	Sample name	Long.	Lat.	Tectonic Unit	Age
GHOMARIDES	MAR_5.1	05° 26' 51"	35° 49' 56"	Beni Hozmar	Silurian
	MAR_4.1	05° 26' 57"	34° 49' 40"	Beni Hozmar	Silurian
	MAR_3.1	05° 27' 10"	35° 49' 24"	Beni Hozmar	Carboniferous
	MAR_19.1	05° 02' 20"	35° 23' 59"	Akaili	Silurian
	MAR_18.1	05° 07' 27"	35° 28' 47"	Akaili	Silurian-Devonian?
	MAR_17.1	05° 09' 52"	35° 30' 29"	Akaili	Devonian
	MAR_15.1	05° 12' 24"	35° 32' 02"	Akaili	Devonian
	MAR_14.1	05° 13' 41"	35° 32' 56"	Akaili	Carboniferous
	MAR_10.1	05° 24' 57"	35° 51' 48"	Akaili	Silurian
	MAR_9.1	05° 24' 57"	35° 51' 48"	Akaili	Carboniferous
MAR_6.1	05° 21' 57"	35° 52' 12"	Akaili	Silurian	
SEBTIDES	MAR_1.2	05° 22' 27"	35° 52' 8"	Tizgarine	Permian
	MAR_1.1	05° 22' 26"	35° 52' 8"	Tizgarine	Permian
	MAR_12.1	05° 23' 31"	35° 52' 26"	Beni Mezala 2	Permian-Triassic
	MAR_8.1	05° 22' 50"	35° 52' 56"	Beni Mezala 1	Permian-Triassic
	MAR_20.1	05° 01' 16"	35° 23' 28"	Filali	Ordovician-Devonian

#### 4. Methods

TOC (total organic carbon) expresses the percentage of organic carbon weight related to the total weight of the analyzed rock. In this **work** data were acquired using a TOC Elementar model TOC VARIO Select **analyzer**, coupled with an oven (max temperature of 850°C).



1  
2  
3 Raman spectroscopic analyses allowed to determine the degree of order of the organic matter and thus  
4  
5 paleo-temperatures experienced by the rocks during prograde metamorphism (e.g. Raman spectroscopy on  
6  
7 carbonaceous material geothermometer – RSCM; BEYSSAC *et alii*, 2002; LAHFID *et alii*, 2010; LÜNSDORF *et*  
8  
9 *alii*, 2014).

10  
11  
12 The Raman spectrum of carbonaceous material consists of two main bands at  $\sim 1585\text{ cm}^{-1}$  (the graphite peak,  
13  
14 G ) and  $1350\text{ cm}^{-1}$  (the disorder peak, D; TUINSTRA & KOENIG, 1970). These bands occur as the result of the  
15  
16 hybridised atomic orbital configuration of carbon atoms and the relative amount of  $sp^2$  carbon bonds  
17  
18 (graphite-like, trigonal planar symmetry) bounded by  $sp^3$  sites (diamond-like, tetrahedral symmetry;  
19  
20 ROBERTSON & OREILLY, 1987). The G band is assigned to the  $E_{2g}$  symmetry in-plane vibration of the carbon  
21  
22 atoms in the graphene sheets. On the other hand, the D band has been interpreted either by double resonant  
23  
24 Raman scattering ( $A_{1g}$ -mode of small graphite crystallites; THOMSEN & REICH, 2000) or to ring breathing  
25  
26 vibration in the graphite sub-unit or polycyclic aromatic compounds (CASTIGLIONI *et alii*, 2001; DI DONATO  
27  
28 *et alii*, 2004; NEGRI *et alii*, 2004; LÜNSDORF, 2016). Their mutual relationships change with maturity level of  
29  
30 organic matter (e.g. temperature; TUINSTRA & KOENIG, 1970) up to the graphitic stage (BEYSSAC *et alii*,  
31  
32 2002). The number of bands that composes the carbonaceous material Raman spectrum, decreases with  
33  
34 increasing ordering (i.e. temperature **increase**) passing from **more than five bands in diagenetic organic**  
35  
36 **matter to** a single band in pure graphite (Fig. 4; HENRY *et alii*, 2019 for a **complete** review).  
37  
38  
39  
40  
41  
42  
43  
44  
45  
46  
47  
48  
49  
50  
51  
52  
53  
54  
55  
56  
57  
58  
59  
60

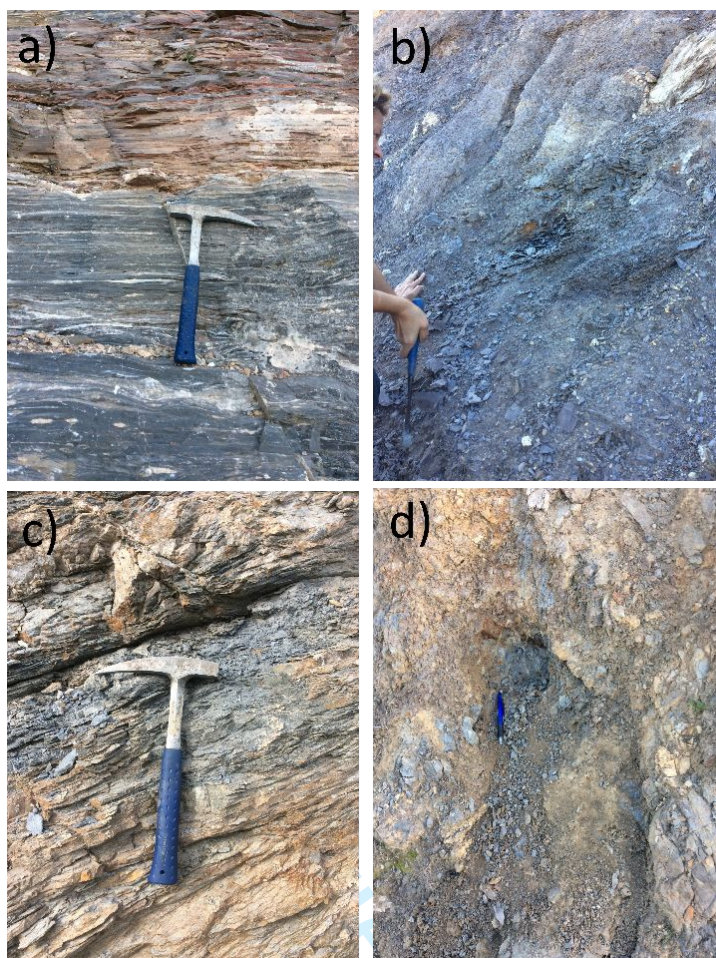


Figure 3 Outcrop examples of a) schists from BM 2 Unit; b) black phyllites from Tizgarine Unit; c) Devonian pelites from the Ghomarides; d) Carboniferous pelites from the Ghomarides.

Analyses in this work were performed on petrographic thin sections according to recommendation in BEYSSAC *et alii* (2002) and LÜNSDORF *et alii* (2017), using a Jobin Yvon micro-Raman LabRam system with a Neodymium-Yag laser of 532nm (green laser) as a light source and a CCD detector. Spectra were acquired in the first order Raman spectral range ( $700$  to  $2300\text{ cm}^{-1}$ ). The **power of the laser was 40mW and was reduced to less than 0.4 mW by optical filters to avoid heating alteration of the organic matter. The integration time for each data was of 20 s repeated for three times under a 50x magnification lens** (as defined by SCHITO *et alii*, 2017).

Temperatures were derived according to **two different approaches in order to check the comparability between the relatively new method of LÜNSDORF *et alii*. (2017) with the classic fitting approach proposed by BEYSSAC *et alii*. (2002) for high metamorphism or by LAHFID *et alii*. (2010) for low metamorphism. The automatic method proposed by LÜNSDORF & LÜNSDORF (2016) and LÜNSDORF *et alii* (2017) is designed**

1  
2  
3 to offer a comparability of Raman results at different stages of “organic metamorphism”. The method is  
4 based on the IFORS software that curve-fits Raman spectra of carbonaceous material modelling  
5 simultaneously the background with a fifth-order polynomial curve and the Raman signal with pseudo-  
6 Voigt bands. The optimization of the curve is an iterative process that adds pseudo-Voigt functions (note  
7 that the number of bands is not imposed *a priori*) until the best-representation of the baseline-subtracted  
8 spectrum is reached (LÜNSDORF & LÜNSDORF, 2016; LÜNSDORF *et alii*, 2017). Among Raman parameters  
9 carried out from this process, the normalized intensities of the D and G bands (STA-D, STA-G) are used to  
10 calculate paleo-temperature by means of the third-degree polynomial equation proposed by LÜNSDORF  
11 *et alii* (2017). The correlation against temperatures provided in LÜNSDORF *et alii* (2017) is based on a  
12 reference series of 26 samples collected across the central and western Alps in a range comprised between  
13 100 and 700°C.

14  
15  
16  
17  
18  
19  
20  
21  
22  
23  
24  
25  
26  
27  
28  
29  
30  
31  
32  
33  
34  
35  
36  
37  
38  
39  
40  
41  
42  
43  
44  
45  
46  
47  
48  
49  
50  
51  
52  
53  
54  
55  
56  
57  
58  
59  
60

RA2 or R2 parameters and related paleo-temperatures, were calculated, depending on the shape of the  
spectra, by means of a four-to-three bands deconvolution as suggested by BEYSSAC *et alii* (2002) for  
graphitic carbon (Figs. 4b and c) or by a five bands deconvolution proposed by LAHFID *et alii* (2010) for low-  
metamorphic organic matter (Fig. 4a). Bands deconvolution was performed using LabSpec software by  
Horiba. Paleo-temperatures were calculated according to the following equations:

$$T (^{\circ}\text{C}) = -445 \times R2 + 641 \quad (1)$$

$$T (^{\circ}\text{C}) = \frac{RA2 - 0.27}{0.0045} \quad (2)$$

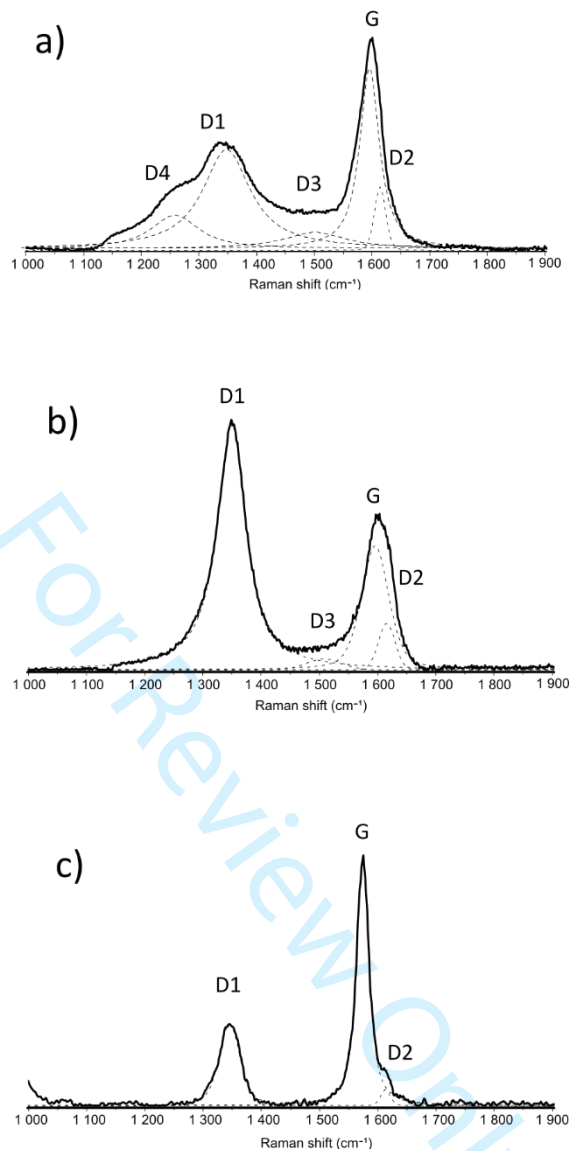


**Figure 4** Examples of Raman spectra and related bands assignment for different temperature intervals in the Internal Rif chain. a) Very disordered Raman spectrum from Carboniferous pelites of the Akaili Unit (Gomarides); b) spectrum from Silurian shales of the Akaili Unit (Ghomarides); c) spectrum of graphitic carbon from the Filali Unit (Sebtides).

## 5. Results

TOC data in Sebtide samples indicate values between 0.7 and 0.8% except for sample 12.1 from the Beni Mezala 2 Unit where TOC is higher than 2%. In the Ghomarides, samples show values ranging between about 0.6 and 3.9% in the Akaili Unit and between 0.6 and 1.6% in the Beni Hozmar Unit, generally indicating high organic carbon content (Tab. 2).

1  
2  
3 Between 14 to 35 Raman spectra on organic fragments were acquired for each sample, to obtain a reliable  
4 temperature estimation (Table 2). High fluorescing spectra with a low signal-to-noise ratio were discarded  
5  
6  
7 **after acquisition** during a first qualitative **evaluation**.  
8

9  
10 In zone 1, Raman spectra on organic matter from the BM 2 Unit show a well-developed D band and a strongly  
11 asymmetric G band due to the presence of a clearly defined D2 band. In the Tizgarine Unit, the G band shows  
12 lower intensities with respect to the D band and the D2 band shows lower intensities and wavenumber  
13  
14 position. Such features correlate to **paleo-temperatures** of approximately 365°C in the BM 2 Unit and  
15  
16 **between 324 and 337°C (according to different approaches, see Tab. 2)** in the Tizgarine Unit.  
17  
18

19  
20 In zone 1, samples 10.1, **6.1** and 9.1 from the Ghomarides show very different spectral features. Spectra in  
21  
22 sample 10.1 **and 6.1** are characterized by two well-developed D and G bands with similar intensities (Fig. 5a),  
23  
24 whereas in sample 9.1 the G band shows higher intensities with respect to the D band and a shoulder toward  
25  
26 lower wavenumbers occurs on the D band (and 5c). Such differences, **shown in Figs. 5a and c**, correspond to  
27  
28 a drop of more than 100°C between **Lower Paleozoic (300-305°C in 10.1 and 296-299°C in 6.1) and**  
29  
30 **Carboniferous samples (195-197°C in sample 9.1). A similar interval gap was also observed the Beni-**  
31  
32 **Hozmar unit where paleo-temperatures range between 352 and 372°C in the Silurian sample 5.1 and**  
33  
34 **between 285 and 288 °C in the Carboniferous sample 3.1 (Tab. 2 and Figs. 5b and d).**  
35  
36  
37

38  
39 In zone 2, the only sample from Filali unit shows spectra at an advanced stage of graphitization, characterized  
40  
41 by a narrow G band with higher intensities with respect to the D band corresponding to temperature of **486-**  
42  
43 **488°C (Fig 4c)**. Moving toward the NE in the Ghomarides, Raman spectra show a progressive increase of  
44  
45 structural disorder with the increase of the D band intensity in samples 18.1 and 17.1 and with a broadening  
46  
47 of both G and D bands in samples 15.1 and 14.1. Raman temperatures indicate a temperature decrease from  
48  
49 the SW to the NE passing from 442-**446°C** in sample 19.1, **to 340-370°C** for samples 18.1 and 17.1 and 246-  
50  
51 **304°C** at 15.1 and 14.1 sampling sites (Fig. 6, **Tab. 2**).  
52  
53  
54  
55  
56  
57  
58  
59  
60

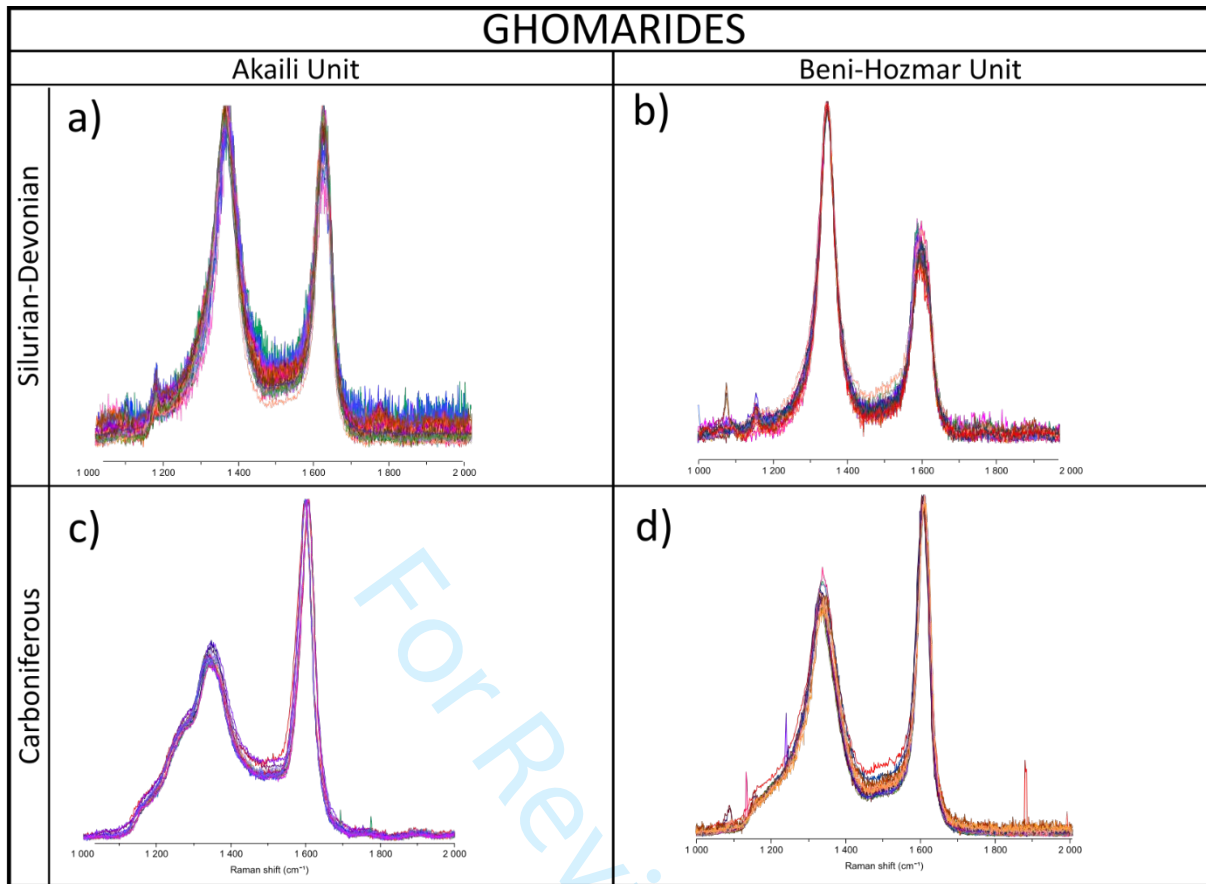


**Figure 5 Differences between Carboniferous and pre- Carboniferous Raman spectra in the Akaili and Beni-Hozmar Units.**

Table 2. TOC data and Raman derived temperatures for the analysed samples. \* Values in *Italic* represent R2 ratio according to Beyssac *et alii*, 2002 ; values in **bold** RA2 ratio according to Lahfid *et alii*, 2010.

Sample	Unit	TOC (%)	T°C mean (LÜNSDORF <i>et alii</i> , 2014)	std T°C	R2/RA2*	std R2/RA2*	T°C mean RA2/R2	std T°C	n° of spectra
Mar 8.1	Beni Mezala 1	0.4	n.d.	n.d.	n.d.	n.d.	n.d.	n.d.	n.d.
Mar 12.1	Beni Mezala 2	2	365.21	19.75	<i>0.62</i>	<i>0.03</i>	365.52	14.26	20
Mar 1.1	Tizgarine	0.7	324.62	17.39	<i>0.68</i>	<i>0.01</i>	337.87	6.80	20
Mar 1.2	Tizgarine	0.8	325.64	16.66	<i>0.66</i>	<i>0.04</i>	332.19	10.31	22
Mar 10.1	Akaili	0.7	298.11	15.39	<b>1.62</b>	<b>0.07</b>	300.91	15.97	32
Mar 9.1	Akaili	0.8	197.00	13.72	<b>0.89</b>	<b>0.13</b>	195.22	29.35	21
Mar 6.1	Akaili	0.4	299.35	21.91	<b>1.60</b>	<b>0.05</b>	296.57	11.13	32
Mar 5.1	Beni Hozmar	0.6	372.24	12.20	<i>0.65</i>	<i>0.03</i>	352.80	12.43	33
Mar 3.1	Beni Hozmar	1.6	285.76	10.95	<b>1.57</b>	<b>0.08</b>	288.57	18.49	27
Mar 4.1	Beni Hozmar	0.4	368.54	15.52	<i>0.64</i>	<i>0.02</i>	356.30	11.01	28
Mar 14.1	Akaili	1.5	246.55	8.93	<b>1.14</b>	<b>0.14</b>	246.86	30.96	21
Mar 15.1	Akaili	1.9	295.71	18.98	<b>1.64</b>	<b>0.08</b>	304.79	18.87	35
Mar 17.1	Akaili	0.7	368.27	9.38	<i>0.65</i>	<i>0.03</i>	380.84	8.02	22
Mar 18.1	Akaili	3.9	342.46	15.28	<i>0.66</i>	<i>0.03</i>	347.64	11.70	24
Mar 19.1	Akaili	1.2	442.23	13.16	<i>0.64</i>	<i>0.03</i>	446.34	7.67	22
Mar 20.1	Filali	0.7	488.07	5.71	<i>0.36</i>	<i>0.06</i>	486.15	6.67	14

## 6. Discussion

### 6.1 RSCM temperatures

The RSCM geothermometer is one of the most used methods to assess the peak temperatures reached during prograde metamorphism (see HENRY *et alii*, 2019 for a complete review). It is based on the variation of the Raman spectrum of graphitic carbon at increasing temperatures, detected by curve-fit derived parameters (PASTERIS & WOPENKA, 1991). Different correlations between Raman parameters and

1  
2  
3 **temperatures have been proposed depending on the fitting approach and the metamorphic types and**  
4 **degree** (BEYSSAC *et alii*, 2002; AOYA *et alii*, 2010; LAHFID *et alii*, 2010; LÜNSDORF *et alii*, 2017; MORI *et alii*,  
5 2017; HENRY *et alii*, 2019; LI *et alii*, 2020). **Among them the most used are those of BEYSSAC *et alii* (2002)**  
6 **and LAHFID *et alii* (2010), based on the R2 and RA2 parameters for high and low-grade metamorphism,**  
7 **respectively. At the highest-grades, CM spectrum is composed by one band in pure graphite and by four**  
8 **bands at about 330°C (BEYSSAC *et alii*, 2002), while in the interval between 200 and 320°C it can be**  
9 **adequately fitted with five Lorentzian bands (LAHFID *et alii*, 2010). While this fitting approach has been**  
10 **successfully applied in a number of studies (BEYSSAC *et alii*, 2004, 2019; NEGRO *et alii*, 2006; GALY *et alii*,**  
11 **2008; DELCHINI *et alii*, 2016; COCHELIN *et alii*, 2018; LAHFID *et alii*, 2019, among others) it has been**  
12 **demonstrated that the parameters calculation can be strongly influenced by the operator fitting approach**  
13 **(LÜNSDORF *et alii*, 2014). For this reason an automatic method has been proposed by LÜNSDORF &**  
14 **LÜNSDORF (2016) to provide higher comparability to the RSCM geothermometer.**

15  
16  
17  
18  
19  
20  
21  
22  
23  
24  
25  
26  
27  
28  
29  
30  
31  
32  
33  
34  
35  
36  
37  
38  
39  
40  
41  
42  
43  
44  
45  
46  
47  
48  
49  
50  
51  
52  
53  
54  
55  
56  
57  
58  
59  
60

In this work, the automatic approach of LÜNSDORF & LÜNSDORF (2016) is particularly suitable since many samples lie in the paleo-temperature range between 300 and 350°C (Tab. 2). This is the interval where the two geothermometers by BEYSSAC *et alii* (2002) and LAHFID *et alii* (2010) overlap and the choice of a bad fitting approach can lead to paleo-temperatures misinterpretation. Nevertheless, in order to constrain as much as possible our thermal data and avoid errors that can derived from the automatic processing of some spectra with low signal-to-noise ratio (Fig. 5), the RSCM temperatures derived with the IFORS software have been double checked by calculating the R2 or RA2 ratio and derived paleo-temperatures. Results shown in Table 2 indicate that maximum differences reached 20°C only in sample 3.1 and that they are lower than 10°C in most of the dataset. This evidence indicate a general agreement in paleo-temperature results considering that the error of the RSCM methods is always comprised between 40-50°C (BEYSSAC *et alii*, 2002); LAHFID *et alii*, 2010; LÜNSDORF & LÜNSDORF, 2016).

The approach based on a comparative between two fitting procedures strengthen the quality of the data presented in this work and further confirms the validity of the IFORS software.



## 6.2 Thermal evolution of the Rif and comparison with previous works

The Rif-Betic orogen is a key area in the Mediterranean puzzle to decipher the western Mediterranean geodynamic evolution (ROYDEN & FACCENNA, 2018 for a review) and it offers the opportunity to study both exhumed root of the Alpine orogen (e.g. Sebides) and terranes derived from the fragmented Variscan chain (e.g. Ghomarides).

The metamorphic evolution of **the internal units of the Rif-Betic orogen** has been the subject of detailed studies focused on the outcrops of Beni Mzala antiform and around the Beni Bousera peridotite (KORNPROBST, 1974; DURAND-DELGA, 1980; CHALOUAN AND MICHARD, 1990; MICHARD *et alii*, 2006; NEGRO *et alii*, 2006; CHALOUAN *et alii*, 2008; PLATT *et alii*, 2013, MARRONE *et alii*, 2021).

In the Federico Unit, cropping out at the core of the Beni Mzala antiform, paleo-temperatures derived from the analyses of carbonaceous material **were** not present in literature given the moderate-to-low TOC content (NEGRO *et alii.*, 2006 and Table 2). Despite this, we were able to carry out enough CM spectra whose RSCM geothermometer shows values of about 320°C in the Tizgarine Unit and of about 365°C in BM 2 one. Data from Tizgarine **Unit** suggest that **it** suffered slightly warmer conditions than those calculated by the cookeite-pyrophyllites-phengite association (about 300°C according to BOUYBAOUENE *et alii.*, 1998). On the other hand, the average temperature calculated for BM2, **even if slightly lower, seem to confirm** the minimum temperatures of 380°C provided by the presence of relict Mg-Carpholite **estimated by** BOUYBAOUENE *et alii*, (1998) **rather than those of** 450°C calculated by VIDAL *et alii* (1999) by means of Chl-Cld thermometer. Results for the BM2 should be considered only as a first approximation, since we were able to derive Raman maximum temperature only on one sample and therefore need to be further validated in the future.

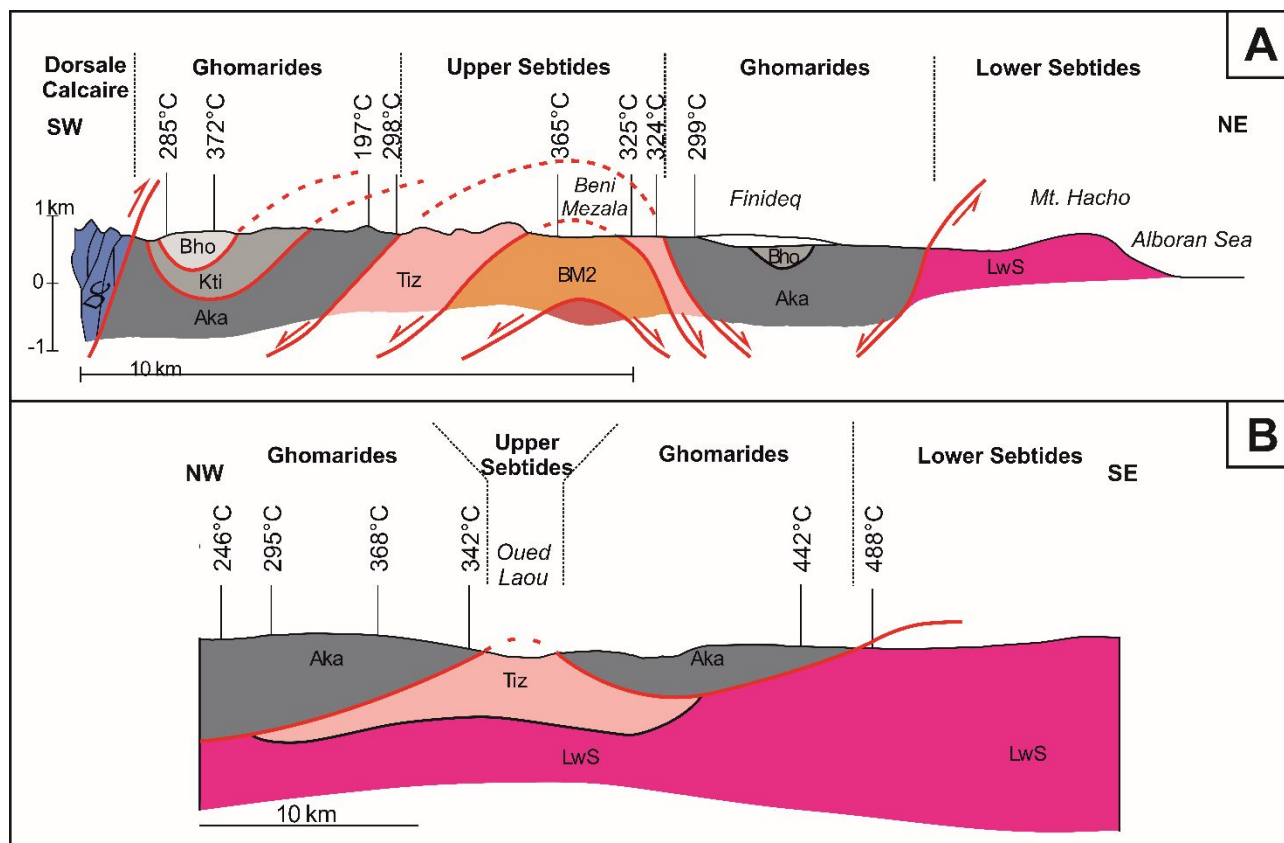


**Figure 6** Raman-derived temperatures plotted on cross-sections 1 and 2 located in Fig. 1. Redrawn and modified after NEGRO *et alii*, 2006 and CHALOUAN *et alii*, 2008. Temperature shown in the figure are derived from the IFORS software (LÜNSDORF & LÜNSDORF, 2016). For comparison with other RSCM approaches see Table 2 and section 6.1. Acronyms: DC – Dorsale Calcaire; BHo – Beni Hozmar; KTi – Koudiat Tiziane; Aka – Akaili; Tiz – Tizgarine; BM2 – Beni Mzala; Lws – Lower Sebides.

In the Ghomarides cropping out on the flanks of the Beni Mezala antiform, NEGRO *et alii* (2006) already provided Raman measurements on four samples from the Akaili Unit and on one sample from Koudiat Tiziane unit, suggesting temperature always below 330°C, as this is the lower calibration limit of the RSCM geothermometer based on R2 parameter proposed by BEYSSAC *et alii* (2002). **This limit can now be overcome since new correlations at low metamorphism are now available in literature** for low metamorphism (RAHL *et alii*, 2005; LAHFID *et alii*, 2010; LÜNSDORF *et alii*, 2017) and in diagenesis (SCHITO *et alii*, 2017; 2019; HENRY *et alii*, 2019) allowing to use the RSCM geothermometers in a variety of geological conditions (MUIRHEAD *et alii*, 2019; KEDAR *et alii*, 2020; NIRRENGARTEN *et alii*, 2020).

1  
2  
3 Our data on the Ghomarides in the northern sector of the Rif belt, outline a paleo-temperature jump  
4 between pre-Carboniferous and Carboniferous successions both in the Akaili and Beni Hozmar units. In  
5 detail, the maximum temperatures acquired during the Eo-Variscan phases by the pre-Carboniferous rocks  
6 are at the boundary between anchizone and epizone (about 300°C, FREY *et alii*, 1987) in the Akaili Unit and  
7 in the epizone (about 370°C) in the Beni-Hozmar (Table 2 and Fig. 7). On the contrary, Visean rocks in the  
8 Akaili Unit show values typical of deep diagenetic/low anchizone conditions (about 200°C) reached during  
9 the late Variscan phase, while temperatures in rocks with the same age are about 280°C in the Beni-Hozmar  
10 unit. Previous data from illite crystallinity (CHALOÜAN & MICHARD, 1985) also indicated lower  
11 metamorphism for Carboniferous rocks in the Ghomarides, but with no significant differences among their  
12 units (CHALOUAN & MICHARD, 1985; CHALOUAN & MICHARD, 1990). Thus our data show thus for the first  
13 time in detail the thermal structure across the Paleozoic Ghomarides, highlighting that the Beni-Hozmar  
14 Unit suffered metamorphism at higher temperatures with respect to the Akaili Unit both during Eo and  
15 Late Varsican events. It is particularly interestingly to note that almost the same gap in paleo-temperatures  
16 between 80 and 100°C is recorded above and below the Variscan unconformity among the two units and  
17 this could suggest that they kept some similar structural relationship during both events.

18  
19 As matter of fact very little is known about the Variscan history of the Paleozoic units in the Ghomarides or  
20 in similar units in the Maghreb chain. In the Malaguides (southern Spain), the pre-Alpine deformation  
21 in Paleozoic rocks is very poorly constrained (MARTIN-ALGARRA *et alii*, 2009). HT/LP mineralogical  
22 assemblage, associated to paleo-temperatures of about 500°C were locally found in the lowermost  
23 Ordovician-Silurian rocks near the Ronda peridotite (RUIZ-CRUZ & GALÁN, 2002; RUIZ-CRUZ & NOVÁK,  
24 2003; NEGRO *et alii*, 2006), while clay mineralogical analyses (ABAD *et alii*, 2003) and CAI (Conodont  
25 Alteration Index) determination (MARTIN-ALGARRA *et alii*, 2009) failed to precisely detect variation at  
26 lower paleo-temperature and the whole Palaeozoic section is generally described to have suffered  
27 anchizone to epizone metamorphism. In both Greater and Lesser Kabylia (northern Algeria), similarly to the  
28 Ghomarides, MICHARD *et alii* (2006) describe a Late Devonian Eo-variscan phase that led to greenschists  
29 metamorphism and a Late-Variscan phase responsible for the folding of the unconformable Carboniferous  
30 deposits. These domains, together with the Calabria-Peloritan arc are thought to share a similar structural

1  
2  
3 position in a western (southwestern? RAUMER *et alii*, 2002) sector of the Paleotethys, rather than in the  
4  
5 Rheic realm such as other Variscan sectors in Iberia and Morocco ( i.e. Balearic, Iberian and Moroccan  
6  
7 mesetas), and to suffered similar metamorphisms (CHALOUAN & MICHARD, 1990; RAUMER *et alii*, 2002;  
8  
9 MARTIN-ALGARRA *et alii*, 2009). This hypothesis is mainly based on stratigraphic and structural affinities  
10  
11 of the Paleozoic successions, even if at low metamorphic degree the lack of a more comprehensive dataset  
12  
13 hampers a full understanding. The RSCM approach proposed in this work has shown to be promising. Thus,  
14  
15 it could be applied in similar areas and provide evidence (or not) of a common metamorphic history of the  
16  
17 Variscan terranes in the Mediterranean area.  
18  
19  
20  
21  
22  
23  
24  
25  
26  
27  
28  
29  
30  
31  
32  
33  
34  
35  
36  
37  
38  
39  
40  
41  
42  
43  
44  
45  
46  
47  
48  
49  
50  
51  
52  
53  
54  
55  
56  
57  
58  
59  
60

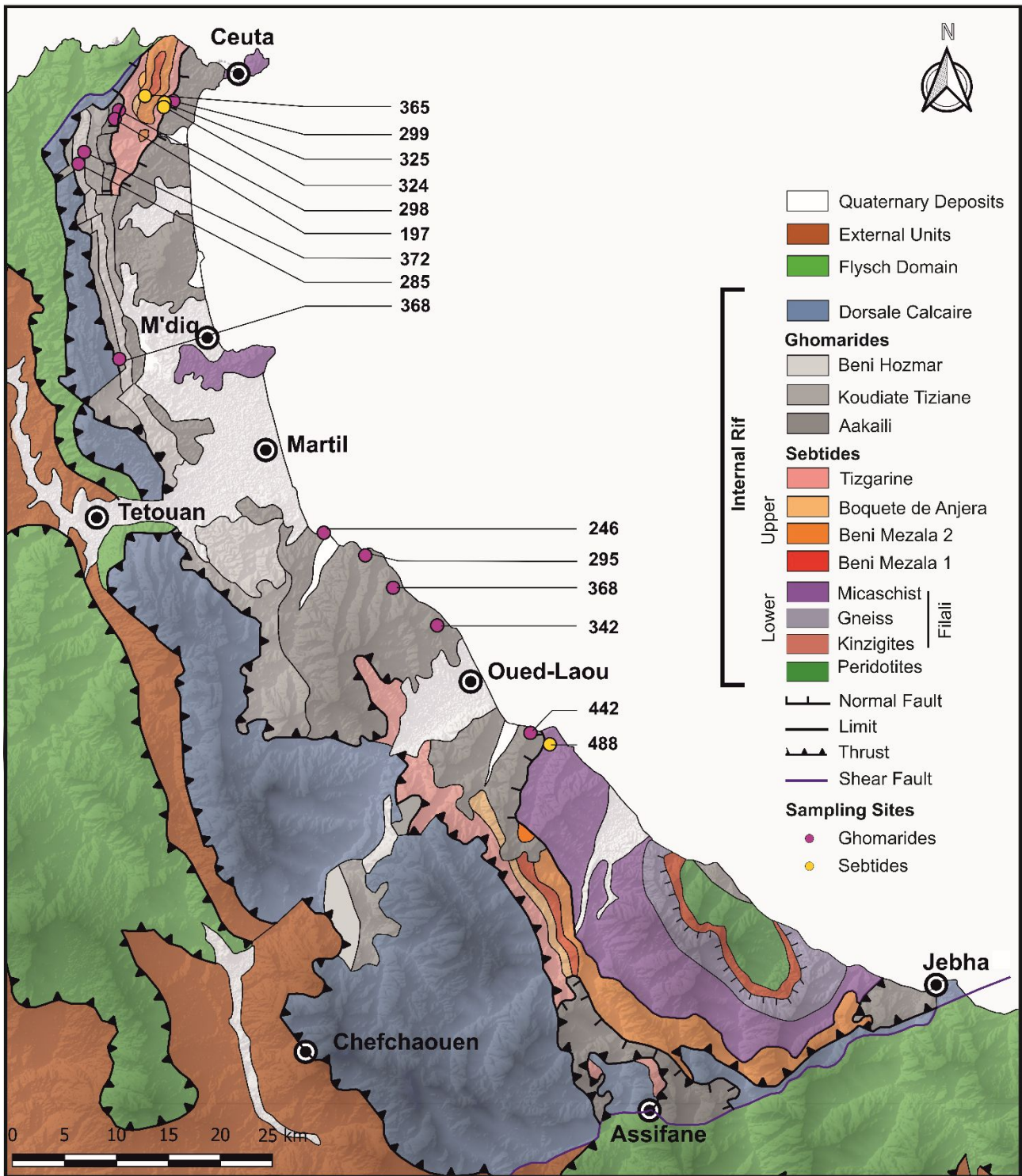


Figure 7. Geological map of internal Rif with indicated Raman-derived maximum paleo-temperatures. Temperature shown in the figure are derived from the IFORS software (LÜNSDORF & LÜNSDORF, 2016). For comparison with other RSCM approaches see Table 2 and section 6.1.

1  
2  
3 In the southern sector (Zone 2), samples were collected along the route from Ras Mazari to Cape Zaouia (Fig.  
4  
5 **7). The main contribution of this work was to unravel paleo-temperatures for the Devonian and**  
6  
7 **Carboniferous rocks (samples 15.1 and 14.1) that were previously reported to be lower than 330°C by**  
8  
9 **NEGRÒ *et alii* (2006). New data show a jump in paleo-temperature of about 50°C between Carboniferous**  
10  
11 **and Devonian rocks moving from Ras Mazari to Tamrabete area south of Tetouan town (Fig. 7). This gap**  
12  
13 **is lower than that observed in the northern sector for the Akaili unit. Moreover, the observation that**  
14  
15 **paleo-temperatures of the pre-Carboniferous samples are similar, suggest that Carboniferous rocks here**  
16  
17 **experienced higher thermal stress probably due to a Late Oligocene (Early Miocene?) thermal event that**  
18  
19 **affected the area (see discussion below).**

20  
21  
22  
23 **As matter of fact,** MICHARD *et alii*. (2006) showed in this area that K/Ar on white mica isotopic ages tend to  
24  
25 increase moving from the Ghomaride–Sebtide tectonic contact (Zaouia Fault, 25My) to the Ras Mazari area  
26  
27 where the apparent ages are of about 183 My. This age distribution, coupled with the increase of Raman  
28  
29 temperature from Ras Mazari to the Zaouia Fault (Fig. 8 from NEGRÒ *et alii*, 2006) has been interpreted as a  
30  
31 thermal event connected to the emplacement of the Beni-Boussera peridotites. Nevertheless, recent works  
32  
33 recently questioned the hypothesis of “hot” exhumation of the Rif–Betic peridotites during the Alpine  
34  
35 orogeny (ROSSETTI *et alii*, 2020; FARAH *et alii*, 2021). **By means of** geochronological data on the migmatitic  
36  
37 rocks that form the envelopment of the Beni Bousera peridotite, ROSSETTI *et alii*, (2020) point out a main  
38  
39 Hercynian thermal event, associated with intra-crustal emplacement of the peridotite, **occurred and was**  
40  
41 **followed by cooling and exhumation from deep to shallower crustal conditions. The final stage of exhumation**  
42  
43 **is constrained by the authors to the Early Miocene and is coeval with the main stage of the Alboran basin**  
44  
45 **back-arc extension. At this time, the westward retreat of the Tethyan subduction caused lithosphere**  
46  
47 **delamination and asthenosphere upwelling that led to crustal partial melting and diffuse magmatism as**  
48  
49 **outlined by the andalusite-bearing dykes that intruded the Beni Bousera units (ROSSETTI *et alii*, 2013). All**  
50  
51 **these pieces of evidence suggest that the thermal gradient depicted by Raman data in the present work and**  
52  
53 **in NEGRÒ *et alii* (2006), as well as the thermal reset of the K/Ar on white mica isotopic ages (MICHARD *et alii*,**  
54  
55 **2006), related to an Alpine HT metamorphic event that is independent from the peridotite emplacement.**  
56  
57  
58  
59  
60 Given this, our data show some differences with respect to **the paleo-temperature pattern** provided by

1  
2  
3 NEGRÒ *et alii* (2006). **This can be observed**, particularly, in the area between Ras Mazari and R Mekkad,  
4  
5 where **paleo**-temperatures estimations differ for more than 100°C (Fig. 7). Considering that we followed the  
6  
7 analytical procedure for Raman spectra acquisition by BEYSSAC *et alii* (2002), a possible source of error could  
8  
9 be **envisaged** in different fitting methods. **However, in our case, the paleo-temperatures from R2 shown in**  
10  
11 **Tab. 2 show a very good agreement with to those calculated with the IFORS software, strengtning our**  
12  
13 **results.** The fitting procedure **or the user interpretation could in part** justify differences **observed** among  
14  
15 similar spectra as shown in Fig. 7b (comparison spectra at 442-485°C and 488-508°C), **but cannot be held**  
16  
17 **responsible for spectra related to samples near Tamkerte, which show very different features. . In this**  
18  
19 **case, the differences are due to different heating conditions** (Fig. 8b). Working with organic matter,  
20  
21 differences in thermal maturity (maximum paleo-temperature) can be usually ascribed to the presence of  
22  
23 reworked material (LACZO & JAMBOR, 1988; LUCCA *et alii*, 2018; QIN *et alii*, 2018; BALESTRA *et alii*, 2019),  
24  
25 but this **does not** seem to be the case, since spectra in our samples are very homogeneous. This piece of  
26  
27 evidence suggests that paleo-temperatures in this sector of **the** Ghomarides, has higher spread than  
28  
29 previously assessed. One possible explanation for this spread could be the effect of localized shear/strain  
30  
31 (KITAMURA *et alii*, 2012; KUO *et alii*, 2014, 2017; KEDAR *et alii*, 2020) **that could have locally increased the**  
32  
33 **thermal stress.** Moreover, as shown by MÜNCH *et alii*. (2021) in the area near Ceuta town, the internal zone  
34  
35 of the Rif chain has been dissected by E-W and NNW-SSE normal faults between about 18 an 11 My and this  
36  
37 can explain why a regular trend of increasing paleo-temperatures from Ras Mazari to Cape Zaouia has not  
38  
39 been **detected** (Fig. 8).  
40  
41  
42  
43  
44  
45  
46  
47  
48  
49  
50  
51  
52  
53  
54  
55  
56  
57  
58  
59  
60

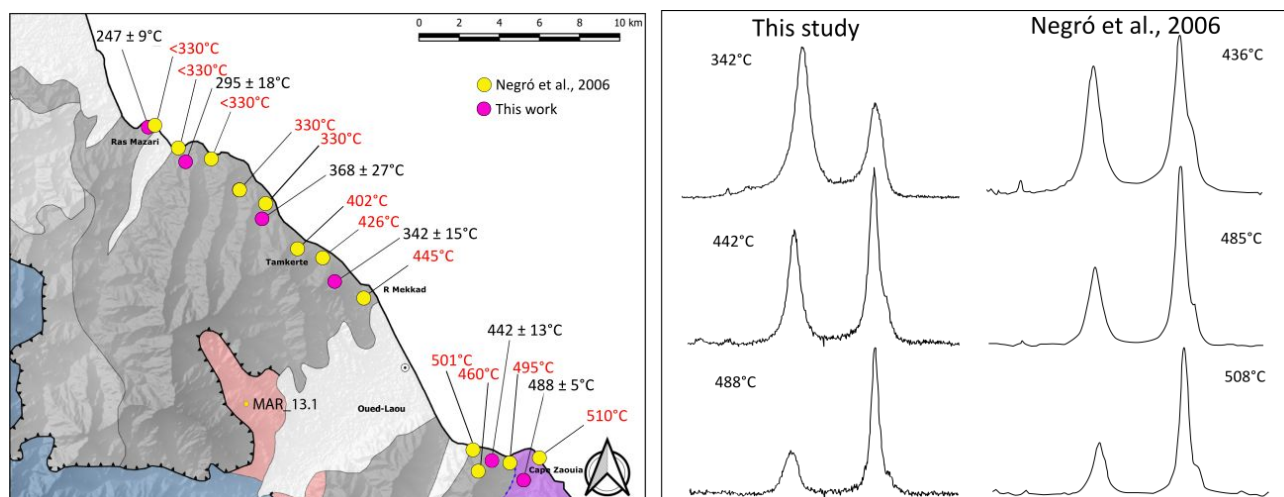


Figure 8 a) Raman paleo- temperatures from this work and from NEGRO *et alii.* (2006), plotted in zone 2 for comparison. b) Comparison between Raman spectra and related paleo-temperatures from this work and NEGRO *et alii.* (2006). Spectra on the same row correspond to samples from the same sampling area. Paleo-temperature shown in the figure are derived from the IFORS software (LÜNSDORF & LÜNSDORF, 2016). For comparison with other RSCM approaches see Table 2 and section 6.1.

## Conclusion

In this work we implemented the paleo-thermal database of the Internal Rif in Morocco providing a new set of data in the Sebtime and Ghomaride successions through Raman spectroscopy on dispersed organic matter. In the upper Sebtime cropping out in the Beni Mezala antiform we show that Tizgarine and BM 2 Units experienced maximum paleo-temperature of about 320 and 370°C, respectively. In the same area, data from Ghomarides show a temperature jump across the Eo-Variscan unconformity in both Akaili and Beni Hozmar Units. Interestingly, our data also indicate higher paleo-temperatures in Beni Hozmar suggesting higher metamorphic conditions suffered by this unit.

In the southern area between Ras Mazari and Cape Zaouia, samples collected from the Akaili Unit show increasing paleo-temperatures moving towards the tectonic contact with the Filali Unit connected with a Late Oligocene high temperature metamorphic event **and** not related to emplacement of the Beni-Bousera peridotite.



## Acknowledgments

We are greatly indebted with M.N. Zaghloul for fruitful discussions and for introduce us to Rif geology. We kindly acknowledge the Editor in chief Federico Rossetti, the associated editor Giulio Viola and two anonymous reviewers for their constructive criticisms that improved the original version of this paper.

## References

- ABAD I., NIETO F., PEACOR D.R. AND VELILLA N. (2003) - *Prograde and retrograde diagenetic and metamorphic evolution in metapelitic rocks of Sierra Espuna (Spain)*. Clay Minerals, **38**, 1–23.
- AOYA M. KOUKETSU Y., ENDO S., SHIMIZU H., MIZUKAMI T., NAKAMURA D., WALLIS S. (2010) - *Extending the applicability of the Raman carbonaceous-material geothermometer using data from contact metamorphic rocks*. Journal of Metamorphic Geology, **28**, 895–914,
- ATOUBAT A., CORRADO S., SCHITO A., HAISSAN F., GIMENO-VIVES O., MOHN G.,FRIZON DE LAMOTTE D. (2020) - *Validating Structural Styles in the Flysch Basin Northern Rif (Morocco) by Means of Thermal Modeling*. Geosciences, **10**, 325.
- AZDIMOUSA A., BOURGOIS J., POUPEAU G., VÁZQUEZ M., ASEBRIY L. ,LABRIN E. (2014) - *Fission track thermochronology of the Beni Bousera peridotite massif (Internal Rif, Morocco) and the exhumation of ultramafic rocks in the Gibraltar Arc*. Arabian Journal of Geosciences, **7**, 1993–2005.
- BALESTRA M., CORRADO S., ALDEGA L., MORTICELLI M.G., SULLI A., RUDKIEWICZ J.-L.,SASSI W. (2019) - *Thermal and structural modeling of the Scillato wedge-top basin source-to-sink system: Insights into the Sicilian fold-and-thrust belt evolution (Italy)*. GSA Bulletin, **131**, 1763–1782.
- BEYSSAC O., GOFFÉ B., CHOPIN C., ROUZAUD J. N. (2002). *Raman spectra of carbonaceous material in metasediments: a new geothermometer*. Journal of Metamorphic Geology, **20**(9), 859-871.
- BEYSSAC O., BOLLINGER L., AVOUAC J.P., GOFFÉ B. (2004) - *Thermal metamorphism in the lesser Himalaya of Nepal*

- 1  
2  
3 *determined from Raman spectroscopy of carbonaceous material. Earth and Planetary Science Letters,*  
4  
5 **225**, 233–241
- 6  
7 BEYSSAC O., PATTISON D.R.M., BOURDELLE F. (2019) - *Contrasting degrees of recrystallization of*  
8  
9 *carbonaceous material in the Nelson aureole, British Columbia and Ballachulish aureole, Scotland, with*  
10  
11 *implications for thermometry based on Raman spectroscopy of carbonaceous material. Journal of*  
12  
13 *Metamorphic Geology*, **37**, 71–95.
- 14  
15  
16 BOOTH-REA G., RANERO C.R., MARTÍNEZ-MARTÍNEZ J.M., GREVEMEYER I. (2007) - *Crustal types and Tertiary*  
17  
18 *tectonic evolution of the Alborán sea, western Mediterranean. Geochemistry, Geophysics, Geosystems,*  
19  
20 **8**(10).
- 21  
22  
23 BOUILLIN J. (1986) - *Le "bassin maghrebin"; une ancienne limite entre l'Europe et l'Afrique à l'ouest des Alpes.*  
24  
25 *Bulletin de la Société Géologique de France*, **2**, 547–558.
- 26  
27  
28 BOUYBAOUENE M., MICHARD A., GOFFE B. (1998) - *High-pressure granulites on top of the Beni Bousera*  
29  
30 *peridotites, Rif Belt, Morocco; a record of an ancient thickened crust in the Alboran Domain. Bulletin de*  
31  
32 *la Société Géologique de France*, **169**, 153–162.
- 33  
34  
35 CALVO M., CUEVAS J., TUBIA J.M. (2001) - *Preliminary palaeomagnetic results on Oligocene–early Miocene*  
36  
37 *mafic dykes from southern Spain. Tectonophysics*, **332**, 333–345.
- 38  
39  
40 CASTIGLIONI C., MAPELLI C., NEGRI F., ZERBI G. (2001) - *Origin of the D line in the Raman spectrum of graphite:*  
41  
42 *A study based on Raman frequencies and intensities of polycyclic aromatic hydrocarbon molecules.*  
43  
44 *Journal of Chemical Physics*, **114**, 963–974.
- 45  
46  
47 CHALOUAN A. (1986). *Les nappes Ghomarides (Rif septentrional, Maroc), un terrain varisque dans la chaîne*  
48  
49 *alpine. Thèse de doctorat Université Louis Pasteur (Strasbourg). Vol 1, 333 p.*
- 50  
51  
52 CHALOUAN A. & MICHARD A. (1990) - *The Ghomarides nappes, Rif coastal range, Morocco: a variscan chip in*  
53  
54 *the Alpine belt. Tectonics*, **9**, 1565–1583.
- 55  
56  
57 CHALOUAN A. & MICHARD A. (2004) - *The Alpine Rif Belt (Morocco): a case of mountain building in a*  
58  
59 *subduction-subduction-transform fault triple junction. Pure and Applied Geophysics*, **161**, 489–519.
- 60  
61  
62 CHALOUAN A., MICHARD A., EL KADIRI K., NEGRO F., FRIZON DE LAMOTTE D., SOTO J.-I., SADDIQUI O. (2008)-  
63  
64 *The Rif belt. In: Michard, A. (Ed.), The Geology of Morocco. Springer, Berlin*, **116**, 203–302,

- 1  
2  
3 CHALOUAN A. & MICHARD A. (1985) - *Age anté-Viséen de la phase varisque paroxysmale dans les nappes*  
4  
5 *ghomarides du Rif interne (Maroc)/Pre-Visean age of the main Variscan folding in the Ghomarides*  
6  
7 *nappes, Inner Rif, Morocco. Sciences Géologiques, Bulletins et Mémoires, 38, 165–174.*  
8  
9  
10 COCHELIN B., LEMIRRE B., DENÈLE Y., DE SAINT BLANQUAT M., LAHFID A., DUCHÊNE S. (2018) - *Structural*  
11  
12 *inheritance in the central pyrenees: The variscan to Alpine tectonometamorphic evolution of the Axial*  
13  
14 *Zone. Journal of the Geological Society, 175, 336–351.*  
15  
16  
17 DELCHINI S., LAHFID A., PLUNDER A., MICHARD A. (2016) - *Applicability of the RSCM geothermometry*  
18  
19 *approach in a complex tectono-metamorphic context: The Jebilet massif case study (Variscan Belt,*  
20  
21 *Morocco). Lithos, 256, 1–12.*  
22  
23  
24 DI DONATO E., TOMMASINI M., FUSTELLA G., BRAMBILLA L., CASTIGLIONI C., ZERBI G., SIMPSON C.D.,  
25  
26 MÜLLEN K., NEGRI F. (2004) - *Wavelength-dependent Raman activity of D2h symmetry polycyclic*  
27  
28 *aromatic hydrocarbons in the D-band and acoustic phonon regions. Chemical Physics, 301, 81–93.*  
29  
30  
31 DIDON J., DURAND-DELGA M., KORNPORST J. (1973) - *Homologies géologiques entre les deux rives du détroit*  
32  
33 *de Gibraltar. Bulletin de la Société Géologique de France, 7, 77–105.*  
34  
35  
36 DOCHERTYC. & BANDA E. (1995) - *Evidence for the eastward migration of the Alboran Sea based on regional*  
37  
38 *subsidence analysis: a case for basin formation by delamination of the subcrustal lithosphere? Tectonics,*  
39  
40 *14, 804–818.*  
41  
42  
43 DUCOUX M., JOLIVET L., CALLOT J. P., AUBOURG C., MASINI E., LAHFID A., HOMMONNAY E., CAGNARD F.,  
44  
45 GUMIAUX C., BAUDIN T. (2019) - *The Nappe des Marbres Unit of the Basque-Cantabrian Basin: The*  
46  
47 *Tectono-thermal Evolution of a Fossil Hyperextended Rift Basin. Tectonics, 38, 3881–3915.*  
48  
49  
50 DURAND-DELGA M. (1980) - *Le cadre structural de la Méditerranée occidentale. Geologie des chaines alpines*  
51  
52 *issues de la Tethys, BRGM ed., Orleans, pp. 67–85.*  
53  
54  
55 DURAND-DELGA M. & OLIVIER P. (1988) - *Evolution of the Alboran block margin from Early Mesozoic to Early*  
56  
57 *Miocene time. In: The Atlas System of Morocco. Springer, Berlin, pp. 463–480.*  
58  
59  
60 EL KADIRI K., LINARES A., OLORIZ F. (1992) - *La Dorsale calcaire rifaine (Maroc septentrional): Evolution*  
*stratigraphique et géodynamique durant le Jurassique-Crétacé. Notes et mémoires du Service*  
*géologique, 217–265.*

1  
2  
3  
4  
5  
6  
7  
8  
9  
10  
11  
12  
13  
14  
15  
16  
17  
18  
19  
20  
21  
22  
23  
24  
25  
26  
27  
28  
29  
30  
31  
32  
33  
34  
35  
36  
37  
38  
39  
40  
41  
42  
43  
44  
45  
46  
47  
48  
49  
50  
51  
52  
53  
54  
55  
56  
57  
58  
59  
60

- FARAH A., MICHARD A., SADDIQI O., CHALOUAN A., CHOPIN C. (2021) - *The Beni Bousera marbles, record of a Triassic-Early Jurassic hyperextended margin in the Alpujarrides-Sebtides units (Rif belt)*, BSGF - Earth Sciences Bulletin, **192**(1), 26.
- FAVRE P. & STAMPFLI G.M. (1992) - *From rifting to passive margin: the examples of the Red Sea, Central Atlantic and Alpine Tethys*. Tectonophysics, **215**, 69–97.
- FRIZON DE LAMOTTE D., RAULIN C., MOUCHOT N., WROBEL-DAVEAU J., BLANPIED C., RINGENBACH J. (2011) - *The southernmost margin of the Tethys realm during the Mesozoic and Cenozoic: Initial geometry and timing of the inversion processes*. Tectonics, **30**(3), TC3002.
- GALY V., BEYSSAC O., FRANCE-LANORD C., EGLINTON T. (2008) - *Recycling of graphite during Himalayan erosion: A geological stabilization of carbon in the crust*. Science, **322**, 943–945.
- GARCÍA-DUEÑAS V., BALANYÁ J.C., MARTÍNEZ-MARTÍNEZ J.M. (1992) - *Miocene extensional detachments in the outcropping basement of the northern Alboran basin (Betics) and their tectonic implications*. Geomarine Letters, **12**, 88–95.
- GIMENO-VIVES O., FRIZON DE LAMOTTE D., LEPRÊTRE R., HAISSSEN F., ATOUABAT A., MOHN G. (2020) - *The structure of the Central-Eastern External Rif (Morocco); Poly-phased deformation and role of the underthrusting of the North-West African paleo-margin*. Earth-Science Reviews, 103198.
- GIMENO-VIVES O., MOHN G., BOSSE V., HAISSSEN F., ZAGHLOUL M.N., ATOUABAT A., FRIZON DE LAMOTTE D. (2019) - *The Mesozoic margin of the Maghrebian Tethys in the Rif belt (Morocco): Evidence for polyphase rifting and related magmatic activity*. Tectonics, **38**, 2894–2918.
- GUEDES A., VALENTIM B., PRIETO A.C., RODRIGUES S., NORONHA F. (2010) - *Micro-Raman spectroscopy of collotelinite, fusinite and macrinite*. International Journal of Coal Geology, **83**, 415–422.
- GUERRERA F., MARTÍN-ALGARRA A., PERRONE V. (1993) - *Late Oligocene-Miocene syn-/late-orogenic successions in western and central Mediterranean chains from the Betic Cordillera to the southern Apennines*. Terra Nova, **5**, 525–544.
- GUERRERA F., MARTÍN-MARTÍN M., PERRONE V., TRAMONTANA M. (2005) - *Tectono-sedimentary evolution of the southern branch of the Western Tethys (Maghrebian Flysch Basin and Lucanian Ocean): consequences for Western Mediterranean geodynamics*. Terra Nova, **17**, 358–367.

- 1  
2  
3 GUEYDAN F., PITRA P., AFIRI A., POUJOL M., ESSAIFI A., PAQUETTE J. (2015). *Oligo-Miocene thinning of the*  
4  
5 *Beni Bousera peridotites and their Variscan crustal host rocks, Internal Rif, Morocco*. *Tectonics*, **34**,  
6  
7 1244–1268.  
8  
9  
10 HENRY D.G., JARVIS I., GILLMORE G., STEPHENSON M., EMMINGS J.F. (2018) - *Assessing low-maturity organic*  
11  
12 *matter in shales using Raman spectroscopy: Effects of sample preparation and operating procedure*.  
13  
14 *International Journal of Coal Geology*, **191**, 135–151.  
15  
16 HENRY D.G., JARVIS I., GILLMORE G., STEPHENSON M. (2019) - *Raman spectroscopy as a tool to determine*  
17  
18 *the thermal maturity of organic matter: Application to sedimentary, metamorphic and structural*  
19  
20 *geology*. *Earth-Science Reviews*, **198**, 102936.  
21  
22  
23 KEDAR L., BOND C.E., MUIRHEAD D. (2020). *Carbon ordering in an aseismic shear zone: Implications for*  
24  
25 *Raman geothermometry and strain tracking*. *Earth and Planetary Science Letters*, **549**, 116536.  
26  
27  
28 KITAMURA M., MUKOYOSHI H., FULTON P.M., HIROSE T. (2012) - *Coal maturation by frictional heat during*  
29  
30 *rapid fault slip*. *Geophysical research letters*, **39**, L16302.  
31  
32  
33 KORNPORST J. (1974) - *Contribution h l'Etude petrographique et structurale de la zone interne du Rif (Maroc*  
34  
35 *Septentrional)*. *Notes et Memoirs de la Service Geologique de Maroc*, 251, 256 pp.  
36  
37  
38 KUO L.W., LI H., SMITH S.A.F., DI TORO G., SUPPE J., SONG S.R., NEILSEN S., SHEU H.S., SI J. (2014) - *Gouge*  
39  
40 *graphitization and dynamic fault weakening during the 2008 Mw 7.9 Wenchuan earthquake*. *Geology*,  
41  
42 **42**, 47–50.  
43  
44  
45 KUO L.W., DI FELICE, F., SPAGNOLO E., DI TORO G., SONG S.R., ARETUSINI S., LI H., SUPPE J., SI J., WEN C.Y.  
46  
47 (2017) - *Fault gouge graphitization as evidence of past seismic slip*. *Geology*, **45**, 979–982.  
48  
49  
50 LACZO I. & JAMBOR A. (1988) - *Secondary Heating of Vitrinite: Some Geological Implications*. in *The*  
51  
52 *Pannonian Basin: A Study in Basin Evolution*. AAPG Special Volumes. **M45**, 311-318.  
53  
54  
55 LAHFID A., BEYSSAC O., DEVILLE E., NEGRO F., CHOPIN C., GOFFÉ B. (2010) - *Evolution of the Raman spectrum*  
56  
57 *of carbonaceous material in low-grade metasediments of the Glarus Alps (Switzerland)*. *Terra Nova*, **22**,  
58  
59 354–360.  
60  
61  
62 LAHFID A., BAIDDER L., OUANAIMI H., SOULAIMANI A., HOEPFFNER C., FARAH A., SADDIQUI O., MICHARD A.  
63  
64 (2019) - *From extension to compression: high geothermal gradient during the earliest Variscan phase of*

1  
2  
3  
4  
5  
6  
7  
8  
9  
10  
11  
12  
13  
14  
15  
16  
17  
18  
19  
20  
21  
22  
23  
24  
25  
26  
27  
28  
29  
30  
31  
32  
33  
34  
35  
36  
37  
38  
39  
40  
41  
42  
43  
44  
45  
46  
47  
48  
49  
50  
51  
52  
53  
54  
55  
56  
57  
58  
59  
60

*the Moroccan Meseta; a first structural and RSCM thermometric study*. European Journal of Mineralogy, **31**, 695–713.

LEBLANC D. (1979) - *Étude Géologique Du Rif Externe Oriental Au Nord de Taza (Maroc)*. Éditions du Service géologique du Maroc, **281**, 293 pp.

LEPRÊTRE R., FRIZON DE LAMOTTE D., COMBIER V., GIMENO-VIVES O., MOHN G., ESCHARD R. (2018) - *The Tell-Rif orogenic system (Morocco, Algeria, Tunisia) and the structural heritage of the southern Tethys margin*. BSGF-Earth Sciences Bulletin, **189**(2), 10.

LI C.Z. (2007) - *Some recent advances in the understanding of the pyrolysis and gasification behaviour of Victorian brown coal*. Fuel, **86**, 1664–1683.

LI K., RIMMER S.M., PRESSWOOD S.M., LIU Q. (2020) - *Raman spectroscopy of intruded coals from the Illinois Basin: Correlation with rank and estimated alteration temperature*. International Journal of Coal Geology, **219**, 103369.

LUCCA A., STORTI F., MOLLI G., MUCHEZ P., SCHITO A., ARTONI A., BALSAMO F., CORRADO S., SALVIOLI-MARIANI E. (2018) - *Seismically enhanced hydrothermal plume advection through the process zone of the Compione extensional Fault, Northern Apennines, Italy*. Bulletin of the Geological Society of America, **131**, 547–571.

LÜNSDORF N.K. (2016) - *Raman spectroscopy of dispersed vitrinite - Methodical aspects and correlation with reflectance*. International Journal of Coal Geology, **153**, 75–86.

LÜNSDORF N.K. & LÜNSDORF J.O. (2016) - *Evaluating Raman spectra of carbonaceous matter by automated, iterative curve-fitting*. International Journal of Coal Geology, **160**, 51–62.

LÜNSDORF N.K., DUNKL I., SCHMIDT B.C., RANTITSCH G., VON EYNATTEN H. (2014) - *Towards a higher comparability of geothermometric data obtained by Raman spectroscopy of carbonaceous material. Part I: evaluation of biasing factors*. Geostandards and Geoanalytical Research, **38**, 73–94.

LÜNSDORF N.K., DUNKL I., SCHMIDT B.C., RANTITSCH G., VON EYNATTEN H. (2017) - *Towards a Higher Comparability of Geothermometric Data Obtained by Raman Spectroscopy of Carbonaceous Material. Part 2: A Revised Geothermometer*. Geostandards and Geoanalytical Research, **41**, 593–612.

MARRONE S., MONIÉ P., ROSSETTI F., LUCCI F., THEYE T., BOUYBAOUENE M.L., NAJIB ZAGHLOUL M. (2020) -

1  
2  
3 *The Pressure-Temperature-time-deformation history of the Beni Mzala unit (Upper Sebtides, Rif belt,*  
4 *Morocco): Refining the Alpine tectono-metamorphic evolution of the Alboran Domain of the Western*  
5 *Mediterranean.* *Journal of Metamorphic Geology.* **39**(5), 591-615.

6  
7  
8  
9  
10 MARTIN-ALGARRA A., MAZZOLI S., PERRONE V., RODRIGUEZ-CANERO R., NAVAS-PAREJO P. (2009) - *Variscan*  
11 *tectonics in the Malaguide Complex (Betic Cordillera, southern Spain): stratigraphic and structural*  
12 *Alpine versus pre-Alpine constraints from the Ardales area (Province of Malaga). I. Stratigraphy.* *The*  
13 *Journal of geology,* **117**, 241–262.

14  
15  
16  
17  
18  
19 MELCHIORRE M., ÁLVAREZ-VALERO A.M., VERGÉS J., FERNANDEZ M., BELOUSOVA E.A., EL MAZ A.,  
20 MOUKADIRI A. (2017). *In situ U-Pb zircon geochronology on metapelitic granulites of Beni Bousera*  
21 *(Betic-Rif system, N Morocco).* *Geological Society of America Special Papers,* **526**, 151–171.

22  
23  
24  
25  
26  
27  
28  
29  
30  
31  
32  
33  
34  
35  
36  
37  
38  
39  
40  
41  
42  
43  
44  
45  
46  
47  
48  
49  
50  
51  
52  
53  
54  
55  
56  
57  
58  
59  
60  
MICHARD A., NEGRO F., SADDIQI O., BOUYBAOUENE M.L., CHALOUAN A., MONTIGNY R., GOFFÉ B. (2006) -  
*Pressure–temperature–time constraints on the Maghrebide mountain building: evidence from the Rif–*  
*Betic transect (Morocco, Spain), Algerian correlations, and geodynamic implications.* *Comptes Rendus*  
*Geoscience,* **338**, 92–114.

MICHARD A., MOKHTARI A., CHALOUAN A., SADDIQI O., ROSSI P., RJIMATI E.-C. (2014) - *New ophiolite slivers*  
*in the External Rif belt, and tentative restoration of a dual Tethyan suture in the western Maghrebides.*  
*Bulletin de la Société Géologique de France,* **185**, 313–328.

MILLIARD Y. (1959). *Les massifs métamorphiques et ultrabasiques de la zone paléozoïque interne du Rif.* *Notes*  
*Mem. Serv. Géol. Maroc,* **18**, 125–160.

MORI H., MORI N., WALLIS S., WESTAWAY R., ANNEN C. (2017). *The importance of heating duration for*  
*Raman CM thermometry: evidence from contact metamorphism around the Great Whin Sill intrusion,*  
*UK.* *Journal of Metamorphic Geology,* **35**, 165–180, <https://doi.org/10.1111/jmg.12225>.

MUIRHEAD D.K., BOND C.E., WATKINS H., BUTLER R.W.H., SCHITO A., CRAWFORD Z., MARPINO A. (2019) -  
*Raman Spectroscopy: an effective thermal marker in low temperature carbonaceous fold-thrust belts.*  
*Geological Society, London, Special Publications,* **490**, 135-151.

MÜNCH P., CAILLAUD J., MONIÉ P., GRAUBY O., CORSINI M., RICCI J., ROMAGNY A., PILIPPON M., LANSON B.,  
AZDIMOUSSA A., BEN MOUSSA A., ARNAUD N. (2021) - *Direct dating of brittle extensional deformation*

- 1  
2  
3 *contemporaneous of Neogene exhumation of the internal zones of the Rif Chain*. *Tectonophysics*, **807**,  
4  
5 228800.  
6  
7  
8 NEGRI F., DI DONATO E., TOMMASINI M., CASTIGLIONI C., ZERBI G., MÜLLEN K. (2004) - *Resonance Raman*  
9  
10 *contribution to the D band of carbon materials: Modeling defects with quantum chemistry*. *Journal of*  
11  
12 *Chemical Physics*, **120**, 11889–11900.  
13  
14 NEGRO F., BEYSSAC O., GOFFÉ B., SADDIQI O., BOUYBAOUENE M.L. (2006) - *Thermal structure of the Alboran*  
15  
16 *Domain in the Rif (northern Morocco) and the Western Betics (southern Spain). Constraints from Raman*  
17  
18 *spectroscopy of carbonaceous material*. *Journal of Metamorphic Geology*, **24**, 309–327.  
19  
20  
21 NIRRENGARTEN M., MOHN G., SCHITO A., CORRADO S., GUTIÉRREZ-GARCÍA L., BOWDEN S.A. AND DESPINOIS  
22  
23 F. (2020) - *The thermal imprint of continental breakup during the formation of the South China Sea*.  
24  
25 *Earth and Planetary Science Letters*, **531**, 115972.  
26  
27  
28 PASTERIS J.D. & WOPENKA B. (1991) - *Raman spectra of graphite as indicators of degree of metamorphism*.  
29  
30 *The Canadian Mineralogist*, **29**, 1–9.  
31  
32 PÉROUSE E., VERNANT P., CHÉRY J., REILINGER R., MCCLUSKYS. (2010) - *Active surface deformation and sub-*  
33  
34 *lithospheric processes in the western Mediterranean constrained by numerical models*. *Geology*, **38**,  
35  
36 823–826.  
37  
38  
39 PLATT J.P., BEHR W.M., JOHANESSEN K., WILLIAMS J.R. (2013) - *The Betic-Rif arc and its orogenic hinterland:*  
40  
41 *a review*. *Annual Review of Earth and Planetary Sciences*, **41**, 313–357.  
42  
43  
44 QIN J., WANG S., SANEI H., JIANG C., CHEN Z., REN S., XU X., YANG J., ZHONG N. (2018) - *Revelation of organic*  
45  
46 *matter sources and sedimentary environment characteristics for shale gas formation by petrographic*  
47  
48 *analysis of middle Jurassic Dameigou formation, northern Qaidam Basin, China*. *International Journal of*  
49  
50 *Coal Geology*, **195**, 373–385.  
51  
52  
53 RAHL J.M., ANDERSON K.M., BRANDON M.T., FASSOULAS C. (2005) - *Raman spectroscopic carbonaceous*  
54  
55 *material thermometry of low-grade metamorphic rocks: Calibration and application to tectonic*  
56  
57 *exhumation in Crete, Greece*. *Earth and Planetary Science Letters*, **240**, 339–354.  
58  
59  
60 ROBERTSON J. & OREILLY E.P. (1987). *Electronic and atomic structure of amorphous carbon*. *Physical Review*  
  
B, **35**, 2946–2957.



- 1  
2  
3 RODRÍGUEZ-RUIZ M.D., ABAD I., BENTABOL M., CRUZ M.D.R. (2020) - *Evidences of talc-white mica*  
4 *assemblage in low-grade metamorphic rocks from the internal zone of the Rif Cordillera (N Morocco).*  
5 *Applied Clay Science*, **195**, 105723.  
6  
7  
8  
9  
10 ROSSETTI F., THEYE, T., LUCCI F., BOUYBAOUENNE M.L., DINI A., GERDES A., PHILLIPS D., COZZUPOLI D. (2010)  
11 - *Timing and modes of granite magmatism in the core of the Alboran Domain, Rif chain, northern*  
12 *Morocco: implications for the Alpine evolution of the western Mediterranean.* *Tectonics*, **29**(2), TC2017.  
13  
14  
15  
16  
17 ROSSETTI F., DINI A., LUCCI F., BOUYBAOUENNE M., FACCENNA C. (2013) - *Early Miocene strike-slip tectonics*  
18 *and granite emplacement in the Alboran Domain (Rif Chain, Morocco): significance for the geodynamic*  
19 *evolution of Western Mediterranean.* *Tectonophysics*, **608**, 774–791.  
20  
21  
22  
23  
24 ROSSETTI F., LUCCI F., THEYE T., BOUYBAOUENNE M.L., GERDES A., OPITZ J., DINI A., LIPP C. (2020). *Hercynian*  
25 *anatexis in the envelope of the Beni Bousera peridotites (Alboran Domain, Morocco): Implications for*  
26 *the tectono-metamorphic evolution of the deep crustal roots of the Mediterranean region.* *Gondwana*  
27 *Research*. **83**, 157-182.  
28  
29  
30  
31  
32  
33 ROYDENL. & FACCENNA C. (2018). *Subduction orogeny and the Late Cenozoic evolution of the Mediterranean*  
34 *Arcs.* *Annual Review of Earth and Planetary Sciences*, **46**, 261–289.  
35  
36  
37  
38 RUIZ-CRUZ M.D. & GALÁN E. (2002). *Mineralogy and origin of spots in spotted slate from the Maláguide*  
39 *complex, betic cordilleras, spain: an XRD, EMPA and TEM–AEM study.* *The Canadian Mineralogist*, **40**,  
40 1483–1503.  
41  
42  
43  
44 RUIZ-CRUZ M.D. & NOVÁK J.K. (2003) - *Metamorphic chlorite and “vermiculitic” phases in mafic dikes from*  
45 *the Maláguide Complex (Betic Cordillera, Spain).* *European Journal of Mineralogy*, **15**, 67–80.  
46  
47  
48  
49 SCHITO A. & CORRADO S. (2018) - *An automatic approach for characterization of the thermal maturity of*  
50 *dispersed organic matter Raman spectra at low diagenetic stages.* *Geological Society, London, Special*  
51 *Publications*, **484**, 107-119.  
52  
53  
54  
55 SCHITO A., ROMANO C., CORRADO S., GRIGO D., POE B. (2017) - *Diagenetic thermal evolution of organic*  
56 *matter by Raman spectroscopy.* *Organic Geochemistry*, **106**, 57–67.  
57  
58  
59  
60 SCHITO A., SPINA A., CORRADO S., CIRILLI S., ROMANO C. (2019) - *Comparing optical and Raman*  
*spectroscopic investigations of phytoclasts and sporomorphs for thermal maturity assessment: the case*

1  
2  
3  
4  
5  
6  
7  
8  
9  
10  
11  
12  
13  
14  
15  
16  
17  
18  
19  
20  
21  
22  
23  
24  
25  
26  
27  
28  
29  
30  
31  
32  
33  
34  
35  
36  
37  
38  
39  
40  
41  
42  
43  
44  
45  
46  
47  
48  
49  
50  
51  
52  
53  
54  
55  
56  
57  
58  
59  
60

*study of Hettangian continental facies in the Holy cross Mts. (central Poland)*. Marine and Petroleum Geology, **104**, 331–345.

SCHMIDT J.S., HINRICHS R., ARAUJO C. V. (2017) - *Maturity estimation of phytoclasts in strew mounts by micro-Raman spectroscopy*. International Journal of Coal Geology, **173**, 1–8.

SORCI A., CIRILLI S., CLAYTON G., CORRADO S., HINTS O., GOODHUE R., SCHITO A., SPINA A. (2020). *Palynomorph optical analyses for thermal maturity assessment of Upper Ordovician (Katian-Hirnantian) rocks from Southern Estonia*. Marine and Petroleum Geology, **120**, 104574.

SOTO J.I., PLATT J.P., SÁNCHEZ-GÓMEZ M., AZAÑÓN J.M. (1999) - *Pressure–temperature evolution of the metamorphic basement of the Alboran Sea: thermobarometric and structural observations*. In: Proceedings of the Ocean Drilling Program, Scientific Results. pp. 263–279.

TAYLOR G.H., TEICHMÜLLER M., DAVIS A., DIESSEL C.F.K., LITKE R., ROBERT P. (1998) - *Organic petrology*. Gebrüder Borntraeger, Berlin, Stuttgart. pp. 704.

TEICHMÜLLER M. (1986) - *Organic petrology of source rocks, history and state of the art*. Organic Geochemistry, **10**, 581–599.

THOMSEN C. & REICH S. (2000) - *Double resonant raman scattering in graphite*. Physical Review Letters, **85**, 5214–5217.

TUINSTRA F. & KOENIG J.L. (1970) - *Raman Spectrum of Graphite*. The Journal of Chemical Physics, **53**, 1126–1130.

VAN HINSBERGEN D.J.J., VISSERS R.L.M., SPAKMAN W. (2014) - *Origin and consequences of western Mediterranean subduction, rollback, and slab segmentation*. Tectonics, **33**, 393–419.

VON RAUMER J., STAMPFLI G., BOREL G., BUSSY F. (2002) - *Organization of pre-Variscan basement areas at the north-Gondwanan margin*. International Journal of Earth Sciences, **91**, 35–52.

WILKINS R.W.T., BOUDOU R., SHERWOOD N., XIAO X. (2014) - *Thermal maturity evaluation from inertinites by Raman spectroscopy : The ‘ RaMM ’ technique*. International Journal of Coal Geology, **128–129**, 143–152.

WILLIAMS J.R. & PLATT J.P. (2018) - *A new structural and kinematic framework for the Alborán Domain (Betic–*

1  
2  
3 *Rif arc, western Mediterranean orogenic system*). Journal of the Geological Society, **175**, 465–496.

4  
5 ZAGHLOUL M.N., CRITELLI S., PERRI F., MONGELLI G., PERRONE V., SONNINO M., TUCKER M., AIELLO M.,  
6  
7 VENTIMIGLIA C. (2010). *Depositional systems, composition and geochemistry of Triassic*  
8 *rifted-continental margin redbeds of the Internal Rif Chain, Morocco*. Sedimentology, **57**, 312–350.  
9  
10  
11  
12  
13  
14  
15  
16  
17  
18  
19  
20  
21  
22  
23  
24  
25  
26  
27  
28  
29  
30  
31  
32  
33  
34  
35  
36  
37  
38  
39  
40  
41  
42  
43  
44  
45  
46  
47  
48  
49  
50  
51  
52  
53  
54  
55  
56  
57  
58  
59  
60

For Review Only